

Agriculture, Trade, Migration, and Climate Change *

Hyeseon Shin †

April 17, 2025

[Click for the Most Recent Version](#)

Abstract

Climate change affects agricultural production through land productivity and multicropping capacities. Given agriculture's substantial contribution to both income and employment in developing economies, evolving agro-climatic conditions can reshape labor reallocation and agricultural production. I develop a dynamic spatial general equilibrium model incorporating farmers' optimal crop choices, international trade, and forward-looking migration. Under RCP 8.5, global welfare effects on agricultural workers are modest but vary significantly across countries. Results highlight that the general equilibrium effects of labor mobility are nontrivial, and domestic structural transformation can play a crucial role in mitigating the adverse impacts of climate change.

Keywords: agricultural production, climate change, migration, structural transformation

JEL-Codes: F16, Q17, Q54

*I gratefully acknowledge the financial support from The Andersons Program in International Trade and express my deepest gratitude to my advisor, Ian Sheldon, for his continuous support and guidance. I also gratefully acknowledge the computing power support provided by [Ohio Supercomputer Center \(1987\)](#). I extend my thanks to my committee members, Yongyang Cai, Abdoul Sam, and Seungki Lee, for their valuable feedback. I am also grateful to Steven Redding, Banu Demir Pakel, Yan Bai, Eli Fenichel, Alex Hollingsworth, Kensuke Suzuki, Chengyuan He, Yixuan Wang, Kunxin Zhu, and all other seminar and conference participants for their insightful comments and discussions at various stages of this paper, including the Camp Resources XXX Workshop, 2024 Agricultural & Applied Economics Association Annual Meeting, 2024 Summer School in International Economics by the Journal of International Economics, the 88th Annual Meeting of the Midwest Economics Association, the 2023 Annual Meeting of the International Agricultural Trade Research Consortium, and the 2023 Interdisciplinary PhD Workshop in Sustainable Development at Columbia University. All remaining errors are mine.

†The Ohio State University (e-mail: shin.774@osu.edu).

1 Introduction

Climate change has heterogeneous impacts across regions and sectors, with agriculture standing out as a particularly vulnerable and concerning sector (e.g., [Rudik et al., 2022](#); [Nath, 2023](#); [Zappala, 2024](#)). Given the sector's significant role in both income and employment in many developing economies¹, it has emerged as a crucial agenda to understand the potential consequences of climate change on the agricultural sector. From a production perspective, climate change can directly influence agricultural production through two primary channels: yield and multicropping. The impact on yields is highly heterogeneous across countries, especially given the current geographical distribution of irrigation resources, with the potential to reshape patterns of comparative advantage across countries and crops. Additionally, climate change can affect the capacity of multicropping—the practice of growing crops more than once per year—which can influence the effective size of harvested areas. On the labor market side, climate change may affect labor reallocation through income shocks; yet, these adjustments are imperfect and are long-term processes due to existing frictions. Furthermore, the labor reallocation due to climate change is likely to interact with the underlying forces of structural transformation shaping long-term economic growth, as historical patterns have indicated. While there has been a growing body of studies that attempt to evaluate the impact of climate change, a critical gap remains in the literature connecting the fundamental economic forces between adaptation in agricultural production and labor reallocation within a dynamic general equilibrium framework.

This paper develops and quantifies a dynamic spatial general equilibrium model to examine the effects of climate change on agricultural production and labor markets. The model incorporates three key market mechanisms: optimal crop choices (crop switching), international trade, and labor mobility. First, each country grows multiple crops on a given land and optimizes its land allocation among crops in response to climate change shocks, including yield and multicropping capacity changes. The general equilibrium framework allows us to capture both Ricardian (comparative advantage) and Heckscher-Ohlin (relative factor abundance) effects in agricultural production resulting from agro-climatic changes, accounting for substantial heterogeneity across countries and crops. Second, as crops are traded internationally, an agro-climatic shock in one country can propagate through global markets, influencing crop prices, production, and consumption choices around the world. Third, households make forward-looking migration decisions, choosing whether to relocate across countries and sectors—agriculture and non-agriculture—based on expected lifetime utility. Labor markets with higher utility attract more workers, though migration is subject to bilateral frictions. To capture the full interaction of these market adjustment forces, the model builds on the heterogeneous land model ([Eaton and Kortum, 2002](#); [Sotelo, 2020](#)), incorporates [Armington \(1969\)](#) trade, and features dynamic migration decision of heterogeneous agents as in [Artuç et al. \(2010\)](#) and [Caliendo et al. \(2019\)](#).

This study leverages detailed spatial data on agro-climatic conditions from the Global Agro-

¹The average employment share in the agriculture sector is 34.2% among non-OECD countries, while it is 4.8% among OECD countries. The average GDP share of the agriculture sector is 15% among non-OECD countries, while it is 2.5% among OECD countries. The author's calculation is based on the year 2020, using World Bank data.

Ecological Zones (GAEZ) v4 project, including information on potential yield, multicropping capacity, and irrigation distribution around the world. The model is quantified for 60 countries (regions), aggregating 145 countries globally, and covers 10 major crops, with simulation periods projected through the end of this century. Using dynamic hat algebra developed in [Caliendo et al. \(2019\)](#), I find a transition path of the global agricultural production model toward the sequential equilibrium, by expressing time-varying variables as time differences and solving a system of non-linear equations of these time differences. This approach enables the identification of equilibrium solutions without requiring estimation of a large set of fundamental variables²—a particularly useful feature given that agro-climatic potential yield data from GAEZ does not precisely reflect levels of land productivity within the model.

When mapping the model to data, the framework captures the heterogeneous forces and frictions governing labor reallocation across countries and sectors. Leveraging dynamic hat algebra, the model is quantified without explicitly estimating bilateral migration costs. Instead, the sequential equilibrium solution is conditioned on observed initial migration flows, which inherently embed information on the economic forces and barriers shaping labor reallocation. For example, a large share of domestic migration from agriculture to non-agriculture reflects a substantial income gap between the two sectors and relatively low migration costs. Given the limitation on the availability of global migration flow data, this study introduces a novel approach to capturing these heterogeneous labor reallocation dynamics within a global, cross-country, and cross-sector framework. Migration flow data are constructed to ensure that domestic *net* sectoral flows precisely capture observed changes in sectoral populations over time while incorporating population growth. Accounting for heterogeneity in domestic sectoral flows is crucial for two reasons. First, domestic sectoral migration is a key characterization of structural transformation, reallocating labor between agriculture and non-agriculture. Second, domestic sectoral flows constitute the predominant form of labor mobility, far exceeding cross-country international migration flows. The model simulations here explicitly capture cross-country heterogeneity in structural transformation: countries such as Vietnam and China experience relatively rapid transitions out of agriculture, while parts of Latin America and Southern Africa exhibit reversals in structural transformation trends.

The model simulations provide valuable insights into the economic impacts of climate change on agricultural production and labor dynamics. Over time, the model captures a gradual decline in agricultural employment share across most countries, reflecting domestic sectoral labor mobility and structural transformation in the labor market. Additionally, the results suggest that negative income shocks induced by climate change can accelerate structural transformation out of agriculture, leading to a lower share of agricultural employment by the end of the century. In regions such as Northern and Western Africa, agricultural employment declines more rapidly in the presence of climate change than in its absence, whereas in Central Asia, positive income shocks are projected to slow structural transformation, resulting in a relatively higher share of agricultural employment under climate change.

²The fundamental variable refers to the exogenous state variable ([Caliendo et al., 2019](#)). Specifically, the model solution does not require levels of land productivity, total factor productivities in agriculture and non-agriculture, bilateral trade costs, and migration costs.

The welfare analysis under the pessimistic climate scenario RCP 8.5 reveals that the global aggregate impact of climate change on agricultural workers is close to zero (0.01%), while there exists considerable heterogeneity across countries. Higher-latitude countries, such as Canada, the U.S., Russia, and those in Northern Europe, generally benefit, while countries in northern Africa, as well as many in Latin America and South-eastern Asia, are negatively affected. The model simulation also captures the timing and extent of land reallocation across crops. In Latin America, for instance, Brazil and Argentina reallocate a significant share of cropland from soybeans to maize, yet still face welfare losses. The welfare effects are particularly pronounced in highly specialized agricultural economies: Mongolia and Australia, where over 90% their land is dedicated to wheat production, are expected to experience starkly divergent outcomes, with Mongolia realizing the greatest welfare gain (+3.85%) and Australia suffering the largest loss (-1.23%). Lastly, an alternative welfare evaluation using a model that excludes labor mobility reveals amplified welfare effects in both directions, with losses reaching (-5.16%) and gains up to (+7.46%). This result underscores the crucial role of labor mobility in mitigating the adverse effects of climate change and suggests that abstracting from dynamic labor market adjustments may result in an overestimation of these impacts.

To further investigate the role of labor mobility, I conduct counterfactual exercises in which bilateral migration costs are assumed to rise to prohibitive levels, effectively eliminating cross-country and cross-sector mobility. The results highlight substantial welfare implications of labor mobility: in the baseline scenario, where migration costs remain at current levels, agricultural workers experience a global welfare gain of +14.24% compared to a scenario with no mobility. These effects are unevenly distributed, with the largest gains observed in Vietnam, the Philippines, and China—countries where labor flows out of agriculture are most pronounced. A second counterfactual exercise isolates the role of domestic sectoral mobility by prohibiting international migration while allowing labor reallocation across sectors within countries. The results suggest that welfare effects under this scenario closely resemble those in the first counterfactual exercise, consistent with empirical evidence that most labor mobility occurs domestically rather than internationally. These findings underscore the critical role of domestic structural transformation in mitigating the adverse welfare effects of climate change for agricultural workers. Although international migration remains limited by high barriers, facilitating sectoral mobility within countries could serve as a key policy instrument to address prevalent income disparities between agricultural and non-agricultural workers, complementing broader climate adaptation efforts.

To the best of my knowledge, this is the first dynamic spatial general equilibrium model to evaluate the impact of climate change on global agricultural production while incorporating forward-looking labor mobility within a multi-country, multi-crop production framework. Notably, the model captures heterogeneous forces and frictions governing structural transformation across countries, addressing a critical gap in the literature. Furthermore, the quantification approach accounts for rich heterogeneity in climate change shocks across countries and crops, integrating both yield and multicropping capacity shocks based on existing irrigation distributions. This framework extends beyond prior studies ([Costinot et al., 2016](#); [Gouel and Laborde, 2021](#)), which primarily focus

on potential yield changes, offering a more comprehensive evaluation of the impact of climate change on global agriculture. Finally, the optimal land allocation over time across countries and crops is explicitly addressed in the model framework, with simulation results providing useful and practical insights for policymakers and farmers seeking to optimize land use under future climate conditions.

Related Literature — This study relates to and contributes to several branches of literature. Firstly, this study closely connects to the literature on heterogeneous land models in a spatial general equilibrium framework (e.g., [Costinot et al., 2016](#); [Gouel and Laborde, 2021](#); [Sotelo, 2020](#); [Pellegrina, 2022](#); [Conte, 2022](#); [Farrokhi and Pellegrina, 2023](#)). These studies have incorporated the modern Ricardian trade framework à la [Eaton and Kortum \(2002\)](#) to generate predictions for land shares across crops, by exploiting high-resolution crop-yield data from the GAEZ project. In particular, [Costinot et al. \(2016\)](#) and [Gouel and Laborde \(2021\)](#) analyze the impact of agricultural productivity shocks under climate change and emphasize the role of crop switching and international trade as measures to mitigate adverse welfare impacts. This study closely relates to and complements [Costinot et al. \(2016\)](#) and [Gouel and Laborde \(2021\)](#) by explicitly addressing labor mobility and structural transformation, and by enriching the model quantification. Recent studies by [Pellegrina \(2022\)](#) and [Conte \(2022\)](#) develop spatial general equilibrium models that incorporate both trade and migration. These studies are set in a static context and focus on a single country, Brazil ([Pellegrina, 2022](#)), or a continent, sub-Saharan Africa ([Conte, 2022](#)).

This study also contributes to the literature analyzing the interactions between climate change and migration. In particular, recent advancements in tractable quantitative models and computational methods (e.g., see [Redding, 2016](#); [Redding and Rossi-Hansberg, 2017](#); [Caliendo et al., 2019](#); [Kleinman et al., 2023](#)) have spurred rapid growth in the literature on dynamic spatial general equilibrium models. These studies quantify the impact of climate change in a spatial general equilibrium model with internal or international forward-looking migration, focusing on different aspects of the economy: investment decision and technological diffusion ([Desmet and Rossi-Hansberg, 2015](#); [Desmet et al., 2018, 2021](#)); sectoral and geographical specialization ([Conte et al., 2021](#)); education-specific migration ([Burzyński et al., 2022](#)); endogenous use of fossil fuels and clean energy ([Cruz, 2023](#)); sectoral productivity and local amenity shocks ([Rudik et al., 2022](#)); impact of storms and extreme heat waves ([Bilal and Rossi-Hansberg, 2023](#)). In these studies, agriculture is often considered an aggregate sector or a part of the aggregate economy, without addressing the adjustment role of crop choices within the agriculture sector. Another group of studies empirically assesses the impact of weather shocks on internal or international migration patterns (e.g., [Cattaneo and Peri, 2016](#); [Peri and Sasahara, 2019](#)).

Additionally, this study connects to the classical macroeconomics literature on the structural transformation of an economy (e.g., see [Herrendorf et al., 2014](#)). In the literature, it has been well-understood that sectoral allocation of labor appears to be distorted in many developing economies ([Vollrath, 2009](#); [Gollin et al., 2014](#)) and that labor market frictions are the key contributor prohibiting the labor reallocation from agriculture to non-agriculture, resulting an excessively large share of labor remaining in the agricultural sector with low labor productivity ([Restuccia et al.,](#)

2008; Tombe, 2015). While there is a relatively large body of literature analyzing labor reallocation from agriculture to non-agriculture sector or rural to urban areas within specific countries (e.g., Herrendorf et al. (2013) for the US; Tombe and Zhu (2019); Adamopoulos et al. (2024) for China; Munshi and Rosenzweig (2016); Imbert and Papp (2020) for India; Lagakos et al. (2023) for Bangladesh)³, there are relatively fewer studies that examine structural transformation in labor markets across many countries around the world. An exception is Cruz (2023), which develops a model incorporating sectoral reallocation, dynamic labor mobility, and an endogenous climate system, where temperature increases have heterogeneous impacts on productivity across regions and sectors. This study also considers bilateral migration costs across region- and sector-specific labor markets but takes a different approach to constructing its migration flow matrix.⁴ Nath (2023) also examines potential sectoral reallocation between agriculture and non-agriculture in response to climate change but does not account for the economy’s dynamic features or the costs of mobility across space and sectors.

2 Background and Motivation

This section briefly introduces the data and the empirical patterns that motivate the selection of model components. To assess the impact of climate change on future agricultural production, this study utilizes projections from the GAEZ version 4 dataset, provided by the FAO. The GAEZ dataset includes projections of agro-climatic potential yield, potential for multiple cropping practices, and the current geographical distribution of irrigation availability, all at a 5 arc-minute spatial resolution⁵. Following Costinot et al. (2016), I use the climate model HadGEM2-ES and adopt the pessimistic scenario RCP 8.5 as the baseline scenario.⁶ This paper considers 10 major crops and 60 countries (regions) covering 145 countries globally.

Potential Yield — The GAEZ data provides information on agro-climatic potential yield, evaluating agro-climatic environments based on climatic factors such as precipitation and temperature, as well as soil and terrain conditions (Fischer et al., 2021). The potential yield is assessed under a high-input scenario—including full mechanization, a management system, and the optimal use of intermediate inputs such as pesticides and fertilizers—thereby providing the upper limit of agronomically feasible production under specific climatic conditions. The agro-climatic potential yield estimates are provided for all terrains on Earth for historical, current, and future potential climate scenarios, irrespective of whether the land is currently used for growing certain crops or not, and

³For a more extensive review of the literature on structural transformation out of the agricultural sector, see Gollin (2023).

⁴Cruz (2023) constructs a migration flow dataset encompassing international and intranational migration flows, with six sectors and 287 regions worldwide. The study first constructs region-sector migration stocks and employs a Poisson regression model to estimate migration flows. In contrast, this paper constructs migration flows by capturing domestic sectoral net flows, which exactly reflect observed population changes in the region-sector labor market.

⁵This is approximately 9 x 9 km at the equator.

⁶In the GAEZ project, future projections are based on five climate models (GFDL-ESM2M, HadGEM2-ES, IPSL-CM5A-LR, MIROC-ESM-CHEM, and NorESM1-M) and four climate scenarios (RCP 2.6, 4.5, 6.0, and 8.5), with projections extending to the end of the century (Fischer et al., 2021). The sensitivity of the results under different climate models and scenarios is presented in Appendix E.2.

are provided for two water supply scenarios: irrigation and rain-fed conditions.

A stable water supply is a critical factor influencing potential yields. Additionally, there is large spatial heterogeneity in the availability of irrigation facilities across croplands, which further affects how countries will be hit differently by climate change. See Figure C.4 for the share of croplands equipped with irrigation by country. I use current irrigation distribution data from the GAEZ dataset to adjust potential yields based on irrigation availability and aggregate the results at the country level, which is the unit of analysis for this study. See Appendix C.1 for details.

Figure 1a summarizes future changes in potential yield for the highest-revenue crop in each country under the RCP 8.5 scenario, depicting the percentage change in potential yield by 2100 relative to the year 2020. For example, the figure shows that maize, China's highest-revenue crop in the current period, is expected to see an increase in potential yield, while Brazil's highest-revenue crop, soybeans, is expected to experience a decrease in potential yield. This figure suggests significant heterogeneity across countries in future potential yield changes, suggesting that some countries may be at higher risks if cropland allocation is not adjusted to account for the evolving agro-climatic environment, particularly given current irrigation availability.

The potential for climate change to reshape comparative advantage across both countries and crops in agricultural production has been well-emphasized by Costinot et al. (2016). As climate change alters agro-climatic potential yields, some countries may experience an either absolute or relative increase in potential yield, while others may experience a decline. Similarly, within a country, certain crops may see an either absolute or relative increase in potential yield, whereas others may face a decrease. These shifts in potential yield are likely to alter the comparative advantage in agricultural production from a traditional Ricardian perspective, driving changes in land allocation as countries devote more land to crops where they gain a comparative advantage.

Multicropping and Harvested Areas — It is important to note that the size of physical cropland areas can differ significantly from the size of harvested areas—the total area of croplands actually harvested—due to multicropping practices, where crops are grown multiple times throughout the year. For example, some regions in Southern Asia and Latin America may cultivate crops up to three times per year. As noted by Gouel and Laborde (2021), neglecting multicropping practices can introduce substantial bias into model predictions. Previous studies, such as Costinot et al. (2016) and Gouel and Laborde (2021), examined productivity shocks from climate change but were unable to properly address the gap between physical and harvested areas due to limited data availability. The latest version of the GAEZ dataset (version 4) includes multicropping zone information, enabling us to distinguish between physical and harvested areas more accurately.

The GAEZ project classifies all lands on Earth into 9 zones based on multicropping potential, ranging from zero cropping to triple rice cropping. Similar to the agro-climatic potential yield estimates, multicropping potential is assessed solely based on agro-climatic characteristics, such as the length of growing periods and temperature, and is provided for two different water scenarios—irrigation and rain-fed conditions—covering both historical and future periods. Multicropping may involve planting different crops (e.g., maize and bean) or growing identical crops (e.g., rice) sequentially in the same field after harvest. While multicropping in practice may involve specific

combinations of crops planted together to optimize production, the current version of the GAEZ data provides multicropping zone information only as the number of potential multicropping practices for all crops, except for rice. Given this data constraint and to reduce the complexity of model quantification, I have simplified the multicropping zone information by regrouping the 9 zones into 4 classifications, ranging from zero to triple cropping, irrespective of crop types. Similar to potential yield, I use the irrigation distribution data to adjust multicropping potentials based on current irrigation availability. See appendix C.2 for details of data construction.

Essentially, climate change can alter multicropping potential, which may, in turn, affect the effective size of harvested areas, assuming the physical land area remains constant over time. Thus, the impact of climate change on agricultural production involves not only changes in relative productivity, as emphasized in the Ricardian framework but also changes in relative factor abundance, as highlighted by the Heckscher-Ohlin model. Figure 1b displays the percentage change in multicropping potential by 2100 compared to 2020. Countries in the mid-latitudes of the northern hemisphere are expected to see an increase in multicropping potential, while most countries in the southern hemisphere are projected to experience a decline.

Structural Transformation — The final empirical pattern motivating the model choice is the structural transformation in the labor market. Structural transformation broadly refers to the reallocation of economic activity or resources across sectors—agriculture, manufacturing, and services—in the process of economic development (Herendorf et al., 2013, 2014). A central feature of this process is the reallocation of the labor force, typically from less productive sectors (e.g., agriculture) to more productive sectors (e.g., manufacturing or services), often captured by changes in employment shares. Figure 2a summarizes the historical transition in the share of agricultural employment, aggregated at the sub-regional level, indicating a widespread decline in agricultural employment over the past 30 years (1990–2020). Developing economies with previously higher shares of agricultural employment, particularly in Asia and Africa, have experienced a rapid decline, while developed economies have seen a more gradual decrease, as their agricultural employment share is already relatively low. However, not all developing economies with a high share of agricultural employment have experienced declining trends at the same pace, indicating the existence and potential heterogeneity of barriers associated with structural transformation out of agriculture. The evidence on the barriers of structural transformation has also been documented in the existing literature (e.g., Restuccia et al., 2008; Herendorf and Schoellman, 2018).

While there is no straightforward consensus on the driving force of structural transformation⁷,

⁷In earlier closed-economy models, such as the Solow-Swan framework (Solow, 1956; Swan, 1956), any income-improving economic shock, including agricultural productivity, combined with non-homothetic preferences—where the income elasticity for agricultural goods is less than one—leads to a decline in both agricultural employment and the agricultural sector’s value-added share. In open-economy models, however, structural transformation may not be explained by productivity growth. For instance, Matsuyama (1992) demonstrates that countries with relatively high agricultural productivity may fully specialize in agricultural production, without experiencing a contraction in the agricultural sector. Gollin (2023) further emphasizes that the effect of an agricultural productivity shock on the agricultural employment share depends critically on the specific country and crop. In cases where a country experiences a productivity shock in crops with high global demand and prices, the shock may result in expanded production and an increase in the agricultural sector’s value-added share. Conversely, if the crop primarily serves inelastic local demand, the productivity shock may lead to lower prices, potentially reducing the agricultural sector’s value-added. Whether

structural transformation is closely related to the income gap between sectors. To see if this relationship exists, I run a simple regression as follows:

$$y_{it} = \beta \log(x_{it}) + D_i + D_t + \epsilon_{it}, \quad (1)$$

where y_{it} is the share of domestic *net* migration flows from agriculture to non-agriculture (with 5-year intervals)⁸, and $\log(x_{it})$ denotes the log ratio of per capita income between non-agricultural and agricultural workers (calculated as 5-year averages), defined as the log of GDP per capita in the non-agricultural sector divided by GDP per capita in the agricultural sector. This equation is estimated after controlling for country (D_i) and year (D_t) fixed effects, using panel data for 60 countries (regions) from 1990 to 2015 at 5-year intervals. In Figure 2b, the slope (β) depicts this relationship between the income gap and structural transformation through migration flows out of agriculture, by partialling out the country and year-fixed effects from both the dependent and independent variables. The results are clear and intuitive: a larger income gap between sectors is positively associated with a higher share of workers transitioning out of agriculture. This aligns with the classical view that labor reallocation should eventually lead to equalization of the marginal product of labor across sectors—even though income per capita does not exactly correspond to the marginal product of labor, they are closely related—if there are no barriers across sectors. Furthermore, these findings suggest that sectoral income shocks from climate change have the potential to influence structural transformation; In a country where income from the agricultural sector becomes relatively less attractive due to climate change, the force driving transformation out of agriculture may become stronger. Conversely, if the agricultural sector becomes more attractive, the force of structural transformation may weaken.

These empirical patterns together highlight the importance of incorporating labor mobility when assessing the long-term impacts of climate change, and rationalize the model choice of labor mobility as a dynamic discrete choice problem à la [Artuç et al. \(2010\)](#) and [Caliendo et al. \(2019\)](#). In the model, labor mobility is considered across both spatial (cross-country) and sectoral (cross-sector) dimensions, where the relative income gap (through utility) drive labor flows, and households encounter frictions when switching countries or sectors. Among these flows, domestic cross-sector mobility from agriculture to non-agriculture, in particular, captures structural transformation. Although the term migration is often associated with cross-country population movements, I use it to refer to all labor flows, in line with common usage in the literature.

such a productivity shock increases or decreases agricultural employment may also depend on the labor intensity of the crops involved. For a more comprehensive review of the relevant literature, see e.g., [Gollin \(2023\)](#).

⁸For domestic net migration flows, a positive value indicates a net movement of people from the agricultural sector to the non-agricultural sector, while a negative value signifies the reverse. Details on the construction of migration flows are provided in Section 5.3 and Appendix D.2.

3 A Quantitative Structural Model

This section presents a dynamic spatial model to evaluate the general equilibrium impact of agricultural productivity shocks induced by climate change, incorporating three crucial aspects of market adjustment mechanisms: farmers' optimal crop choice, international trade, and labor reallocation. Essentially, the static component of agricultural production builds upon the heterogeneous land model in [Sotelo \(2020\)](#), while the dynamic component of labor mobility closely follows [Caliendo et al. \(2019\)](#). The productivity shock on agriculture is expected to be highly heterogeneous across countries and even across crops within a single country, potentially resulting in large-scale variation in comparative advantages around the world. Farmers in each country will re-optimize their choice of crop production such that their choice maximizes the return to land, with crop prices being adjusted through international crop markets. Furthermore, countries with severely negative agricultural productivity shocks may experience a reduction in income for households working in the agricultural sector, altering the forces of labor reallocation across countries and sectors. The quantitative structural framework in this paper allows us to study the general equilibrium effects resulting from interactions of crop-level production adjustments, market adjustments through international trade, and labor dynamics.

3.1 Environment

Consider a world economy consisting of N countries, where each country's economy is divided into two output sectors: agriculture (A) and non-agriculture (M). Countries are indexed by $n \in \mathcal{N} \equiv \{1, \dots, N\}$, and the sector is indexed by $s \in \mathcal{S} \equiv \{A, M\}$. In the agricultural sector, labor, land, and intermediate inputs are used to produce crop products $j \in \mathcal{J}^c \equiv \{1, \dots, J\}$, where \mathcal{J}^c is a set of crops. The non-agricultural sector consists of a single good $j \in \mathcal{J}^o \equiv \{0\}$, which is an aggregate of all other products and serves as a numeraire. The production of non-agricultural goods requires labor and structure inputs⁹. Time is discrete and denoted by $t = 0, 1, 2, \dots$.

The endogenous state variable considered in this model is population L_t^{ns} for each labor market of the country-sector pair. The initial allocation of population L_0^{ns} is taken as given. Apart from labor, each country is endowed with an exogenous supply of other production inputs: The agricultural land in country n is comprised of a continuum of heterogeneous plots indexed by $\omega \in \Omega_t^n$, where Ω_t^n is the set of plots in country n , and the total amount of land is denoted by H_t^n . The intermediate inputs M_t^n used for crop production include fertilizers, pesticides, the use of mechanization, etc., and the structure input is a composite of local inputs, both of which are considered to be supplied exogenously in each country.

The model consists of four types of agents. In each labor market, there are households maximizing their lifetime utility by consuming goods and making dynamic migration decisions each period. Each household inelastically supplies one unit of labor and receives a competitive market wage from the local labor market. Local farmers produce crop products by hiring labor, land, and intermediate inputs from the local market. Non-agricultural products are also produced by local

⁹Structure input is essentially non-accumulating capital.

firms that hire labor and structure inputs from the local market. All factor and output markets are assumed to be perfectly competitive, resulting in zero profits for local farmers and firms. Finally, local governments, owning land, intermediate inputs, and structure inputs in each country, redistribute rental revenues to households residing in each country.

3.2 Prices and wages

In country n , the local price of good j is denoted by p_t^{nj} . The rental rate of plot ω for crop j in country n is $r_t^{nj}(\omega)$, while the rental rates of intermediate input and structure input are z_t^n and ℓ_t^n , respectively. Each sector within a country has its own market wages, $w_t^n A$ and $w_t^n M$ for the agricultural sector and non-agricultural sector, respectively.

3.3 International Trade

Trade is subject to a standard iceberg cost $\tau_t^{m,n,j} \geq 1$, such that $\tau_t^{m,n,j}$ units of products need to be produced and shipped from country m for one unit to be consumed in country n . Then no-arbitrage requires:

$$p_t^{m,n,j} = \tau_t^{m,n,j} p_t^{mj}, \quad (2)$$

where p_t^{mj} is the local price of product j in origin country m . Note that, by definition, the trade value of good j imported from country m to n is $X_t^{m,n,j} = \tau_t^{m,n,j} p_t^{m,j} c_t^{m,n,j}$, where $c_t^{m,n,j}$ is the consumption of good j in country n imported from country m . For the case of domestic consumption, the iceberg trade cost is simply set to be $\tau_t^{n,n,j} = 1$.

3.4 Preferences

Households have logarithmic utility $u_t^{ns} = \log(C_t^{ns})$, where C_t^{ns} represents the aggregate consumption of a household located in country n and working for sector s , hereafter referred to as labor market ns . The aggregate consumption C_t^{ns} is defined as:

$$C_t^{ns} = (c_t^{ns,A})^{\phi^n} (c_t^{ns,M})^{1-\phi^n}, \quad (3)$$

where $c_t^{ns,A}$ and $c_t^{ns,M}$ are agricultural and non-agricultural consumption, respectively, and ϕ^n is a preference parameter capturing the expenditure share of the agricultural consumption in country n .

Agricultural consumption, $c_t^{ns,A}$, is a CES composite of various crop products with its associated aggregate price index, P_t^n , given by:

$$\begin{aligned} c_t^{ns,A} &= \left(\sum_{j \in \mathcal{J}^c} (\phi^{n,j})^{1/\varkappa} (c_t^{ns,j})^{(\varkappa-1)/\varkappa} \right)^{\varkappa/(\varkappa-1)} \\ P_t^n &= \left(\sum_{j \in \mathcal{J}^c} \phi^{n,j} (P_t^{nj})^{1-\varkappa} \right)^{1/(1-\varkappa)}, \end{aligned} \quad (4)$$

where $c_t^{ns,j}$ is the consumption of crop j by a household in labor market ns , and P_t^{nj} is the consumption price index of crop j in country n . Here, $\phi^{n,j} \geq 0$ is a preference parameter for crop j in country n , and $\varkappa > 0$ is the elasticity of substitution between different crop products.

The consumption of each crop product is assumed to be an Armington composite of the given product from different origins (Armington, 1969). Accordingly, $c_t^{ns,j}$ and its associated price index, P_t^{nj} , are given by:

$$\begin{aligned} c_t^{ns,j} &= \left(\sum_{m \in \mathcal{N}} (\phi^{m,n,j})^{1/\delta} (c_t^{m,ns,j})^{(\delta-1)/\delta} \right)^{\delta/(\delta-1)} \\ P_t^{nj} &= \left(\sum_{m \in \mathcal{N}} \phi^{m,n,j} (p_t^{m,n,j})^{1-\delta} \right)^{1/(1-\delta)}, \end{aligned} \quad (5)$$

where $c^{m,ns,j}$ is the consumption of crop j imported from country m , consumed by a household in labor market ns , and $p_t^{m,n,j}$ is the price of crop j imported from country m and paid by consumers in country n . The parameter $\phi^{m,n,j} \geq 0$ captures preference for crops imported from country m and consumed by country n , and $\delta > 0$ is the elasticity of substitution between crop products from various origins. The Armington assumption considers agricultural products from different countries as imperfect substitutes, despite their often homogeneous nature. This CES-type specification is useful and has been adopted in previous studies, as it simplifies the problem by eliminating the need to determine whether a country is a net exporter or importer, as well as its trading partners (Costinot et al., 2016).

3.5 Household Migration

The migration decision of households is a dynamic discrete choice problem following Artuç et al. (2010) and Caliendo et al. (2019). For each country-sector pair, the labor market consists of a mass L_t^{ns} of households at the beginning of time t . Each household inelastically provides one unit of labor, receives a competitive market wage w_t^{ns} , and makes consumption. At the end of each period, households have the option to relocate to a different labor market, but there is a publicly known migration cost $\zeta^{ns,mz} \geq 0$, capturing spatial and sectoral reallocation frictions. Households also learn about their idiosyncratic preference shock ϵ_t^{mz} , which will be realized for any potential country m and sector z they move to. With complete information and forward-looking behavior, households optimally choose a labor market maximizing their expected lifetime utility at a discount factor β , given the migration costs and future realizations of idiosyncratic shocks. Then the household's dynamic discrete choice problem is expressed as:

$$\mathbf{v}_t^{ns} = u_t^{ns} + \max_{m \in N, z \in \mathcal{S}} \left\{ \beta \mathbb{E}_t(\mathbf{v}_{t+1}^{mz}) - \zeta^{ns,mz} + \nu \epsilon_t^{mz} \right\}, \quad (6)$$

where \mathbf{v}_t^{ns} is the lifetime utility of a household in country n evaluated at time t , and ν is a parameter scaling the idiosyncratic shock.

Following the standard assumptions in dynamic discrete choice literature, idiosyncratic shock ϵ_t^{mz} follows a Type-I extreme value distribution (Gumbel) with mean zero, and is independently and identically distributed across individuals, countries, sectors, and time. Then the household's

dynamic problem can be rewritten as:

$$V_t^{ns} = u_t^{ns} + \nu \log \left(\sum_{m \in \mathcal{N}} \sum_{z \in \mathcal{S}} \exp \left(\frac{\beta V_{t+1}^{mz} - \zeta^{ns,mz}}{\nu} \right) \right), \quad (7)$$

where $V_t^{ns} \equiv \mathbb{E}_t(\mathbf{v}_t^{ns})$ is the expected lifetime utility of the household over a vector of preference shock $\epsilon_t = \{\epsilon_t^{mz}\}_{m \in \mathcal{N}, z \in \mathcal{S}}$. Exploiting the properties of extreme value distributions, the migration share of households from labor market ns to mz is derived as:

$$\mu_t^{ns,mz} = \frac{\exp((\beta V_{t+1}^{mz} - \zeta^{ns,mz})/\nu)}{\sum_{\tilde{m} \in \mathcal{N}} \sum_{\tilde{z} \in \mathcal{S}} \exp((\beta V_{t+1}^{\tilde{m}\tilde{z}} - \zeta^{ns,\tilde{m}\tilde{z}})/\nu)}. \quad (8)$$

The above expression for migration share suggests that country-sector pairs with higher expected lifetime utility, net of migration costs, attract a larger fraction of movers. Also, $1/\nu$ implies the migration elasticity governing how much migration share responds to the relative differences in the expected lifetime utility net of migration costs. As the migration elasticity $1/\nu$ approaches zero, the migration does not respond at all to relative differences in expected lifetime utility across labor markets. Conversely, when the migration elasticity $1/\nu$ goes to infinity, implying there is no heterogeneity in idiosyncratic shocks, the migration will fully respond to relative differences in expected lifetime utility, resulting in no differences in expected lifetime utility across all labor markets.

At the end of time t , but before the migration happens, the population in each country n grows at an exogenous growth rate g_t^n .¹⁰ Provided with the migration share, the evolution of the labor supply in the next period is given by:

$$L_{t+1}^{ns} = \sum_{m \in \mathcal{N}} \sum_{z \in \mathcal{S}} \mu_t^{mz,ns} (1 + g_t^m) L_t^{mz}. \quad (9)$$

3.6 Agricultural Production

The production component of the model closely follows [Sotelo \(2020\)](#) and differs from [Costinot et al. \(2016\)](#) and [Gouel and Laborde \(2021\)](#) in some key aspects. In [Costinot et al. \(2016\)](#) and [Gouel and Laborde \(2021\)](#), Leontief production technology over land and labor is assumed, without allowing for substitution between inputs, with heterogeneous total factor productivity. In this setup, the model assumes Cobb-Douglas technology with heterogeneous land productivity, allowing for the substitution of input factors between land, labor, and intermediate inputs. Additionally, this study considers the unit of land input as the harvested area to account for multicropping practices, whereas physical land area was used for the unit of land input in previous studies.

Production Technology — Crop production features a Cobb-Douglas technology with constant

¹⁰The timeline of the dynamic process is as follows. At the beginning of each time t , the population for each labor market L_t^{ns} is given. Then production occurs within each labor market, workers collect their wages, and learn about their idiosyncratic shock ϵ_t^{mz} for all potential labor markets they can move to. After population growth is realized, workers migrate to their chosen labor market.

returns to scale that combines labor, land, and intermediate inputs. In country n , the quantity of a crop $j \in \mathcal{J}^c$ produced on a plot ω is given by:

$$q_t^{nj}(\omega) = B_t^n \left(\ell_t^{nj}(\omega) \right)^{\alpha^{nj}} \left(m_t^{nj}(\omega) \right)^{\rho^{nj}} \left(h_t^{nj}(\omega) A_t^{nj}(\omega) \right)^{\gamma^{nj}}, \quad (10)$$

where $\ell_t^{nj}(\omega)$ is the labor input, $m_t^{nj}(\omega)$ is the intermediate input (e.g., fertilizers, pesticides, and machinery), and $h_t^{nj}(\omega)$ is the land input. The parameters $\alpha^{nj}, \rho^{nj}, \gamma^{nj}$ denote factor intensities of labor, intermediate, and land inputs, respectively, with a constraint of $\alpha^{nj} + \rho^{nj} + \gamma^{nj} = 1$. Each plot ω is heterogeneous in land productivity, which is represented by $A_t^{nj}(\omega) \geq 0$. The parameter B_t^n captures exogenous country-specific total factor productivity.

Following the Ricardian formulation à la [Eaton and Kortum \(2002\)](#), $A_t^{nj}(\omega) \geq 0$ is assumed to be independently and identically drawn from a Fréchet distribution for each (n, j, ω) , with shape parameter $\theta > 1$ and scale parameter ΥA_t^{nj} . The scale parameter is defined such that $A_t^{nj} = \mathbb{E}[A_t^{nj}(\omega)]$ and $\Upsilon \equiv \Gamma(1 - \frac{1}{\theta})^{-1}$, where $\Gamma(\cdot)$ denotes the Gamma function. Then the joint distribution of productivities of different crops is given by:

$$\prod_{j \in \mathcal{J}} \Pr(A_t^{nj}(\omega) \leq a^j) = \exp \left(- \sum_{j \in \mathcal{J}} \left(\frac{a^j}{\Upsilon A_t^{nj}} \right)^{-\theta} \right).$$

With a Fréchet distribution, the shape parameter $\theta > 1$ governs the dispersion of land productivities within each country, with a higher value denoting smaller heterogeneity in land productivity. The scale parameter $\Upsilon A_t^{nj} > 0$ governs the overall level of efficiency in producing a particular crop in each plot, with a higher value denoting a higher productivity level. If a crop j cannot grow in country n , A_t^{nj} is set to 0.

Profit Maximization — The representative farmer in country n hires labor and land from the input market and decides which crops to grow in each plot such that its profit is maximized. Then the profit maximization problem of the farmer is given by:

$$\begin{aligned} & \max_{\ell_t^{nj}(\omega), m_t^{nj}(\omega), h_t^{nj}(\omega)} \sum_{j=1}^J p_t^{nj} q_t^{nj} - \sum_{j=1}^J \int_{\Omega^n} (w_t^{n,A} \ell_t^{nj}(\omega) + z_t^n m_t^{nj}(\omega) + r_t^{nj}(\omega) h_t^{nj}(\omega)) d\omega \\ & \text{s.t. } q_t^{nj} = \int_{\Omega^n} B_t^n \left(\ell_t^{nj}(\omega) \right)^{\alpha^{nj}} \left(m_t^{nj}(\omega) \right)^{\rho^{nj}} \left(h_t^{nj}(\omega) A_t^{nj}(\omega) \right)^{\gamma^{nj}} d\omega, \end{aligned}$$

Under perfect competition, profit maximization results in zero profit for farmers. The difference between crop revenue and the combined costs of labor and intermediate inputs is exactly equal to the rental cost of land. Since the land market is also competitive, farmers choose a crop that generates the highest rental rate of land. In other words, the profit maximization problem for crop production is equivalent to a discrete choice problem in which farmers choose a crop maximizing the rental rate of land in a given plot ω .

The rental rate of land can be determined in two steps. First, one can solve the cost minimization problem to obtain the cost function of producing a given amount of crop. Second, by exploiting that the marginal cost of production is equal to the crop price under perfect competition, a relation

can be derived between rental rates and crop prices. The rental rate of land from the production of crop j in parcel ω is obtained by:

$$r_t^{nj}(\omega) = R_t^{nj} A_t^{nj}(\omega), \quad (11)$$

where R_t^{nj} is the rental rate per efficiency unit of land, defined as:

$$R_t^{nj} = \left(\frac{p_t^{nj} B_t^n}{\bar{c}^{nj} (w_t^n \mathbf{A})^{\alpha^{nj}} (z_t^n)^{\rho^{nj}}} \right)^{1/\gamma^{nj}}, \quad (12)$$

where $\bar{c}^{nj} = (\alpha^{nj})^{-\alpha^{nj}} (\rho^{nj})^{-\rho^{nj}} (\gamma^{nj})^{-\gamma^{nj}}$. Note that $r_t^{nj}(\omega)$ also follows the Fréchet distribution with shape parameter $\theta > 1$ and scale parameter $\Upsilon R_t^{nj} A_t^{nj}$, given the distributional assumption on $A_t^{nj}(\omega)$. Properties of the extreme value distribution yield a tractable expression for the probability that crop j generates the highest rental rate of land among all other crops in a given plot ω . This probability is equal to the share of land allocated to crop j in country n , as there is a continuum of plots in each country that share the identical probability of crop choices. Therefore, the share of land allocated to each crop j in country n is given by:

$$\pi_t^{nj} = \frac{(R_t^{nj} A_t^{nj})^\theta}{\sum_{k=1}^J (R_t^{nk} A_t^{nk})^\theta}. \quad (13)$$

Equation (13) shows that crops of higher land productivity, higher market price, lower labor and intermediate input costs will take a relatively larger share of land. The shape parameter θ governs how much land allocation responds to changes in the rental rate per efficiency unit of land R_t^{nj} or average level of land productivity A_t^{nj} . Therefore, I refer to θ as land allocation elasticity. A higher value of θ indicates greater homogeneity in land productivity within a country for the given crop, leading to larger shifts in response to variations in R_t^{nj} or A_t^{nj} .

Optimal Revenue and Crop Supply — Given the optimal land allocation, the optimal crop revenue and crop supply can be characterized. First, the average rental rate of land for crop j in country n , conditional on crop j being chosen, denoted as Φ_t^n , can be derived as follows:

$$\Phi_t^n = \mathbb{E} \left[R_t^{nj} A_t^{nj}(\omega) \mid R_t^{nj} A_t^{nj}(\omega) \in \arg \max_{k \in \mathcal{J}^c} R_t^{nk} A_t^{nk}(\omega) \right] = \left(\sum_{k=1}^J (R_t^{nk} A_t^{nk})^\theta \right)^{1/\theta}. \quad (14)$$

Let us denote the optimal revenue per unit of land for a given plot ω as $\psi_t^{nj}(\omega)$. The optimal revenue from growing crop j in country n can be obtained by the product of land size in country n , the share of land assigned to crop j , and the average revenue conditional on the selection of crop j in country n . The country- and crop-level optimal revenue Ψ_t^{nj} is then given by:

$$\begin{aligned} \Psi_t^{nj} &= \mathbb{E} \left[\psi_t^{nj}(\omega) \mid R_t^{nj} A_t^{nj}(\omega) \in \arg \max_{k \in \mathcal{J}^c} R_t^{nk} A_t^{nk}(\omega) \right] \pi_t^{nj} H_t^n \\ &= (R_t^{nj} A_t^{nj})^\theta (\Phi_t^n)^{1-\theta} \left(\frac{H_t^n}{\gamma^{nj}} \right). \end{aligned} \quad (15)$$

Then, the optimal quantity of crop j produced in country n is simply obtained by $q_t^{nj} = (\Psi_t^{nj}/p_t^{nj})$. Furthermore, the aggregate country-level optimal revenue from crop production, denoted as Ψ_t^n , can be characterized as:

$$\Psi_t^n = \sum_{j=1}^J \Psi_t^{nj} = \Phi_t^n H_t^n \sum_{j=1}^J \left(\frac{\pi_t^{nj}}{\gamma^{nj}} \right). \quad (16)$$

Optimal Input Demands — The optimal demands for labor and intermediate inputs can be derived with an approach similar to that employed for optimal crop revenue. Let us denote $\ell_t^{nj}(\omega)$ and $m_t^{nj}(\omega)$ as the optimal input demand per unit of land of a given plot ω for labor and intermediate input, respectively. The country- and crop-level input demand for the production of crop j is the product of the land size of each country, the fraction of land allocated to the crop j , and the average input demand conditional on crop j being the rent-maximizing crop among all crop varieties:

$$\begin{aligned} \ell_t^{nj} &= \mathbb{E} \left[\ell_t^{nj}(\omega) \mid R_t^{nj} A_t^{nj}(\omega) \in \arg \max_{k \in \mathcal{J}^c} R_t^{nk} A_t^{nk}(\omega) \right] \pi_t^{nj} H_t^n = \left(\frac{\alpha^{nj}}{w_t^n \mathbf{A}} \right) \Psi_t^{nj} \\ m_t^{nj} &= \mathbb{E} \left[m_t^{nj}(\omega) \mid R_t^{nj} A_t^{nj}(\omega) \in \arg \max_{k \in \mathcal{J}^c} R_t^{nk} A_t^{nk}(\omega) \right] \pi_t^{nj} H_t^n = \left(\frac{\rho_t^{nj}}{z_t^n} \right) \Psi_t^{nj}. \end{aligned} \quad (17)$$

The equations above suggest that the input cost share equals the country- and crop-level revenue multiplied by the factor intensity, a standard outcome of Cobb-Douglas technology. Additionally, the country-level aggregate input demands for crop production can be derived as follows:

$$\ell_t^n \mathbf{A} = \sum_{j=1}^J \ell_t^{nj} = \frac{\bar{\alpha}_t^n}{w_t^n \mathbf{A}} \Psi_t^n \quad \text{and} \quad m_t^n = \sum_{j=1}^J m_t^{nj} = \frac{\bar{\rho}_t^n}{z_t^n} \Psi_t^n, \quad (18)$$

where $\bar{\alpha}_t^n = \sum_{j=1}^J \chi_t^{nj} \alpha^{nj}$ and $\bar{\rho}_t^n = \sum_{j=1}^J \chi_t^{nj} \rho^{nj}$ are the weighted averages of factor intensities for labor and intermediate inputs, respectively, with the weight, χ_t^{nj} , being the revenue share of crop j . This result suggests that the country-level input cost share equals the weighted factor intensity, similar to the result found at the country- and crop-level input cost shares.

3.7 Non-agricultural Sector

To focus on crop-level agricultural production, the non-agricultural good is modeled with a parsimonious assumption. The non-agricultural product is produced with labor and structure under constant returns to scale technology, described as follows:

$$q_t^{n0} = A_t^{nM} (\ell_t^{nM})^{\xi^n} (S_t^n)^{1-\xi^n}, \quad (19)$$

where ℓ_t^{nM} is the labor input, S_t^n is the structure input. Here, $A_t^{nM} > 0$ is an exogenous total factor productivity (TFP) of the non-agricultural sector and $\xi^n \in (0, 1)$ represents the labor intensity in non-agricultural sector production. Under perfect competition, the returns to labor and structure

inputs in non-agricultural goods production are given, respectively, by:

$$w_t^n \mathbf{M} = A_t^n \mathbf{M} \xi^n (\ell_t^n \mathbf{M})^{\xi^n - 1} (S_t^n)^{1 - \xi^n} \quad \text{and} \quad \iota_t^n = A_t^n \mathbf{M} (1 - \xi^n) (\ell_t^n \mathbf{M})^{\xi^n} (S_t^n)^{-\xi^n}. \quad (20)$$

3.8 Income Transfers and Budget Constraint

To maintain the model's tractability regarding labor mobility, I introduce the assumption of income transfers from local governments to households, similar to [Redding \(2016\)](#).¹¹ Local governments, which own land, intermediate inputs, and structure inputs, evenly redistribute rental revenues from land and intermediate inputs to households working in the agricultural sector. Similarly, the local governments evenly distribute rental revenues from structure inputs to households working in the non-agricultural sector. Perfect competition and zero equilibrium profits imply that all revenues from the agricultural and non-agricultural sectors are paid to their factors of production, respectively. With the income transfer assumptions, the total income of households in the agricultural sector simply reduces to the revenue of agricultural production per worker, while the total income of households in the non-agricultural sector equates to the revenue of non-agricultural production per worker.

$$E_t^{n \mathbf{A}} = \left(\frac{\Psi_t^n}{L_t^{n \mathbf{A}}} \right) \quad \text{and} \quad E_t^{n \mathbf{M}} = \left(\frac{q^{n0}}{L_t^{n \mathbf{M}}} \right). \quad (21)$$

3.9 Market Clearing

Market clearing for crop products $j \in \mathcal{J}^c$ implies that the production of crop j in country n equals the total consumption of that crop in all countries, accounting for trade costs $\tau_t^{n,m,j}$:

$$q_t^{nj} = \sum_{m \in \mathcal{N}} \tau_t^{n,m,j} c_t^{n,m,j}, \quad (22)$$

where $c_t^{n,m,j} = \sum_{s \in \mathcal{S}} c_t^{n,ms,j} L_t^{ms}$ is the total consumption of good j in country m , imported from country n . Input markets are also cleared, ensuring that labor demand and supply are equalized in each country-sector pair of labor markets, as well as for intermediate inputs at the country level.

$$L_t^{ns} = \ell_t^{ns} \quad \text{and} \quad M_t^n = m_t^n. \quad (23)$$

3.10 Competitive Equilibrium

The competitive equilibrium of the economy can be defined following [Caliendo et al. \(2019, 2021\)](#) with a group of state variables that describe the economy. The fundamental variables, or exogenous state variables, include productivities $A_t = \{B_t^n, A_t^{nj}, A_t^n \mathbf{M}\}_{n \in \mathcal{N}, j \in \mathcal{J}^c}$, bilateral migration costs $\zeta =$

¹¹Tracking individual wealth poses considerable challenges in the presence of labor mobility. Consequently, prior studies have proposed several approaches: (1) allowing redistribution of rental revenues from local governments to its local agents, (2) constructing a global portfolio that aggregates rental revenues from the global economy and redistributes them to local agents by giving shares, and (3) allowing local immobile factor owners. For a detailed exploration of distributional assumptions regarding rental revenues, see e.g., [Redding and Rossi-Hansberg \(2017\)](#).

$\{\zeta^{ns,mz}\}_{n,m \in \mathcal{N}, s,z \in \mathcal{S}}$, bilateral trade costs $\tau_t = \{\tau_t^{m,n,j}\}_{m \in \mathcal{N}, n \in \mathcal{N}, j \in \mathcal{J}^c}$, structure endowment $S_t = \{S_t^n\}_{n \in \mathcal{N}}$, land endowment $H_t = \{H_t^n\}_{n \in \mathcal{N}}$, and intermediate input endowment $M_t = \{M_t^n\}_{n \in \mathcal{N}}$. The set of time-varying fundamental variables is denoted by $\Theta_t \equiv \{A_t, \tau_t, S_t, H_t, M_t\}$, and the time-invariant fundamental variable is denoted by $\bar{\Theta} \equiv \{\zeta\}$. The endogenous state variable is the population in the labor market for all country-sector pairs, $L_t = \{L_t^{ns}\}_{n \in \mathcal{N}, s \in \mathcal{S}}$.

Definition 3.1 (Temporary equilibrium). Given $(\Theta_t, \bar{\Theta}, L_t)$, a *temporary equilibrium* of the economy is a set of variables $T_t(\Theta_t, \bar{\Theta}, L_t) \equiv \{c_t, q_t, \pi_t, p_t, u_t, X_t, w_t, z_t, \iota_t\}$, where $c_t = \{c_t^{m,ns,j}\}_{m,n \in \mathcal{N}, s \in \mathcal{S}, j \in \mathcal{J}^c}$, $q_t = \{q_t^{nj}\}_{n \in \mathcal{N}, j \in \mathcal{J}^c}$, $\pi_t = \{\pi_t^{nj}\}_{n \in \mathcal{N}, j \in \mathcal{J}^c}$, $p_t = \{p_t^{nj}\}_{n \in \mathcal{N}, j \in \mathcal{J}^c}$, $u_t = \{u_t^{ns}\}_{n \in \mathcal{N}, s \in \mathcal{S}}$, $X_t = \{X_t^{n,m,j}\}_{n,m \in \mathcal{N}, j \in \mathcal{J}^c}$, $w_t = \{w_t^{ns}\}_{n \in \mathcal{N}, s \in \mathcal{S}}$, $z_t = \{z_t^n\}_{n \in \mathcal{N}}$, and $\iota_t = \{\iota_t^n\}_{n \in \mathcal{N}}$ that satisfy the optimality conditions for (a) household's utility maximization problem in equation (2)-(5), and (21); (b) farmer's profit maximization problem in equation (12)-(18); (c) firm's profit maximization problem in equation (19)-(20); (d) and the market clearing condition defined in equation (22) and (23) of the static problem for each time t .

Definition 3.2 (Sequential equilibrium). Given $(L_0, \{\Theta_t\}_{t=0}^\infty, \bar{\Theta})$, a *sequential equilibrium* is a sequence of variables $\{L_t, \mu_t, V_t, T_t(\Theta_t, \bar{\Theta}, L_t)\}_{t=0}^\infty$, where $\mu_t = \{\mu_t^{ns,mz}\}_{n,m \in \mathcal{N}, s,z \in \mathcal{S}}$ and $V_t = \{V_t^{ns}\}_{n \in \mathcal{N}, s \in \mathcal{S}}$, such that the household dynamic migration problem in equations (7)-(9) is satisfied.

4 Solving the Equilibrium

Developing a global-scale agricultural production model poses challenges in terms of both data availability and computational capacity. A key breakthrough is the application of the dynamic hat algebra approach introduced in [Caliendo et al. \(2019\)](#), which significantly reduces the computational burden of solving the multi-region dynamic optimization problem and the number of fundamental variables to be estimated.¹² With dynamic hat algebra, solving the model involves computing relative changes between time t and $t + 1$, denoting variables in time differences (ratios) as $\dot{x}_{t+1} = (x_{t+1}/x_t)$ for any variable x_t . Suppose an initial allocation of the economy is observed and information on the future sequence of changes in the time-varying fundamental variables $\{\dot{\Theta}_t\}_{t=1}^\infty$ is provided. The economy at $t = 0$ does not need to be in a steady state but it is assumed that the economy is transitioning toward a steady state. To ensure that the model can reach a steady state rather than exploding or shrinking, it is further assumed that the sequence of time differences in the fundamental variables converges to 1 in the long run, i.e., $\lim_{t \rightarrow \infty} \dot{\Theta}_t = 1$, and that the population growth rate eventually becomes zero, i.e., $\lim_{t \rightarrow \infty} \{g_t^n\}_{n \in \mathcal{N}} = 0$. To simplify the notation in the following propositions, let us define the consumption shares as $s_t^{nj} = (P_t^{nj} c_t^{n,s,j} / P_t^n c_t^{n,\mathbf{A}})$ and $s_t^{mnj} = (p_t^{m,n,j} c_t^{m,n,s,j} / P_t^{nj} c_t^{n,s,j})$, respectively, and denote the set of consumption shares as $s_t = \{s_t^{nj}, s_t^{mnj}\}_{m,n \in \mathcal{N}, j \in \mathcal{J}^c}$. Then Proposition 1 and 2 together characterize the sequential equilibrium of the model.

¹²Exact hat algebra, initially introduced in a static trade model by [Dekle et al. \(2007, 2008\)](#), was later extended to a dynamic setting by [Caliendo et al. \(2019\)](#) incorporating labor mobility. For the application of dynamic hat algebra in other models in the recent literature, see e.g., [Caliendo et al. \(2019, 2021\)](#) and [Kleinman et al. \(2023\)](#).

Proposition 1 (Solution to the Temporary Equilibrium). *Given the allocation of temporary equilibrium $\{\pi_t, s_t, L_t, X_t\}$ and time differences $\{\dot{L}_{t+1}, \dot{\Theta}_{t+1}\}$, the solution to the temporary equilibrium at time $t + 1$ solves the following set of equations:*

1) Aggregate-level demand:

$$\dot{C}_{t+1}^{ns} = (\dot{c}_{t+1}^{ns, \mathbf{A}})^{\phi^n} (\dot{c}_{t+1}^{ns, \mathbf{M}})^{1-\phi^n} \quad (24)$$

$$\dot{c}_{t+1}^{ns, \mathbf{A}} = \frac{\dot{E}_{t+1}^{ns}}{\dot{P}_{t+1}^n} \quad \text{and} \quad \dot{c}_{t+1}^{ns, \mathbf{M}} = \dot{E}_{t+1}^{ns} \quad (25)$$

2) Crop-level demand:

$$\dot{c}_{t+1}^{ns,j} = \left(\frac{\dot{P}_{t+1}^{nj}}{\dot{P}_{t+1}^n} \right)^{-\varkappa} \dot{c}_{t+1}^{ns, \mathbf{A}}, \quad \text{for } j \in \mathcal{J}^c \quad (26)$$

$$\dot{P}_{t+1}^n = \left(\sum_{j \in \mathcal{J}^c} s_t^{nj} (\dot{P}_{t+1}^{nj})^{1-\varkappa} \right)^{1/(1-\varkappa)} \quad (27)$$

$$s_{t+1}^{nj} = s_t^{nj} \left(\frac{\dot{P}_{t+1}^{nj}}{\dot{P}_{t+1}^n} \right)^{1-\varkappa} \quad (28)$$

3) Crop- and origin-level demand:

$$\dot{c}_{t+1}^{m,ns,j} = \left(\frac{\dot{\tau}_{t+1}^{m,n,j} \dot{p}_{t+1}^{mj}}{\dot{P}_{t+1}^{nj}} \right)^{-\delta} \dot{c}_{t+1}^{ns,j}, \quad \text{for } j \in \mathcal{J}^c \quad (29)$$

$$\dot{P}_{t+1}^{nj} = \left(\sum_{m \in \mathcal{N}} s_t^{mnj} (\dot{\tau}_{t+1}^{m,n,j} \dot{p}_{t+1}^{mj})^{1-\delta} \right)^{1/(1-\delta)} \quad (30)$$

$$s_{t+1}^{mnj} = s_t^{mnj} \left(\frac{\dot{\tau}_{t+1}^{m,n,j} \dot{p}_{t+1}^{mj}}{\dot{P}_{t+1}^{nj}} \right)^{1-\delta} \quad (31)$$

4) Crop production:

$$\dot{R}_{t+1}^{nj} = \left(\dot{p}_{t+1}^{nj} \dot{B}_{t+1}^n (\dot{w}_{t+1}^{n, \mathbf{A}})^{-\alpha^{nj}} (\dot{z}_{t+1}^n)^{-\rho^{nj}} \right)^{1/\gamma^{nj}} \quad (32)$$

$$\pi_{t+1}^{nj} = \frac{\pi_t^{nj} (\dot{R}_{t+1}^{nj} \dot{A}_{t+1}^{nj})^\theta}{\sum_{k=1}^J \pi_t^{nk} (\dot{R}_{t+1}^{nk} \dot{A}_{t+1}^{nk})^\theta} \quad (33)$$

$$\dot{\Phi}_{t+1}^n = \left(\sum_{k=1}^J \pi_t^{nk} (\dot{R}_{t+1}^{nk} \dot{A}_{t+1}^{nk})^\theta \right)^{1/\theta} \quad (34)$$

$$\begin{aligned} \dot{w}_{t+1}^{n, \mathbf{A}} &= \left(\frac{\sum_{j=1}^J \alpha^{nj} (\gamma^{nj})^{-1} \pi_{t+1}^{nj}}{\sum_{k=1}^J \alpha^{nk} (\gamma^{nk})^{-1} \pi_t^{nk}} \right) \left(\frac{\dot{\Phi}_{t+1}^n \dot{H}_{t+1}^n}{\dot{L}_{t+1}^n} \right) \\ \dot{z}_{t+1}^n &= \left(\frac{\sum_{j=1}^J \rho^{nj} (\gamma^{nj})^{-1} \pi_{t+1}^{nj}}{\sum_{k=1}^J \rho^{nk} (\gamma^{nk})^{-1} \pi_t^{nk}} \right) \left(\frac{\dot{\Phi}_{t+1}^n \dot{H}_{t+1}^n}{\dot{M}_{t+1}^n} \right) \end{aligned} \quad (35)$$

5) *Budget constraint:*

$$\dot{E}_{t+1}^{ns} = \begin{cases} \left(\frac{\sum_{j=1}^J (\gamma^{nj})^{-1} \pi_{t+1}^{nj}}{\sum_{k=1}^J (\gamma^{nk})^{-1} \pi_t^{nk}} \right) \left(\frac{\dot{\Phi}_{t+1}^n \dot{H}_{t+1}^n}{\dot{L}_{t+1}^{n\mathbf{A}}} \right), & \text{if } s \in \{\mathbf{A}\} \\ \dot{A}_{t+1}^{n\mathbf{M}} (\dot{L}_{t+1}^{n\mathbf{M}})^{\xi^n-1} (\dot{S}_{t+1}^n)^{1-\xi^n}, & \text{if } s \in \{\mathbf{M}\} \end{cases} \quad (36)$$

6) *Crop market clearing:*

$$\sum_{m \in \mathcal{N}} X_{t+1}^{n,m,j} = (\dot{R}_{t+1}^{nj} \dot{A}_{t+1}^{nj})^\theta (\dot{\Phi}_{t+1}^n)^{1-\theta} \dot{H}_{t+1}^n \left(\sum_{\tilde{m} \in \mathcal{N}} X_t^{n,\tilde{m},j} \right), \quad \text{for } j \in \mathcal{J}^c \quad (37)$$

$$\text{with } X_{t+1}^{n,m,j} = \left(\frac{\tau_{t+1}^{n,m,j} \dot{p}_{t+1}^{nj}}{\dot{P}_{t+1}^{mj}} \right)^{1-\delta} \left(\frac{\dot{P}_{t+1}^{mj}}{\dot{P}_{t+1}^m} \right)^{1-\varkappa} \left(\frac{\sum_{s \in \mathcal{S}} \dot{E}_{t+1}^{ms} \dot{L}_{t+1}^{ms} E_t^{ms} L_t^{ms}}{\sum_{s \in \mathcal{S}} E_t^{ms} L_t^{ms}} \right) X_t^{n,m,j}.$$

Proof. See Appendix B.1. ■

Proposition 2 (Solution to the Sequential Equilibrium). *Given the initial allocation of the model, $(L_0, \pi_0, s_0, \mu_{-1}, X_0)$, and the converging sequence of exogenous time-varying fundamentals $\{\dot{\Theta}_t\}_{t=1}^\infty$, the solution to the sequential equilibrium, $\{L_{t+1}, \mu_{t+1}, V_{t+1}\}_{t=0}^\infty$, solves the following set of equations:*

$$\mu_{t+1}^{ns,mz} = \frac{\mu_t^{ns,mz} (\dot{v}_{t+2}^{mz})^{\beta/\nu}}{\sum_{\tilde{m} \in \mathcal{N}} \sum_{z \in \mathcal{S}} \mu_t^{ns,\tilde{m}z} (\dot{v}_{t+2}^{\tilde{m}z})^{\beta/\nu}} \quad (38)$$

$$L_{t+1}^{ns} = \sum_{m \in \mathcal{N}} \sum_{z \in \mathcal{S}} \mu_t^{mz,ns} (1 + g_t^m) L_t^{mz} \quad (39)$$

$$\dot{v}_{t+1}^{ns} = \dot{v}_{t+1}^{ns} (\dot{L}_{t+1}, \dot{\Theta}_{t+1}) \left(\sum_{m \in \mathcal{N}} \sum_{z \in \mathcal{S}} \mu_t^{ns,mz} (\dot{v}_{t+2}^{mz})^{\beta/\nu} \right)^\nu, \quad (40)$$

where $v_{t+1}^{ns} = \exp(V_{t+1}^{ns})$ and $\dot{v}_{t+1}^{ns} = \exp(u_{t+1}^{ns})$, and $u_{t+1}^{ns}(\dot{L}_{t+1}, \dot{\Theta}_{t+1})$ satisfies the temporary equilibrium at each time $t+1$, for given $\{\dot{L}_{t+1}, \dot{\Theta}_{t+1}\}$.

Proof. See Appendix B.2. ■

Proposition 1 and 2 together suggest that the solution to the dynamic general equilibrium model can be obtained by solving a set of nonlinear equations without requiring the level values of the fundamental variables. This approach is particularly advantageous as it avoids the difficulties associated with accurately estimating the level of country- and crop-level land productivity (A_t^{nj}), as well as the full matrix of bilateral migration costs ($\zeta^{ns,mz}$) and trade costs ($\tau_t^{n,m,j}$), which is quite challenging given current data limitations in country-level studies as in this paper. Instead, the model solution makes use of information on the initial allocation of migration flows ($\mu_{-1}^{ns,mz}$) and future changes in time-varying fundamental variables ($\{\dot{\Theta}_{t+1}\}_{t=0}^\infty$). The model can be used to simulate the economy's transition path toward steady-state equilibrium when global agricultural production is facing climate change shocks, which potentially affect both land productivity and the size of harvest areas through changes in multicropping practices.

While solving the equilibrium using dynamic hat algebra offers great advantages for spatial models with high dimensionality across both space and time, some limitations of this approach need to be acknowledged. First, because the equilibrium solution for each time period depends on the values from the preceding period, the method struggles to account for situations where a previously zero value becomes positive in the subsequent period. This limitation could restrict the model’s ability to accurately capture crop and migration choices. For instance, if a country allocates no land to a particular crop in the initial period, the equilibrium solution does not allow for any future allocation to that crop following climate change shocks. Similarly, if there are no migration flows between certain labor markets in the initial period, the model does not permit new migration flows to emerge between these markets in subsequent periods. This could lead to an underestimation of the role of crop switching or labor mobility in the equilibrium solution. However, estimating the exact barriers to adopting new crops or entering new labor markets is inherently challenging when observed land allocations or migration flows are at zero. Therefore, the solution obtained using dynamic hat algebra should be interpreted as capturing intensive margins—non-zero adjustments in cropland shares and migration flows—and extensive margins from non-zeros to zeros¹³, but not extensive margins involving shifts from zero to non-zero cropland shares and migration flows.

5 Bringing Model to Data

This section describes how the model is matched with data to evaluate the impact of climate change on agricultural crop production. The model is quantified for 10 major crops—rice, maize, wheat, potato and sweet potato, sugarcane, soybeans, tomatoes, oil palm, cassava, and bananas—and 60 regions, covering 145 countries around the world.¹⁴ The initial year is set to 2020, and the model is solved with 5-year step sizes. While the goal of the model is to evaluate the impact of climate change by 2100, the time horizon extends to 2400 to allow sufficient time for numerical convergence of the sequential equilibrium. Exogenous climate change shocks on agricultural production, TFP growth in both the agricultural and non-agricultural sectors, and population growth are applied through the end of the century (2025–2100), with no further shocks assumed thereafter. The solution algorithm is presented in the Appendix D.1.

5.1 Data

This study combines multiple data sources. The key spatial information regarding agricultural production is obtained from the GAEZ version 4 dataset provided by FAO. This dataset covers projections on the agro-climatic potential yield and the potential number of multicropping practices, along with the current geographical distribution of irrigation availability for croplands. Other historical data on the agricultural sector is sourced from the Food and Agriculture Organization (FAO) dataset, including variables such as production quantity, harvested area, bilateral trade flows, and

¹³If a specific crop productivity shifts from non-zero to zero, i.e., $\hat{A}_t^{nj} = 0$, the land allocation for that crop becomes zero, as implied in equation (33).

¹⁴For list of crops and countries, see Table 9 and 10 in the Appendix C.

producer prices at both the country and crop levels. The future agricultural TFP (\dot{B}_{t+1}^n) is assumed to grow at an exogenous annual rate of 1.12%, following the recent estimates of global agricultural output TFP growth during 2011-2020 (Fuglie et al., 2024). Macroeconomic variables are collected from the World Bank dataset, including sectoral GDP, sectoral employment, population, birth rates, death rates, and inflation rates. Future TFP changes in the non-agricultural sector (\dot{A}_{t+1}^{nM}), as well as population growth rates (g_t^n), are constructed based on projections from KC and Lutz (2017), assuming SSP2 (Shared Socioeconomic Pathways) scenario.¹⁵. All monetary variables are deflated to 2020 USD.

5.2 Climate Change Shocks

In this paper, the climate change shock to the agricultural sector is considered in two dimensions: land productivity and multiple cropping (or multicropping). This subsection describes how the exogenous climate change shocks to agricultural production are introduced into the model quantification.

Land Productivity — Previous studies most closely related to this paper—Costinot et al. (2016) and Gouel and Laborde (2021)—assume a Leontief production technology and directly map the agro-climatic potential yield (A_t^{nj}) from the GAEZ dataset as total factor productivity in their models. Although the Leontief assumption allows total factor productivity to be conveniently interpreted as yield, this approach introduces two potential biases. First, the agro-climatic potential yield from the GAEZ data only captures agro-climatic conditions under a high-input scenario, without accounting for heterogeneity in realized yields across countries or crops due to cultural or technological farming practices or limited access to resources. Consequently, the agro-climatic potential yield can diverge significantly from realized yields, particularly in developing economies with limited access to mechanized equipment and chemical inputs.¹⁶ Second, the potential yield from the GAEZ data is measured as yield per harvest. Therefore, if the model relies on physical land size, using the GAEZ yield directly as total factor productivity may severely bias production quantities, especially in countries where multicropping is prevalent.

In this paper, the total factor productivity parameter B_t^n can be interpreted to absorb all the non-climatic factors affecting yield, thereby leaving agro-climatic attributes only to the land productivity (A_t^{nj}). Importantly, the dynamic hat algebra only exploits the relative changes over time, without requiring the level of land productivity. I interpret that the GAEZ agro-climatic potential yield exhibits a linear relationship with land productivity in the model, i.e., $A_t^{nj} = v^{nj} A_t^{nj}$. Even though the land productivity (A_t^{nj}) and non-climatic efficiencies (B_t^n) are not directly observed, the sequential equilibrium of the model can be solved with dynamic hat algebra by exploiting that future changes in land productivity can be captured by future changes in agro-climatic potential yield,

¹⁵ Assuming an exogenous population path following SSP2, the TFP growth rate is constructed to capture the projected trajectory of GDP growth under SSP2. In this scenario, projected future economic patterns remain largely consistent with historical trends, with developing countries experiencing higher economic growth rates and developed economies exhibiting lower growth rates.

¹⁶On an additional note, GAEZ data also provides information on the ‘achievement ratio (actual/potential)’ for yields.

i.e., $\dot{A}_{t+1}^{nj} = \dot{\mathcal{A}}_{t+1}^{nj}$. By conditioning on the observed quantities in the initial period, the model is exactly matched with the observed quantities of production, consumption, and trade, and can evaluate changes in equilibrium resulting from productivity shocks from climate change. Specifically, these productivity shocks are introduced by constructing an irrigation-adjusted potential yield at the country level, with cubic interpolation applied to generate a full time path through 2100. See appendix C.1 for details.

Multiple Cropping Capacity — Changes in multicropping potentials are closely related to the effective size of harvested areas. For instance, if a field previously used for double cropping per year becomes available only for single cropping, the effective harvested area is reduced to half of its original size. Therefore, in the production function, the land size is measured in terms of harvested areas rather than physical areas. I capture potential changes in the size of harvested areas (\dot{H}_{t+1}^n) in the model by exploiting the changes in multicropping capacity ($\dot{\mathcal{N}}_{t+1}^n$) from the GAEZ data. In other words, this approach assumes that the size of harvested areas increases or decreases at the same ratio as the multicropping potential changes. It should be noted that, similar to agro-climatic potential yield, the multicropping potentials provided by GAEZ data represent the upper limit of multicropping practices given the region's agro-climatic conditions. In reality, observed multicropping practices may not fully reach this potential multicropping capacity. By conditioning on the observed harvested areas for land input in the initial period, the model solution incorporates the realized multicropping practices of the base year, and integrates potential changes in multicropping capacities thereafter. Similar to the potential yield variable, I construct an irrigation-adjusted multicropping capacity variable at the country level and use cubic interpolation to generate a continuous time path by 2100.

5.3 Migration Flows

One of the key pieces of information required to solve the model is the initial allocation of migration flows. Comprehensive data on international migration for all countries is limited. To the best of the author's knowledge, there is no dataset available that captures migration flows at both cross-country and cross-sector levels. I construct an expanded migration flows matrix across countries and sectors, through a migration flow decomposition based on the equation (9). Given the cross-country migration flow estimates from [Abel and Cohen \(2019\)](#), I construct domestic sectoral flows from agriculture to non-agriculture (or vice versa), such that domestic *net* sectoral flows exactly capture observed changes in sectoral population over time, accounting for population growth rates. Details on the migration flow decomposition are provided in the Appendix D.2. The resulting matrix of expanded migration flows is constructed for the period 1990-2015, with 5-year intervals, consistent with the country-level flows from [Abel and Cohen \(2019\)](#). With 60 countries and 2 sectors, the expanded migration flow matrix comprises 14,400 elements.

Figure 3 summarizes the migration flow estimates expanded at the cross-country and sector levels. Figure 3a shows the time trend of migration flow shares over the period 1990-2015, aggregated at the global scale. Excluding migration flows staying in the same labor market, the largest

migration flow is domestic migration from agriculture to non-agriculture, ranging between 2.26% and 4.76% across the period 1990-2015. All other labor market switching patterns are below the 1% level across all periods. Both Figure 3b and Figure 3c present net domestic flows across sectors for the most recent period 2015-2019, with Figure 3b showing results aggregated across 18 subregions and Figure 3c detailing for 60 countries. The values in Figure 3b and 3c are the share of net domestic migration flows out of total migration flows within each country (or subregion), with positive values indicating net domestic flows from agriculture to non-agriculture, and negative values indicating the reverse.

Most regions exhibit *net* domestic flows from agriculture to the non-agricultural sector, with the highest flows observed in Southeastern Asia (4.5%) and Eastern Africa (3.3%). By country, the largest share of net domestic flows are seen in Vietnam (11.39%), Bangladesh (5.60%), Laos (5.26%), and Myanmar (5.17%). However, there are a few exceptions, with regions such as Southern Africa and South America experiencing the opposite trends. Peru (-6.70%) has the highest domestic migration flows from agriculture to non-agriculture, followed by the Rest of Southern Africa (NSAF2) (-5.2%) and the Rest of Northern Latin America (RNLA) (-3.43). These patterns may reflect the middle-income trap and premature deindustrialization, characterized by stagnant economic growth and a lack of structural transformation.¹⁷ In particular, countries such as Peru, South Africa (part of NSFA2), and Ecuador (part of RNLA) are considered potentially experiencing middle-income premature deindustrialization ([Andreoni and Tregenna, 2021](#)). The model simulation takes the migration flows over 5-year periods 2015-2019 as the initial flows (μ_{-1}) and projects labor mobility thereafter.

5.4 Parameters

Preference Parameters — As the aggregate consumption is a Cobb-Douglas form, the preference parameter for the agricultural consumption (ϕ^n) is directly constructed using the FAO data as the consumption share on agricultural goods, based on the year 2020. The CES preference parameters are adopted from [Costinot et al. \(2016\)](#), with an elasticity of substitution across origins, $\delta = 5.4$, and an elasticity of substitution across crops, $\kappa = 2.82$.

Agricultural Production Parameters — The factor intensities for crop production ($\alpha^{nj}, \rho^{nj}, \gamma^{nj}$) are key parameters governing market adjustments in the agricultural sector. To calibrate the crop-level production input factor intensities, I follow and adapt the approach in [Sotelo \(2020\)](#), exploiting the relationship between land share and revenue share. Specifically, revenue share (χ_t^{nj}) can be

¹⁷In advanced economies such as the United States and the European Union, the decline in manufacturing employment share has been a characteristic feature of the post-industrial phase of development and is considered a standard economic growth pattern. However, similar trends are observed in some developing low- or middle-income countries, even before they are considered to have reached their peak industrialization. Such decline in manufacturing among developing economies has been characterized in the literature as ‘premature deindustrialization’ ([Dasgupta and Singh, 2006; Rodrik, 2016](#)). [Rodrik \(2016\)](#) documents that since the 1980s, the manufacturing sector has contracted in both employment share and real value-added, particularly in Latin America and Sub-Saharan Africa. While premature deindustrialization is often associated with a direct transition from agriculture to the service sector, the migration patterns observed here suggest that some countries may be undergoing a process of ‘reverse structural transformation.’

expressed as a function of land share (π_t^{nj}) and land intensity (γ^{nj}) as follows¹⁸:

$$\chi_t^{nj} = \frac{(\gamma^{nj})^{-1}\pi_t^{nj}}{\sum_{k=1}^J (\gamma^{nk})^{-1}\pi_t^{nk}}. \quad (41)$$

The model implies that, for any country n , crops with systematically higher revenue share relative to their land allocation share in equilibrium have lower land intensity, and vice versa. I assume that the country- and crop-specific land intensity can be multiplicatively decomposed into country-specific and crop-specific components, i.e., $\gamma^{nj} = \gamma^n \gamma^j$. Taking log of equation (41), it follows:

$$\log(\chi_t^{nj}) = \underbrace{\log(\pi_t^{nj})}_{D^j} + \underbrace{\log((\gamma^j)^{-1}) + \log((\gamma^n)^{-1}) - \log\left(\sum_{k=1}^J (\gamma^{nk})^{-1}\pi_t^{nk}\right)}_{D_t^n}. \quad (42)$$

Assuming the above relationship is observed with an error term ϵ_t^{nj} , the following equation is considered for regression:

$$\log(\chi_t^{nj}) = \log(\pi_t^{nj}) + D^j + D_t^n + \epsilon_t^{nj}, \quad (43)$$

where D^j denotes crop-specific fixed effects and D_t^n denotes country-by-year fixed effects. Dropping a baseline crop in the regression, a coefficient b^j on the corresponding dummy variable for D^j captures the fixed effect of crop j relative to the baseline crop. The crop-specific component of land intensity, γ^j , can then be captured by:

$$\gamma^j = \frac{1}{\exp(b^j)} \gamma^{\text{base}}, \quad (44)$$

where γ^{base} is a land intensity parameter of the baseline crop. I set *Potato and sweet potato* (RT1) as the baseline crop as it is the most widely grown crop across countries. I use FAO data on harvested areas, production quantity, and trade unit price for the period 2000-2020 to construct a panel dataset on harvested land share and revenue share to run the regression. The regression result is presented in Table 2. The coefficient of $\log(\pi_t^{nj})$ is obtained as 0.951, which is close to the model prediction of 1. A crop dummy coefficient b^j greater than zero indicates that the crop is less land-intensive relative to the base crop, whereas a negative coefficient suggests higher land intensity relative to the base crop. All crop dummy coefficients are statistically significant, except for those of oil palm and sugar cane.

Ideally, the model could be calibrated using country- and crop-specific land intensities to capture both cross-country and cross-crop heterogeneity. However, due to data limitations, I assume that factor intensities are the same across countries, i.e., $\gamma^{nj} = \gamma^j$.¹⁹ Farrokhi and Pellegrina (2023)

¹⁸For derivation, refer to the equation (A.44) in the Appendix A.4.

¹⁹To the best of the author's knowledge, no recent studies systematically estimate the land input cost share specifically for crop production across all countries worldwide. U.S. Department of Agriculture, Economic Research Service (2023) provides input cost share estimates in agricultural production for most countries, but these estimates encompass crop, livestock, and aquaculture sectors (Fuglie, 2015). In countries with significant reliance on aquaculture, for

calibrate the factor intensities in crop production under modern technology to be 0.206 for land, 0.207 for labor, and 0.587 for intermediate inputs, but do not account for crop-specific heterogeneity.²⁰ After estimating the crop-specific coefficient b^j , I normalize the revenue-weighted input share of land to the aggregate level reported in [Farrokhi and Pellegrina \(2023\)](#), i.e., $\bar{\gamma}^n = 0.206$. Specifically,

$$\bar{\gamma}^n = \sum_{j \in \mathcal{J}^c} o^j \gamma^{nj} = \sum_{j \in \mathcal{J}^c} o^j \gamma^n \frac{1}{\exp(b^j)} \gamma^{\text{base}}, \quad (45)$$

where o^j is the revenue share of crop j globally, for which I construct the ten-year average over the 2010–2020 period. The crop-specific component of land intensity for the baseline crop is then given by:

$$\gamma^{\text{base}} = \left(\sum_{j \in \mathcal{J}^c} \alpha^{nj} \exp(-b^j) \right)^{-1} \frac{\bar{\gamma}^n}{\gamma^n}. \quad (46)$$

Substituting the equation (44) and (46) into $\gamma^{nj} = \gamma^n \gamma^j$, the factor intensity of land for crop j is as follows:

$$\gamma^{nj} = \frac{\exp(-b^j)}{\sum_{j \in \mathcal{J}^c} \alpha^{nj} \exp(-b^j)} \bar{\gamma}^n. \quad (47)$$

After recovering land intensities (γ^{nj}), factor intensities for labor (α^{nj}) and intermediate inputs (ρ^{nj}) are calibrated such that the relative input share of labor to intermediate inputs matches the ratio in [Farrokhi and Pellegrina \(2023\)](#), i.e., $\alpha^{nj}/\rho^{nj} = 0.207/0.587$, and factor intensities for all inputs sum to 1.

The calibrated factor intensities for all 10 crops are displayed in Table 3. Crops such as tomatoes and bananas exhibit relatively low land intensity, while cereal crops and staple grains, such as maize, wheat, and soybeans, are relatively more land-intensive. Figure 4 displays the model fit of the estimated land intensities for the targeted moment of equation (41). Without including any fixed effects, the model predicted revenue share ($\hat{\chi}_t^{nj}$), given the estimated land intensities and observed harvested share of land (π_t^{nj}), can explain approximately $R^2 = 86.77\%$ of variation in the observed revenue share, confirming that there exists large heterogeneity in land intensity across crops.

Lastly, the land allocation elasticity is assumed to be $\theta = 1.38$ following estimates in [Farrokhi and Pellegrina \(2023\)](#), which also employs global crop production data. In other studies, [Sotelo \(2020\)](#) estimates this parameter at $\theta = 1.658$ using Peruvian data, and [Costinot et al. \(2016\)](#) estimates this parameter at $\theta = 2.46$.

Non-Agriculture Production Parameters — The labor intensity parameter for non-agricultural production, ξ^n , is constructed using the share of labor compensation in total value added, based on data from the World Input-Output Database (WIOD) for the year 2014.

Migration Elasticity — Solving the sequential equilibrium of the model requires migration elas-

example, the reported input cost shares may not accurately reflect the land input cost share for crop production.

²⁰In [Farrokhi and Pellegrina \(2023\)](#), land use data by crop are also obtained from the GAEZ dataset, whose field-level values are consistent with FAO country-level data upon aggregation, and the unit of land input is harvested area rather than physical area. Additionally, in [Farrokhi and Pellegrina \(2023\)](#), the use of intermediate inputs under modern technology corresponds to the use of chemical fertilizers.

ticity ($1/\nu$), a parameter governing how much migration responds to the relative changes in life-time expected utilities—and ultimately real income—across labor markets. All other things being equal, the migration elasticity is expected to be larger over longer time intervals, as households are more likely to adjust through labor reallocation over an extended period. In previous studies, Caliendo et al. (2019) estimates migration elasticity using internal migration data from the US, finding $\nu = 5.34$ for the quarterly interval and $\nu = 2.02$ for the annual interval, and Caliendo et al. (2021) estimates annual migration elasticity at $\nu = 2$ using migration flows among countries within the EU. At the same time, however, cross-country and cross-sector migration, as in this study, is likely to have lower migration elasticity compared to within-country or intra-EU migration. In a related study, Cruz (2023) estimates this elasticity at $\nu = 6.67$, using a quinquennial step size, with its data covering 6 sectors and 287 regions around the world.

Following Artuç et al. (2010) and Caliendo et al. (2019), I estimate the migration elasticity using the expanded migration flows data, based on the following equation:

$$\frac{1}{\beta} \log(\mu_t^{ns,mz} / \mu_t^{ns,ns}) - \log(\mu_{t+1}^{ns,mz} / \mu_{t+1}^{mz,mz}) = \frac{1}{\nu} \log(E_{t+1}^{mz} / E_{t+1}^{ns}) + D_t^{m,n} + v_{t+1}, \quad (48)$$

where the coefficient of $\log(E_{t+1}^{mz} / E_{t+1}^{ns})$ captures the migration elasticity ($1/\nu$), and $D_t^{n,m}$ represents the origin-destination-time fixed effects.²¹ Two identification concerns arise here. The first, inherent to this structural estimation, is that the OLS estimates $1/\nu$ are likely to be biased if there exist any shocks at time $t + 1$, contained in the error term v_{t+1} , affect both the income at time $t + 1$ and the migration decision at time t . To address this endogeneity, following Artuç et al. (2010), I instrument $\log(E_{t+1}^{mz} / E_{t+1}^{ns})$ with $\log(E_{t-1}^{mz} / E_{t-1}^{ns})$, given the assumption that income at time $t - 1$ is uncorrelated with the contemporaneous shock at time $t + 1$. Under this identification strategy, the panel data used for estimation is restricted to the period 1995–2010, with 5-year intervals, instead of the original 1990–2015 span. The validity of this lagged instrumental variable, however, can be violated if there exists serial correlations in the income variable and the error term (Ahlfeldt et al., 2020). The second concern relates to the migration flows data, as the country-sector level migration flows data is constructed based on assumptions at the sectoral level (see Appendix D.2 for details). While this may introduce noise in the dependent variable, the measurement error does not induce bias if the measurement error is independent of the regressors (Greene, 2017). Given the inherent challenges in estimating migration elasticity for global migration flows, results should be interpreted with caution.

Table 4 reports the estimated migration elasticity ($1/\nu$) ranging from 0.118 to 0.281. Consistent with findings in Artuç et al. (2010), the IV regression yields higher estimates than OLS. Migration elasticity is estimated using the full set of migration flows (columns 1-2), and additionally only for domestic migration flows (columns 3-4).²² The migration elasticity for domestic migration flows ($\nu = 3.564$) is higher than that for the full dataset ($\nu = 7.864$), suggesting greater responsiveness of domestic sectoral migration compared to international migration flows. Given that population

²¹For derivation of equation (48), see Appendix D.3

²²The entire pair of migration share data is constructed as 57,600 combinations: 60 countries \times 60 countries \times 2 sectors \times 2 sectors \times 4 periods. The domestic migration flows correspond to the case with $n = m$.

changes are primarily driven by domestic sectoral migration, while international migration remains relatively limited, a baseline value of $\nu = 4$ is chosen for the analysis. Alternative values are explored in the sensitivity analysis in section 6.3.

6 Results

6.1 Impact of Climate Change on the Agricultural Sector

Structural Transformation — The analysis begins by examining the labor market consequences, with a particular focus on the share of agricultural employment, a key measure of structural transformation. Figure 5a depicts the simulated time path of employment shares in the agriculture sector, aggregated at 18 sub-regions, under the baseline climate change scenario RCP 8.5. The figure shows historical data for the period 1990–2020, with model simulation results extending beyond 2020. The model predicts a consistent and gradual decline in agricultural employment shares across most regions, indicating a structural transformation from agriculture to non-agriculture, driven by sectoral labor mobility. Notable declines in agricultural employment are projected in regions such as Eastern and Middle Africa, and South-eastern Asia. In contrast, Southern Africa and South America deviate from this pattern, with labor reallocating back to the agricultural sector, reflecting a trend of *reverse* structural transformation.²³ These results should be interpreted in light of the model being quantified conditional on the initial period observations, specifically, migration flows $\mu_{-1}^{ns,mz}$ defined over 2015–2019. A sharp decline in agricultural employment share during 2015–2019 suggests that these regions faced a large income gap between agricultural and non-agricultural sectors, combined with relatively low migration frictions, resulting in a strong force of labor reallocation continued in subsequent periods. Conversely, in regions displaying the opposite trend of structural transformation in the model simulation periods, this pattern is consistent with observed migration flows back into the agricultural sector during 2015–2019.

The structural model provides a framework to analyze how climate change shocks affect labor markets within a general equilibrium context. Figure 5b illustrates the percentage point (p.p.) change in the share of agricultural workers under the RCP 8.5 climate scenario, relative to an economy not exposed to the shock, aggregated at the 18 sub-regional level. By 2100, the change in the share of agricultural employment ranges from a decline of 0.719 p.p. to an increase of 0.239 p.p. Notably, regions such as Northern Africa (−0.719 p.p.) and Western Africa (−0.239 p.p.) exhibit a lower agricultural employment share due to the climate change shock, suggesting that structural transformation out of agriculture could be accelerated by negative income shocks in these areas. Conversely, regions such as Central Asia (+0.239 p.p.) and Southern Africa (+0.175 p.p.) are projected to experience an increase in agricultural employment share under the same scenario, implying that positive income shocks in the agricultural sector could slow the pace of structural transformation.

²³In Figure 5a, Northern Africa also shows a slight increase in the agricultural employment share, though this pattern is driven by sub-regional aggregation; at the country level, the agricultural employment share declines over time.

Welfare Effects — The next step involves quantifying the welfare consequences of the climate change shock on the agricultural sector. Following [Caliendo et al. \(2019\)](#), the consumption equivalent variation is employed to measure welfare changes. At time $t = 0$, the consumption equivalent variation in the labor market ns , \mathcal{Q}^{ns} , is defined such that

$$\tilde{V}_0^{ns} - V_0^{ns} = \sum_{t=0}^{\infty} \beta^t \log(\mathcal{Q}^{ns}), \quad (49)$$

where \tilde{V}_0^{ns} denotes the expected lifetime utility of an alternative or counterfactual scenario, and V_0^{ns} is that of the baseline scenario. The consumption equivalent variation then reduces to the following expression²⁴:

$$\hat{W}^{ns} = \log(\mathcal{Q}^{ns}) = \sum_{t=1}^{\infty} \beta^t \log \left(\frac{\hat{C}_t^{ns}}{(\hat{\mu}_t^{ns,ns})^\nu} \right), \quad (50)$$

where $\hat{C}_t^{ns} = (\tilde{C}_t^{ns}/C_t^{ns}) / (\tilde{C}_{t-1}^{ns}/C_{t-1}^{ns})$ and $\hat{\mu}_t^{ns,ns} = (\tilde{\mu}_t^{ns,ns}/\mu_t^{ns,ns}) / (\tilde{\mu}_{t-1}^{ns,ns}/\mu_{t-1}^{ns,ns})$, with \tilde{x} notation referring to the corresponding variables in the alternative scenarios. Given that the percent change is a linear approximation of logarithmic difference for $\mathcal{Q}^{ns} \simeq 1$, the welfare measure \hat{W}^{ns} can be interpreted as the percentage changes in consumption.

Figure 6 presents the welfare effects of climate change under the RCP 8.5 scenario on workers in the agricultural sector. Specifically, Figure 6a shows the welfare effects of climate change on an economy under RCP 8.5, relative to an economy without climate change shocks, using a benchmark model that incorporates labor mobility. The global aggregate welfare effect of climate change on agricultural workers is around 0.01%, calculated by weighting the agricultural worker populations across countries in the year 2020. While this aggregate figure might suggest limited damage from climate change to agricultural workers globally, there is substantial spatial heterogeneity across countries, with effects ranging from -1.23% to $+3.85\%$. Australia (-1.23%), Cambodia (-1.14%), and countries in northern Africa (-1.01%) experience the most significant welfare losses, whereas Mongolia ($+3.85\%$), Norway ($+3.10\%$), Canada ($+2.16\%$), and Russia ($+1.95\%$) see welfare gains from climate change. The welfare effects for workers in the non-agricultural sector are relatively small compared to those in the agricultural sector, as agricultural consumption accounts for a small fraction of income in most countries (see Figure E.1 in the Appendix).

The evolving comparative advantage in crop production over time is reflected in the transition of land share allocated for different crops, as depicted for major countries in Figure 7-9. Notable shifts in land share are projected in some countries: In North America, the United States is expected to increase its share dedicated to wheat, while reducing the land share for maize and soybeans. In South America, both Brazil and Argentina are projected to allocate less land to soybeans, which currently occupy the largest land share, while the land share devoted to maize expands over time. Despite these adjustments, most countries in South America are projected to experience reduced welfare due to climate change. In Europe, Ukraine, a major agricultural producer, is expected to steadily increase its land share in wheat, reflecting a growing comparative advantage in wheat production. In Asia and Oceania, a notable case is Australia, where land allocation remains relatively

²⁴For derivation, refer to Appendix A.2 in [Caliendo et al. \(2019\)](#).

stable, with over 90% of land dedicated to a single crop, wheat. This high degree of specialization, coupled with declining wheat yields and limited multicropping capacity, suggests that Australia's agricultural production may face the most severe negative welfare effects, with limited room for adaptation under the baseline RCP8.5 scenario. High specialization in a single crop does not always lead to negative welfare outcomes. For instance, Mongolia, which also dedicates over 90% of its land to wheat, is expected to experience the greatest welfare gains among the countries studied.

The country-level welfare effects examined in this analysis are relatively modest compared to findings in previous studies ([Costinot et al., 2016](#); [Gouel and Laborde, 2021](#)). In these studies, welfare changes are reported as a percentage of GDP by obtaining equivalent variation, ranging from -49.07% to 1.43% ([Costinot et al., 2016](#)), and from -14.59% to 15.76% ([Gouel and Laborde, 2021](#)). Several factors likely contribute to this discrepancy. First, this study quantifies welfare effects within a dynamic framework, in which climate change shocks unfold incrementally in five-year intervals, allowing gradual market adjustments through production, trade, and labor reallocation. In contrast, previous studies evaluated climate change shocks within a static framework, where a sudden productivity shock is introduced at the 2071-2100 (2080s) level. Notably, labor market adjustments with bilateral migration frictions are explicitly modeled here—an aspect abstracted from earlier analyses. Furthermore, while previous studies assume a Leontief production structure that precludes any substitution among inputs (land and labor), this study employs a Cobb-Douglas production function that permits substitution among land, labor, and intermediate inputs. Consequently, when land productivity is negatively affected by climate change, farmers can adjust by increasing their use of labor or other intermediate inputs. With all market adjustment mechanisms—production, trade, and labor reallocation—in place, the general equilibrium effects of climate change on the agricultural sector can be more modest than previous studies have indicated.

To examine the role of labor mobility under climate change shocks, Figure 6b, displays the welfare effects of climate change under RCP 8.5, as in the previous figure, but without allowing labor mobility. Labor is assumed to remain fixed at its level of initial period across all countries and sectors. A comparison between Figures 6a and 6b reveals that restricting labor mobility significantly amplifies the welfare impact: countries experiencing worsening conditions under climate change deteriorate significantly without mobility, while those benefiting from climate change see markedly enhanced gains in the absence of mobility. Specifically, country-level welfare effects range from -5.16% to +7.46% when labor mobility is not allowed. This outcome reflects households' ability to respond to both positive and negative income shocks from climate change by relocating toward more attractive labor markets and away from less attractive ones. In the absence of this adjustment mechanism, welfare impacts become more pronounced. These results highlight the critical role of labor mobility in mitigating the adverse effects of climate change and suggest that abstracting from labor market adjustments may lead to an overestimation of its impacts.

6.2 Policy Analysis

Migration Costs — The key parameters related to labor mobility are bilateral migration costs, which encompass not only economic but also institutional, political, and cultural barriers. A useful approach to analyzing the implications of migration policy is to examine counterfactual scenarios on different migration costs. In this analysis, I consider counterfactual scenarios where all or some of the migration costs become infinitely high, thereby restricting labor mobility. Outcomes are then compared between two economies with different migration costs, with all else held equal, including the presence of climate change shocks. Welfare effects are again measured in terms of consumption equivalent variation. Details on the derivation for counterfactual analysis are provided in the Appendix B.3.

Before introducing the counterfactual results, it is useful to revisit the Bellman equation. Rearranging the equation (6) and taking expectation over a vector ϵ_t , it follows

$$V_t^{ns} = u_t^{ns} + \beta V_{t+1}^{ns} + \underbrace{\mathbb{E}_t \left[\max_{m \in \mathcal{N}, z \in \mathcal{S}} \left\{ \beta V_{t+1}^{mz} - \beta V_{t+1}^{ns} - \zeta^{ns,mz} + \nu \epsilon_t^{mz} \right\} \right]}_{\equiv \mathcal{O}_t^{ns}}. \quad (51)$$

The above equation shows that the expected lifetime utility of a household in the labor market ns consists of three components; current period utility (u_t^{ns}), base value of staying the same labor market (βV_{t+1}^{ns}), and the value of moving to a potentially better labor market (\mathcal{O}_t^{ns}). The last component has been called the *option value* in the literature (Artuç et al., 2010). Assuming there is no cost staying in the same labor market ($\zeta^{ns,ns} = 0$), it follows $\mathcal{O}_t^{ns} \geq 0$, implying that the possibility of labor mobility in future periods itself can generate welfare gains. However, the net welfare effect of migration depends on both the second and third terms, as labor mobility can also alter the prospects of all labor markets, including the current one.

The first counterfactual analysis examines the welfare effects of baseline labor mobility. This is done by comparing an economy with baseline labor mobility—both cross-country and cross-sector migration at the current level of migration costs—to an economy where labor mobility is entirely restricted, i.e., $\zeta^{ns,mz} \rightarrow \infty$ for all n, s, m, z . Figure 10a shows the welfare effects of labor mobility for workers in the agricultural sector, revealing a global aggregate welfare effect of 14.24%. Substantial welfare gains are projected for countries such as Vietnam (42.65%), the Philippines (30.71%), and China (26.42%), which are countries with relatively high mobility flows out of the agricultural sector. Conversely, countries like Italy (-39.05%), Peru (-35.14%), and Southern Africa (-33.61%) experience welfare losses among agricultural workers as a result of labor mobility. The welfare outcomes are closely related to the model’s assumption that income is defined as sector-specific GDP per capita, with decreasing returns to labor in agricultural production. In labor markets experiencing net outflows (encompassing both domestic and international flows), the base value of remaining in the same market increases as the population in that market declines over time, thereby increasing per capita income; the opposite holds for markets with net inflows. Notably, agricultural workers in countries such as the US, Canada, and Russia experience welfare losses due to labor mobility, despite the agricultural sector in these countries facing domestic net

outflows in the initial period. This occurs because the positive income shock from climate change attracts more labor into the agricultural sector over time, resulting in lower per capita income for agricultural workers in these countries compared to an economy without mobility.

The second counterfactual analysis focuses on the welfare effects of domestic structural transformation. In this scenario, cross-country migration is prohibited, but households can still migrate between sectors domestically. Specifically, domestic sectoral migration costs remain at their current levels, while cross-country migration costs become infinitely high, i.e., $\zeta^{ns,mz} \rightarrow \infty$ for all $n \neq m$, due to a sudden shock in the initial period ($t = 0$). Welfare effects are then similarly examined by comparing an economy with only domestic sectoral labor mobility to one where labor mobility is entirely restricted. Figure 10b shows the welfare effects of allowing domestic labor mobility for agricultural workers are close to the earlier results in Figure 10a. This outcome aligns with the empirical observation in Figure 3a that a large share of labor mobility occurs through domestic sectoral switches rather than cross-country migration. A comparison of welfare effects under baseline mobility and domestic-only mobility is displayed in Figure E.2 in the appendix. Although the welfare effects are highly correlated across the two scenarios, they are slightly higher under the domestic-only mobility scenario for many countries. This result may seem counterintuitive, as restricting mobility options is likely to reduce the option value. This outcome arises because the domestic-only mobility scenario can increase the base value of remaining in the same labor market, leading to higher net welfare effects. For instance, consider a country with net domestic outflows in the agricultural sector—without the possibility of international inflows, the agricultural sector population under the domestic-only mobility scenario can fall below the levels projected under the baseline mobility scenario. Consequently, per capita income for agricultural workers could be higher under the domestic-only mobility scenario in equilibrium, raising the base value of remaining in the same labor market despite restricted mobility options.

Different model assumptions about income redistribution may affect the quantitative magnitude of welfare outcomes, but the primary insight from this policy analysis is that labor mobility has a substantial welfare impact for workers in the agricultural sector—potentially even exceeding the welfare impact of climate change shocks (RCP8.5) itself in many countries. Furthermore, the welfare gains from labor mobility are driven largely by domestic sectoral mobility rather than international migration. This does not mean that international mobility is not effective in improving welfare consequences; rather, it reflects that, given the higher costs associated with international migration compared to domestic cross-sector mobility, the option value of switching sectors can yield much larger welfare gains than the option value of moving across countries. The large welfare gains from labor mobility also reflect a substantial income gap between the agricultural and non-agricultural sectors, suggesting that addressing the systematic and prevalent sectoral income inequality around the world remains an important task, alongside efforts to tackle climate change. Facilitating labor mobility, particularly through structural transformations away from agriculture toward other sectors, appears crucial in mitigating the welfare impacts of climate change shocks for those working in the agricultural sector. This finding aligns with recent studies, such as [Cruz and Rossi-Hansberg \(2023\)](#), in highlighting labor adjustment as a critical adaptation mechanism

against climate change, while offering a complementary perspective that emphasizes the essential role of structural transformation over cross-country geographical migration.

6.3 Sensitivity Analysis

Other Climate Scenarios — While the model simulation uses the RCP 8.5 scenario from HadGEM2-ES as the baseline, I also conduct welfare analysis with other climate scenarios. Five climate scenarios are available for RCP 4.5 and RCP 8.5, respectively, from the following models: GFDL-ESM2M, HadGEM2-ES, IPSL-CM5A-LR, MIROC-ESM-CHEM, and NorESM1-M. The welfare effects of these climate scenarios are provided in the Appendix E.2. Overall, the welfare effects are similar across different climate models, although a few countries, such as Australia, exhibit somewhat varying welfare predictions across scenarios. Additionally, the welfare effects are analyzed separately for yield shocks and multicropping shocks under the baseline RCP 8.5 (HadGEM2-ES) scenario to assess the individual contribution of each shock. See Table 8 for details.

Behavioral Parameters — The sensitivity of the quantitative results to the migration elasticity parameter is examined in Appendix E.3. Welfare outcomes are compared across different migration elasticity values, showing qualitatively similar patterns. A higher ν leads to labor reallocation less responsive to income shocks, resulting in a slightly more amplified distribution of welfare effects.

7 Conclusion

This paper evaluates the impact of climate change shocks on agricultural production by quantifying a dynamic spatial general equilibrium model that incorporates three key market adjustment mechanisms: farmers' crop choice, international trade, and forward-looking dynamic labor reallocation. Findings indicate that, under RCP 8.5, the overall global welfare effect on agricultural workers may remain modest; however, welfare effects vary substantially across countries. The results also highlight labor mobility as a crucial adjustment mechanism in response to climate change shocks. When labor mobility is restricted, the welfare impacts of climate change are amplified in both positive and negative directions. This study's emphasis on labor reallocation complements previous research highlighting the role of market adjustments through crop choice and international trade against climate change shocks (Costinot et al., 2016; Gouel and Laborde, 2021). Finally, counterfactual analysis of migration costs shows that labor mobility brings welfare gains for agricultural workers in most countries. Given current migration frictions, these welfare gains are largely driven by domestic sectoral labor mobility rather than international mobility. This finding suggests that facilitating structural transformation out of agriculture in developing economies—many of which are likely to experience negative income shocks in the agricultural sector—could serve as an important mitigation strategy against potential adverse impacts of climate change.

This study primarily focuses on the effects of climate change shocks on agriculture, while abstracting from certain factors that could be explored in future work. For instance, it does not account for land use changes across sectors, such as conversions between forests, croplands, and

urban areas, which could be integrated into future research. Additionally, the climate change shocks derived from GAEZ data capture average trends in agro-climatic conditions but do not incorporate volatility from extreme events such as floods, typhoons, and other natural disasters. The findings of this study indeed suggest that, while the impact of climate change could remain within a modest range with gradual shifts in agro-climatic conditions and full market adjustments in production, trade, and labor reallocation, the emerging priority could be addressing the heightened risks associated with extreme weather events in the agricultural sector. Modeling these events would involve introducing uncertainty, similar to the stochastic approaches as in [Cai et al. \(2017\)](#) and [Cai and Lontzek \(2019\)](#), though this may present challenges such as the ‘curse of dimensionality’ in complex multi-country, multi-sector models. Extending this dynamic spatial framework to incorporate these and other economic dimensions could offer valuable insights in future studies.

References

- Abel, G. J. and Cohen, J. E. (2019). Bilateral international migration flow estimates for 200 countries. *Scientific Data*, 6(1):82.
- Adamopoulos, T., Brandt, L., Chen, C., Restuccia, D., and Wei, X. (2024). Land Security and Mobility Frictions*. *The Quarterly Journal of Economics*, 139(3):1941–1987.
- Ahlfeldt, G. M., Bald, F., Roth, D., and Seidel, T. (2020). Quality of Life in a Dynamic Spatial Model. Technical Report 3751857, Rochester, NY.
- Andreoni, A. and Tregenna, F. (2021). The Middle-Income Trap and Premature Deindustrialization in South Africa. In *Structural Transformation in South Africa: The Challenges of Inclusive Industrial Development in a Middle-Income Country*. Oxford University Press.
- Armington, P. S. (1969). A Theory of Demand for Products Distinguished by Place of Production (Une théorie de la demande de produits différenciés d'après leur origine) (Una teoría de la demanda de productos distinguiéndolos según el lugar de producción). *Staff Papers (International Monetary Fund)*, 16(1):159–178.
- Artuç, E., Chaudhuri, S., and McLaren, J. (2010). Trade Shocks and Labor Adjustment: A Structural Empirical Approach. *American Economic Review*, 100(3):1008–1045.
- Bilal, A. and Rossi-Hansberg, E. (2023). Anticipating climate change across the united states. Working Paper 31323, National Bureau of Economic Research.
- Burzyński, M., Deuster, C., Docquier, F., and de Melo, J. (2022). Climate Change, Inequality, and Human Migration. *Journal of the European Economic Association*, 20(3):1145–1197.
- Cai, Y., Judd, K. L., and Lontzek, T. S. (2017). The social cost of carbon with economic and climate risks. Hoover Economics Working Paper 18113, Hoover Economics.
- Cai, Y. and Lontzek, T. S. (2019). The social cost of carbon with economic and climate risks. *Journal of Political Economy*, 127(6):2684–2734.
- Caliendo, L., Dvorkin, M., and Parro, F. (2019). Trade and Labor Market Dynamics: General Equilibrium Analysis of the China Trade Shock. *Econometrica*, 87(3):741–835.
- Caliendo, L., Opronolla, L. D., Parro, F., and Sforza, A. (2021). Goods and Factor Market Integration: A Quantitative Assessment of the EU Enlargement. *Journal of Political Economy*, 129(12):3491–3545.
- Cattaneo, C. and Peri, G. (2016). The migration response to increasing temperatures. *Journal of Development Economics*, 122:127–146.
- Conte, B. (2022). Climate Change and Migration: The Case of Africa. Technical Report 4226415, CESifo Working Paper No. 9948, Rochester, NY.
- Conte, B., Desmet, K., Nagy, D. K., and Rossi-Hansberg, E. (2021). Local sectoral specialization in a warming world. *Journal of economic geography*, 21(4):493–530.
- Costinot, A., Donaldson, D., and Smith, C. (2016). Evolving Comparative Advantage and the Impact of Climate Change in Agricultural Markets : Evidence from 1.7 Million Fields around the World. *Journal of Political Economy*, 124(1):205–248.

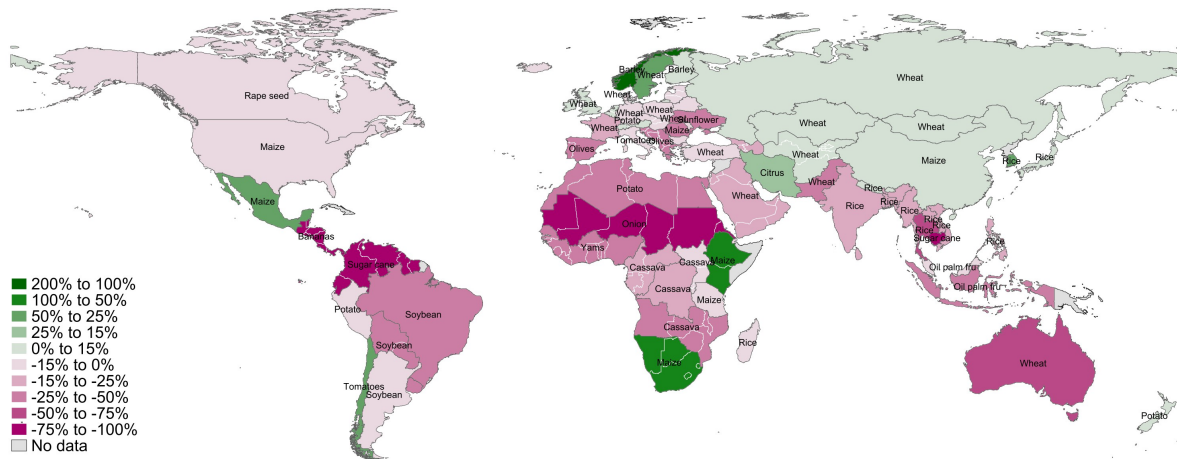
- Cruz, J. L. (2023). Global warming and labor market reallocation. *unpublished manuscript*.
- Cruz, J.-L. and Rossi-Hansberg, E. (2023). The economic geography of global warming. *The Review of Economic Studies*, 91(2):899–939.
- Dasgupta, S. and Singh, A. (2006). Manufacturing, services and premature deindustrialization in developing countries. Technical Report 049, Helsinki, Finland.
- Dekle, R., Eaton, J., and Kortum, S. (2007). Unbalanced Trade. *American Economic Review*, 97(2):351–355.
- Dekle, R., Eaton, J., and Kortum, S. (2008). Global Rebalancing with Gravity: Measuring the Burden of Adjustment. *IMF Staff Papers*, 55(3):511–540.
- Desmet, K., Kopp, R. E., Kulp, S. A., Nagy, D. K., Oppenheimer, M., Rossi-Hansberg, E., and Strauss, B. H. (2021). Evaluating the Economic Cost of Coastal Flooding. *American Economic Journal: Macroeconomics*, 13(2):444–486.
- Desmet, K., Nagy, D. K., and Rossi-Hansberg, E. (2018). The Geography of Development. *Journal of Political Economy*, 126(3):903–983.
- Desmet, K. and Rossi-Hansberg, E. (2015). On the spatial economic impact of global warming. *Journal of Urban Economics*, 88:16–37.
- Eaton, J. and Kortum, S. (2002). Technology, Geography, and Trade. *Econometrica*, 70(5):1741–1779.
- Farrokhi, F. and Pellegrina, H. S. (2023). Trade, technology, and agricultural productivity. *Journal of Political Economy*, 131(9):2509–2555.
- Fischer, G., Nachtergaele, F., van Velthuizen, H., Chiozza, F., Franceschini, G., Henry, M., Mu-choney, D., and Tramberend, S. (2021). *Global Agro-Ecological Zones v4 – Model documentation*. FAO, Rome, Italy.
- Fuglie, K. (2015). Accounting for growth in global agriculture. *Bio-based and Applied Economics*, 4(3):201–234.
- Fuglie, K. O., Morgan, S., Jelliffe, J., and United States. Department of Agriculture. Economic Research Service, i. b. (2024). World agricultural production, resource use, and productivity, 1961–2020.
- Gollin, D. (2023). Agricultural productivity and structural transformation: evidence and questions for african development. *Oxford Development Studies*, 51(4):375–396.
- Gollin, D., Lagakos, D., and Waugh, M. E. (2014). The Agricultural Productivity Gap. *The Quarterly Journal of Economics*, 129(2):939–994.
- Gouel, C. and Laborde, D. (2021). The crucial role of domestic and international market-mediated adaptation to climate change. *Journal of Environmental Economics and Management*, 106:102408.
- Greene, W. H. (2017). *Econometric Analysis*. Pearson, Upper Saddle River, NJ, 8th edition. © 2018.

- Herendorf, B., Rogerson, R., and Valentinyi, A. (2013). Two perspectives on preferences and structural transformation. *American Economic Review*, 103(7):2752–89.
- Herendorf, B., Rogerson, R., and Ákos Valentinyi (2014). Chapter 6 - growth and structural transformation. In Aghion, P. and Durlauf, S. N., editors, *Handbook of Economic Growth*, volume 2 of *Handbook of Economic Growth*, pages 855–941. Elsevier.
- Herendorf, B. and Schoellman, T. (2018). Wages, human capital, and barriers to structural transformation. *American Economic Journal: Macroeconomics*, 10(2):1–23.
- Imbert, C. and Papp, J. (2020). Costs and benefits of rural-urban migration: Evidence from India. *Journal of Development Economics*, 146:102473.
- KC, S. and Lutz, W. (2017). The human core of the shared socioeconomic pathways: Population scenarios by age, sex and level of education for all countries to 2100. *Global Environmental Change*, 42:181–192.
- Kleinman, B., Liu, E., and Redding, S. J. (2023). Dynamic spatial general equilibrium. *Econometrica*, 91(2):385–424.
- Lagakos, D., Mobarak, A. M., and Waugh, M. E. (2023). The Welfare Effects of Encouraging Rural–Urban Migration. *Econometrica*, 91(3):803–837.
- Matsuyama, K. (1992). Agricultural productivity, comparative advantage, and economic growth. *Journal of Economic Theory*, 58(2):317–334.
- Munshi, K. and Rosenzweig, M. (2016). Networks and misallocation: Insurance, migration, and the rural-urban wage gap. *American Economic Review*, 106(1):46–98.
- Nath, I. B. (2023). The Food Problem and the Aggregate Productivity Consequences of Climate Change. Working Paper 27297, Working Paper.
- Ohio Supercomputer Center (1987). Ohio supercomputer center.
- Pellegrina, H. S. (2022). Trade, productivity, and the spatial organization of agriculture: Evidence from Brazil. *Journal of Development Economics*, 156:102816.
- Peri, G. and Sasahara, A. (2019). The Impact of Global Warming on Rural-Urban Migrations: Evidence from Global Big Data.
- Redding, S. J. (2016). Goods trade, factor mobility and welfare. *Journal of International Economics*, 101:148–167.
- Redding, S. J. and Rossi-Hansberg, E. (2017). Quantitative spatial economics. *Annual Review of Economics*, 9(Volume 9, 2017):21–58.
- Restuccia, D., Yang, D. T., and Zhu, X. (2008). Agriculture and aggregate productivity: A quantitative cross-country analysis. *Journal of Monetary Economics*, 55(2):234–250.
- Rodrik, D. (2016). Premature deindustrialization. *Journal of Economic Growth*, 21(1):1–33.
- Rudik, I., Lyn, G., Tan, W., and Ortiz-Bobea, A. (2022). The Economic Effects of Climate Change in Dynamic Spatial Equilibrium. *Conference papers*.

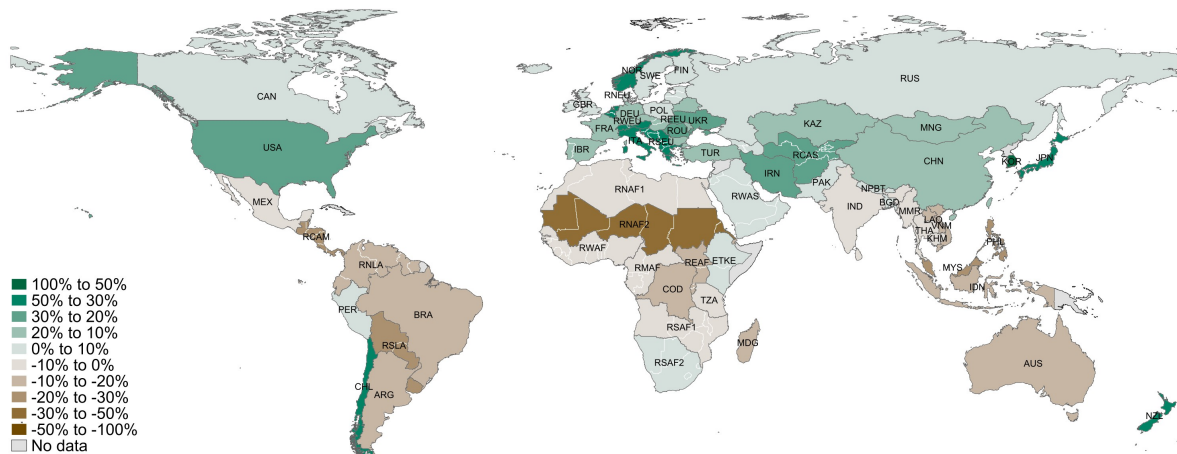
- Solow, R. M. (1956). A Contribution to the Theory of Economic Growth. *The Quarterly Journal of Economics*, 70(1):65–94.
- Sotelo, S. (2020). Domestic Trade Frictions and Agriculture. *Journal of Political Economy*, 128(7):2690–2738.
- Swan, T. W. (1956). Economic growth and capital accumulation. *Economic Record*, 32(2):334–361.
- Tombe, T. (2015). The Missing Food Problem: Trade, Agriculture, and International Productivity Differences. *American Economic Journal: Macroeconomics*, 7(3):226–258.
- Tombe, T. and Zhu, X. (2019). Trade, migration, and productivity: A quantitative analysis of china. *American Economic Review*, 109(5):1843–72.
- U.S. Department of Agriculture, Economic Research Service (2023). International agricultural productivity data product.
- Vollrath, D. (2009). How important are dual economy effects for aggregate productivity? *Journal of Development Economics*, 88(2):325–334.
- Zappala, G. (2024). Estimating sectoral climate impactsin a global production network. *Working Paper*.

Figures

Figure 1: Climate Change Shocks on Agricultural Production under RCP 8.5



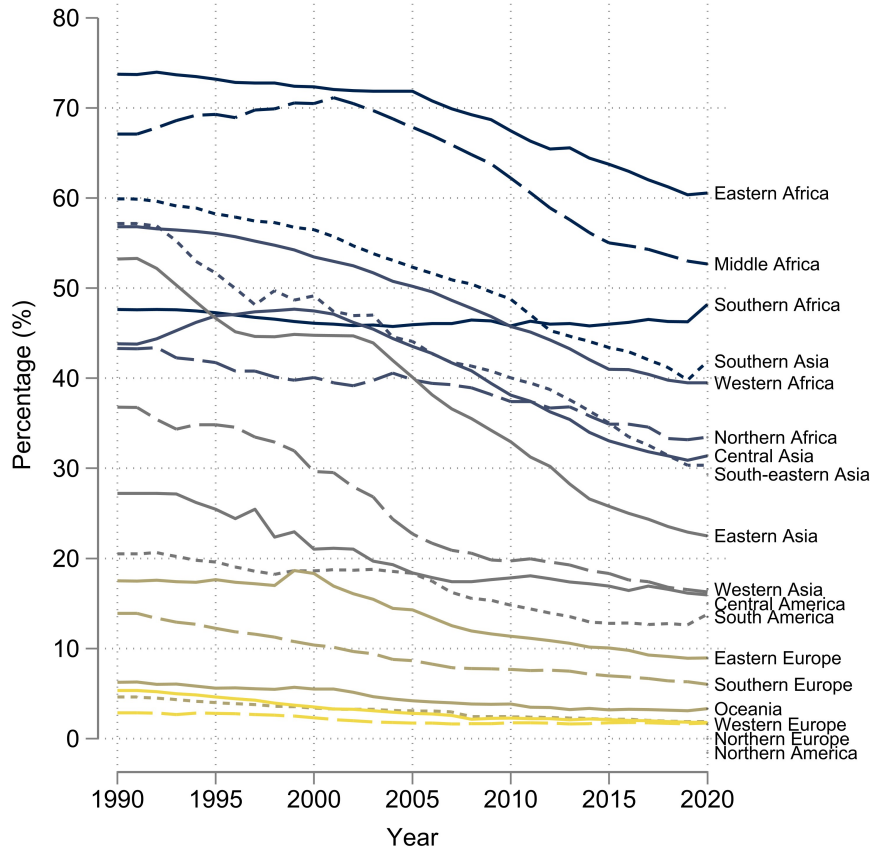
(a) Potential Changes in Yields of the Highest-Revenue Crops



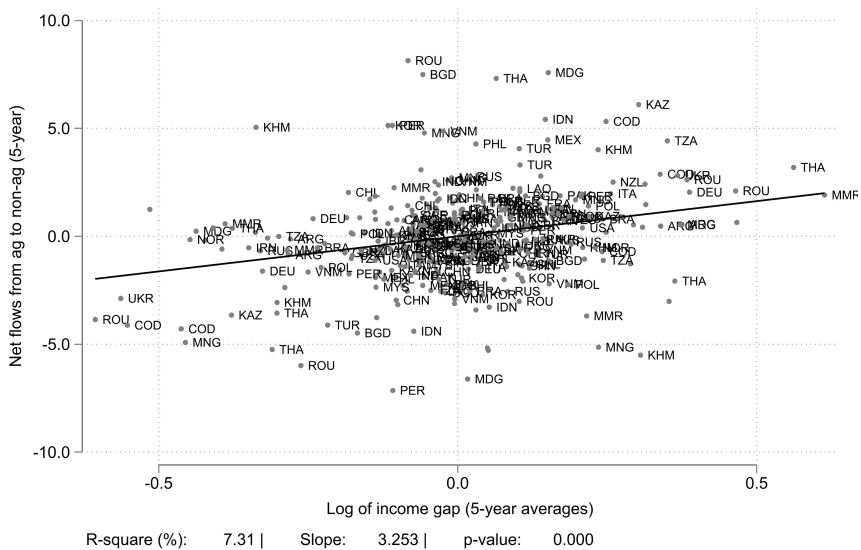
(b) Potential Changes in Multicropping Capacities

Notes: The above graphs illustrate the potential impact of climate change shock on agricultural production under the RCP 8.5 scenario (HadGEM2-ES). Figure 1a displays the potential yield changes by 2100 relative to 2020 for the highest-revenue crops in each country or region. Figure 1b shows the potential multicropping capacity changes by 2100 relative to 2020. For instance, a 10% value means a 10% increase in potential yield or multicropping capacity relative to the level of 2020. Both figures display the irrigation-adjusted values.

Figure 2: Structural Transformation in Labor Markets



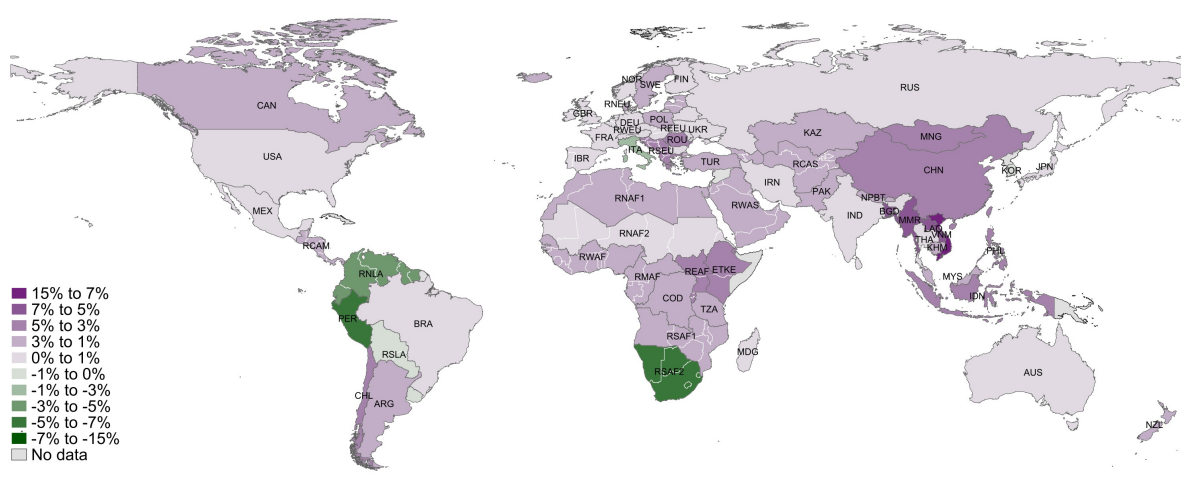
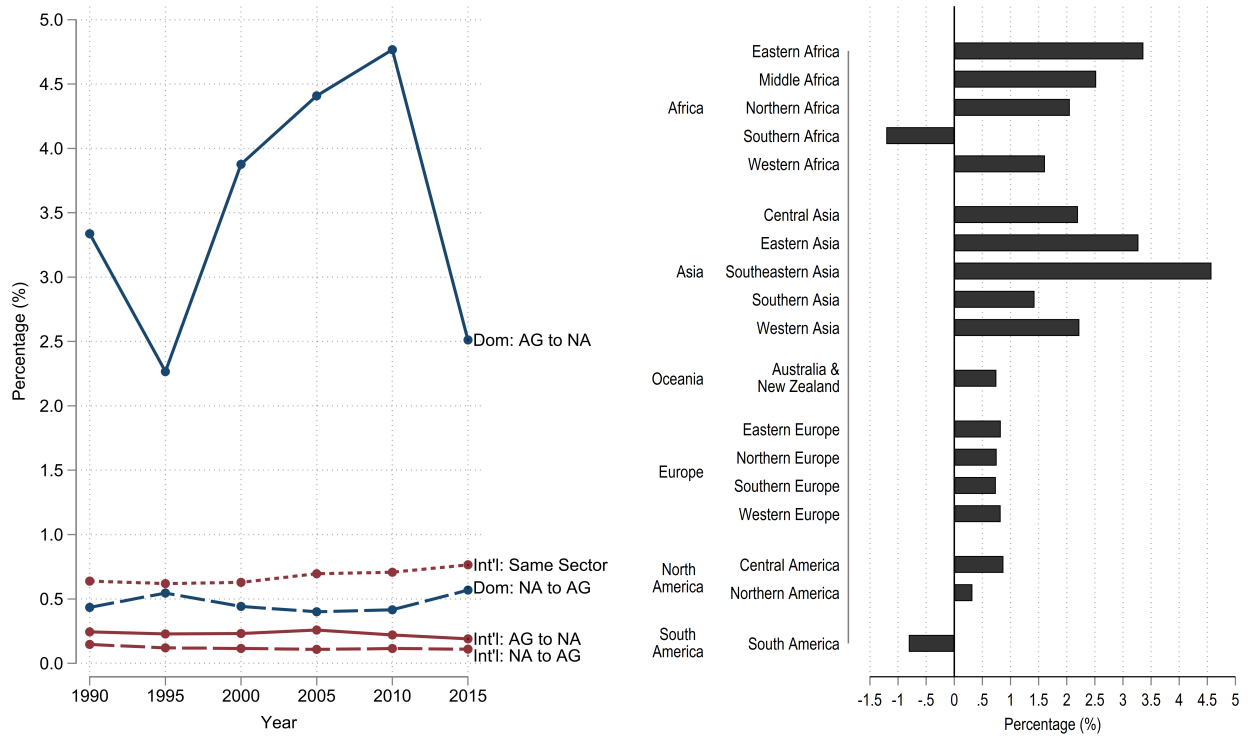
(a) Transition in the Share of Agricultural Employment



(b) Income Gap and Structural Transformation

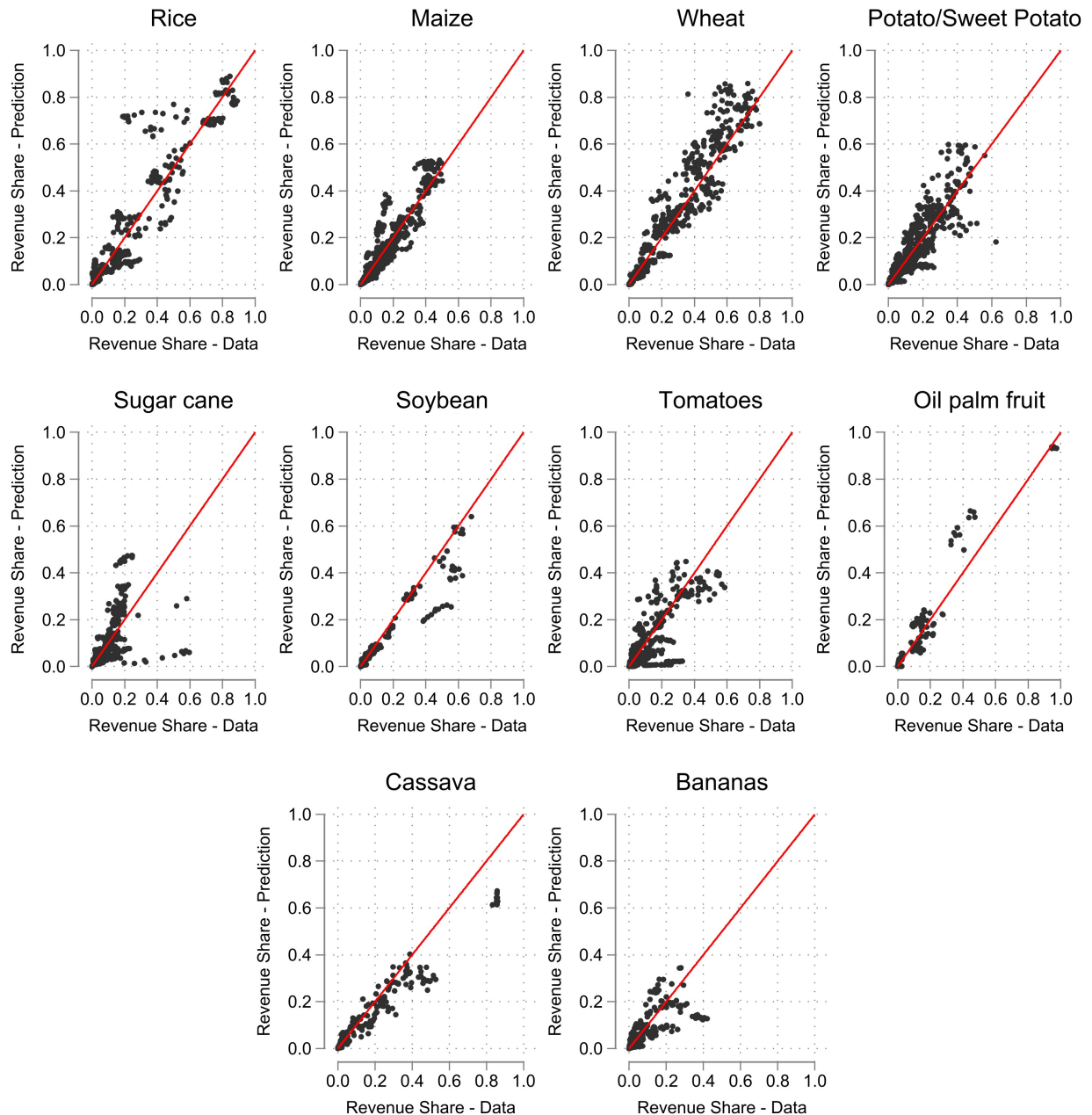
Notes: The graphs above together describe the empirical patterns of historical structural transformation around the world. Figure 2a displays the transition in the share of agricultural employment, aggregated by sub-regional groups, over the period 1990–2020. Figure 2b captures the cross-country relationship between the income gap and the share of domestic net migration flows from the agricultural to the non-agricultural sector for the period 1990–2015, with 5-year intervals, after controlling for year and country fixed effects.

Figure 3: Summary of Migration Flow Estimates



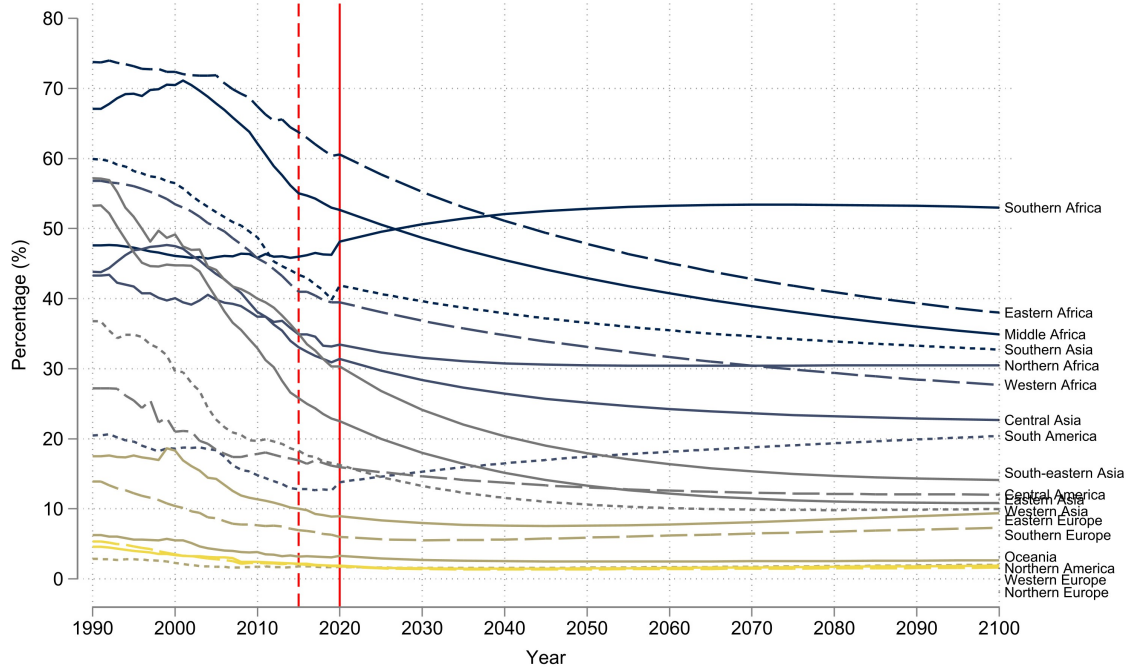
Notes: The graphs above summarize the expanded migration flow estimates. Figure 3a illustrates the percentage of migration flows across countries and sectors over 1990-2015, aggregated at the global level. Both Figure 3b and Figure 3c show the domestic net flows from agriculture to non-agriculture for the period 2015-2019, with Figure 3b presenting results aggregated across 18 sub-regions and Figure 3c presenting across 60 countries.

Figure 4: Fit of the Model–Factor Intensity of Land

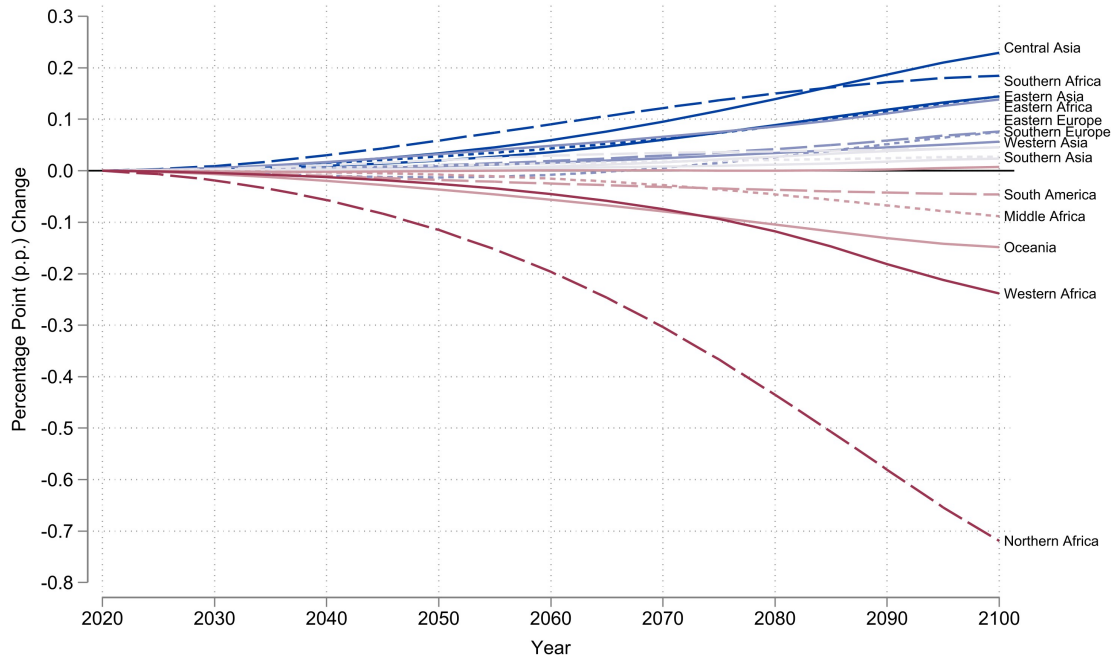


Notes: The figure depicts the fit of the model for factor intensity of land (γ^{nj}). The x-axis represents the observed revenue share (χ_t^{nj}) and x-axis shows the predicted revenue share ($\hat{\chi}_t^{nj}$) from equation (41), given the estimated land intensities and observed harvested share of land (π_t^{nj}). The regression employs country-level panel data from 2000 to 2020. The 45-degree line is shown in red.

Figure 5: Labor Market Effects under the RCP 8.5 Climate Change Scenario



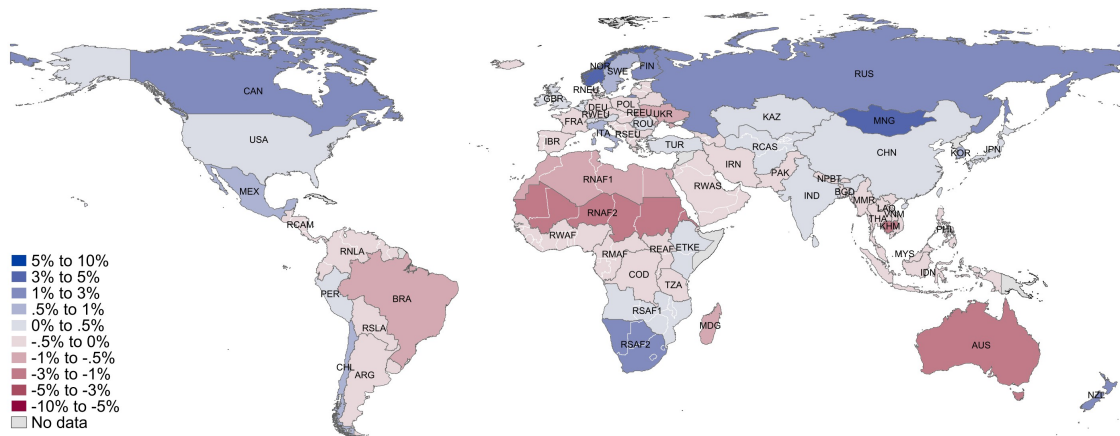
(a) Simulated Time Path of Agriculture Employment Share



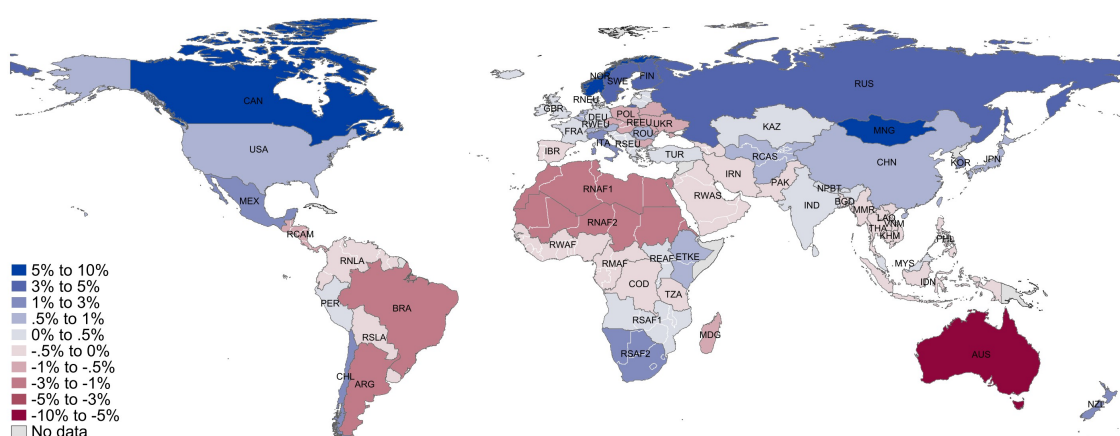
(b) Effects of Climate Change on Agricultural Employment Share

Notes: Figure 5a illustrates the agricultural employment share aggregated at the sub-regional level under the baseline scenario, assuming climate change scenario RCP8.5 (HadGEM2-ES), population scenario SSP2, and an inverse migration elasticity parameter $\nu = 4$. The period from 1990 to 2020 represents the actual historical agricultural employment share, while the post-2020 period shows simulation results. Figure 5b shows the percentage point change in the agricultural employment share under RCP 8.5 relative to the economy without climate change shocks.

Figure 6: The Welfare Effects of Climate Change Shock RCP8.5



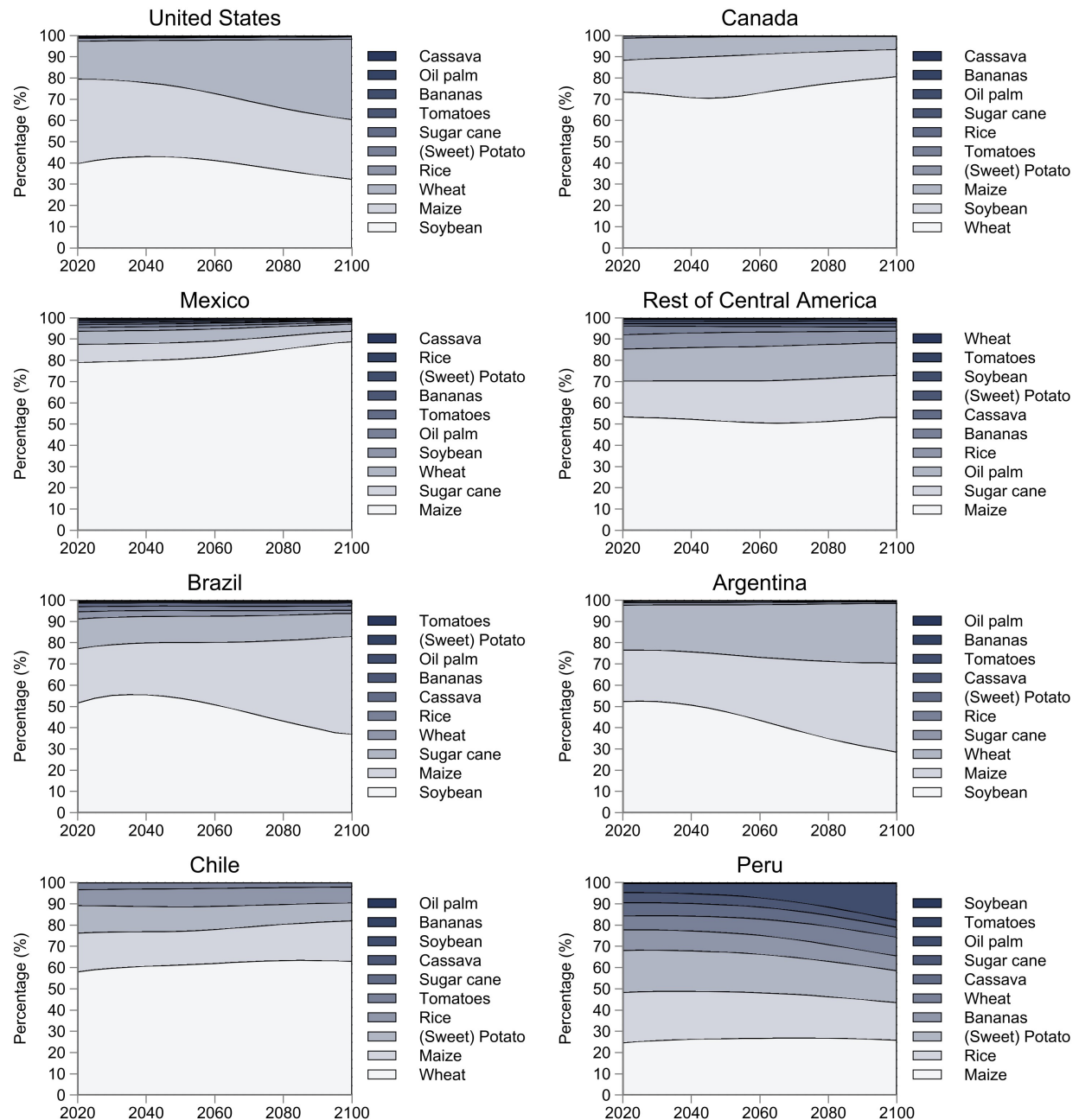
(a) Welfare Effects under Labor Mobility



(b) Welfare Effects under No Labor Mobility

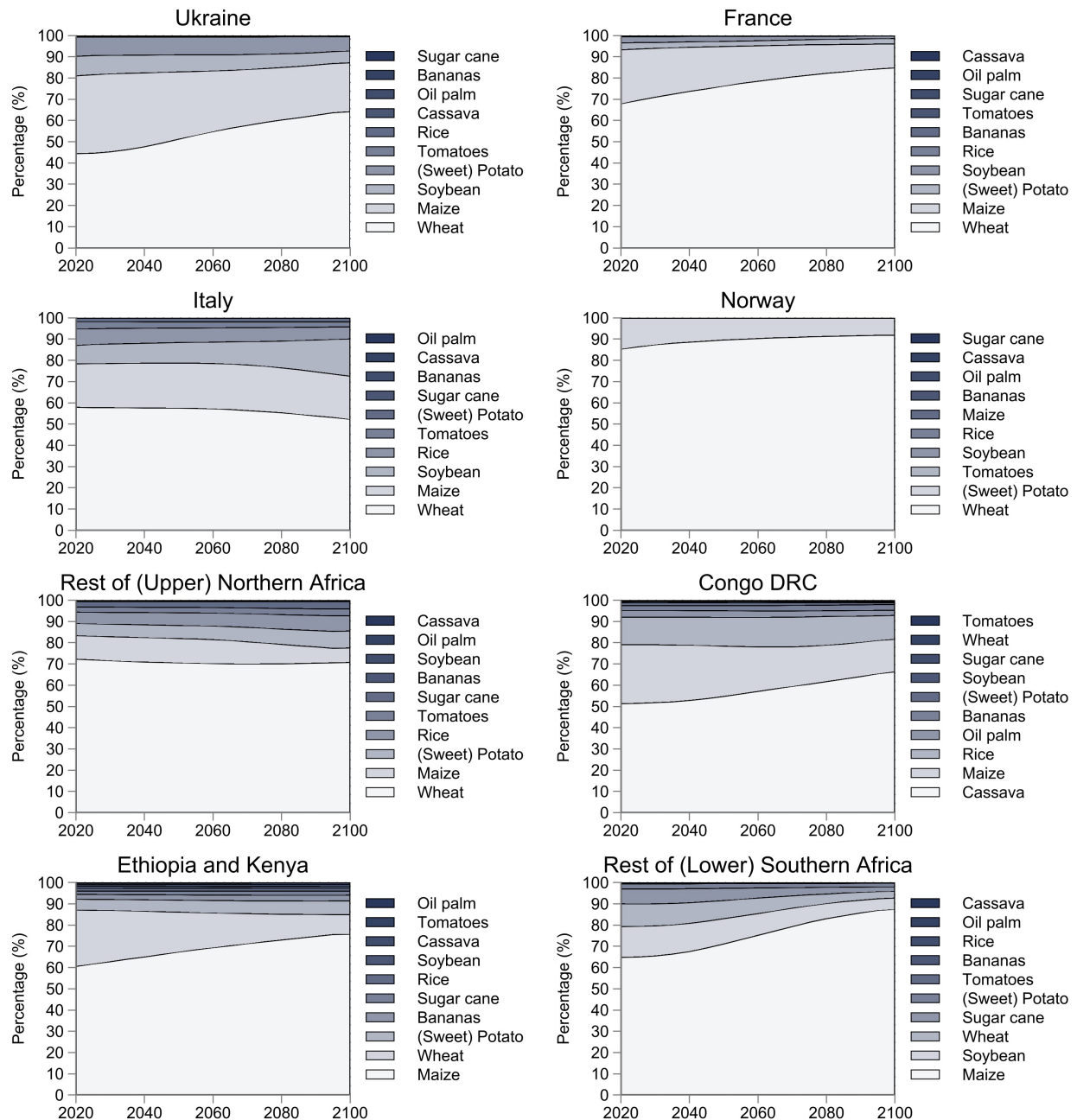
Notes: The figures above show the welfare effects of the climate change RCP 8.5 scenario (HadGEM2-ES), measured by the consumption equivalent variation for workers in the agriculture sector. Figure 6a shows the welfare effects of climate change on an economy under RCP 8.5, relative to an economy without climate change, when the model incorporates labor mobility. Figure 6b similarly depicts the welfare effects of climate change, when the model does not incorporate labor mobility.

Figure 7: Transition in Land Allocation Shares - North and South America



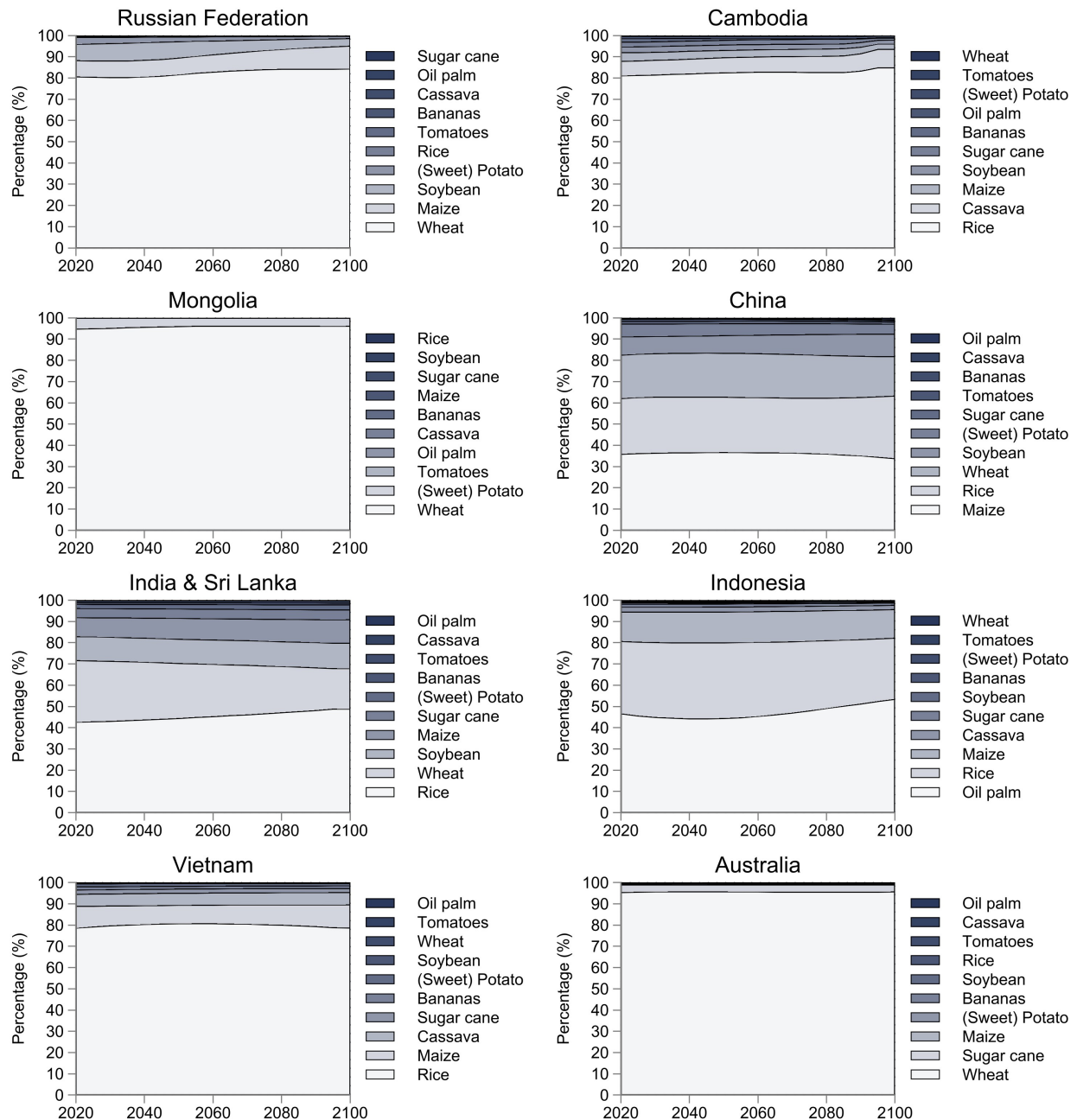
Notes: The figure shows the changes in land allocation shares for major countries under the baseline climate change scenario RCP 8.5 (HadGEM2-ES). The x-axis shows the years from 2020 to 2100, and the y-axis represents the stacked percentage share of land allocated to 10 crops. Crops are ordered such that one with the largest land share in 2020 appears in the lightest color, and those with smaller shares are represented in progressively darker colors.

Figure 8: Transition in Land Allocation Shares - Europe and Africa



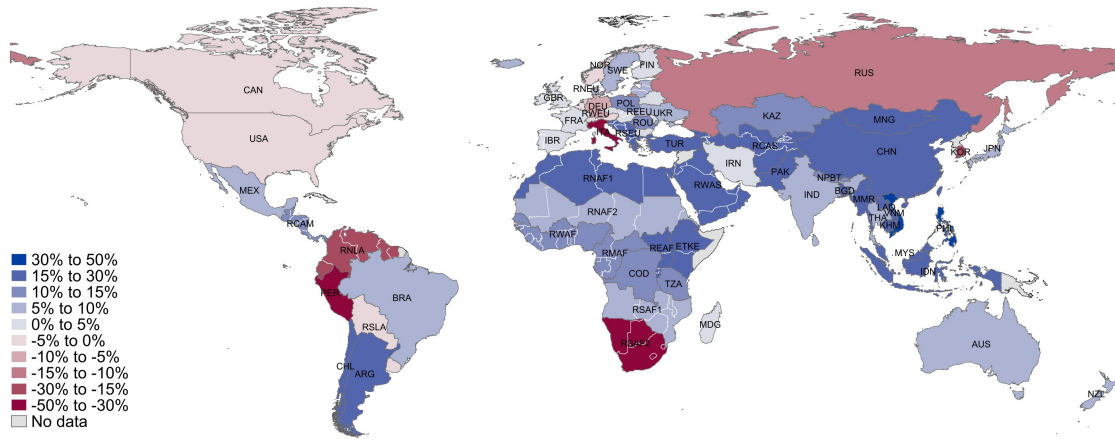
Notes: The figure shows the changes in land allocation shares for major countries under the baseline climate change scenario RCP 8.5 (HadGEM2-ES). The x-axis shows the years from 2020 to 2100, and the y-axis represents the stacked percentage share of land allocated to 10 crops. Crops are ordered such that one with the largest land share in 2020 appears in the lightest color, and those with smaller shares are represented in progressively darker colors.

Figure 9: Transition in Land Allocation Shares - Asia and Oceania

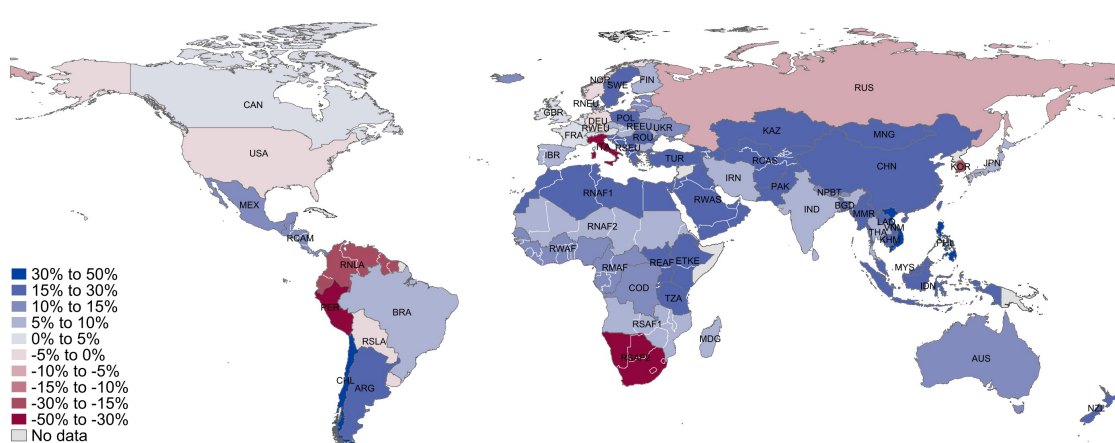


Notes: The figure shows the changes in land allocation shares for major countries under the baseline climate change scenario RCP 8.5 (HadGEM2-ES). The x-axis shows the years from 2020 to 2100, and the y-axis represents the stacked percentage share of land allocated to 10 crops. Crops are ordered such that one with the largest land share in 2020 appears in the lightest color, and those with smaller shares are represented in progressively darker colors.

Figure 10: The Welfare Effects of Migration Policies



(a) Effects of Labor Mobility across Countries and Sectors



(b) Effects of Domestic Labor Mobility across Sectors

Notes: The figures above show the welfare effects of labor mobility under the climate change RCP 8.5 scenario (HadGEM2-ES), measured by the consumption equivalent variation as percentage changes for agricultural workers. Figure 10a shows the welfare effects of labor mobility across both countries and sectors under the current level of migration frictions, relative to an economy with no labor mobility. Figure 10b presents the welfare effects of labor mobility under domestic sectoral mobility only, where within-country sectoral migration costs remain at their current level, relative to an economy with no labor mobility.

Tables

Table 1: Structural Model Parameters and Fundamental Variables

Parameter	Name	Value	Target/Source
<i>Preference</i>			
ϕ^n	consumption share of agricultural goods	...	FAO
δ	elasticity of substitution across origins	5.4	Costinot et al. (2016)
\varkappa	elasticity of substitution across crops	2.82	Costinot et al. (2016)
β	utility discount rate (quinquennial)	(0.96) ⁵	Caliendo et al. (2019)
<i>Production</i>			
$\alpha^{nj}, \gamma^{nj}, \gamma^{nj}$	factor intensity for agriculture	...	Estimation - Eq. (41) and Farrokhi and Pellegrina (2023)
θ	land allocation elasticity	1.38	Farrokhi and Pellegrina (2023)
ξ^n	labor intensity for non-agriculture	...	WIOD
\dot{A}_{t+1}^{nj}	Time differences: land productivity	...	GAEZ
\dot{H}_{t+1}^{nj}	Time differences: harvested areas	...	GAEZ
\dot{B}_{t+1}^n	Time differences: TFP in agriculture	1.056	Fuglie et al. (2024)
\dot{A}_{t+1}^{nM}	Time differences: TFP in non-agriculture	...	SSP2 (KC and Lutz, 2017)
<i>Population Dynamics</i>			
ν	inverse of migration elasticity	4.0	Estimation - equation (8)
g_t^n	population growth rate	...	SSP2 (KC and Lutz, 2017)

Notes: Exogenous shocks—including changes in land productivity, harvested areas, agricultural and non-agricultural TFP, and population growth—are applied through 2100, after which they remain constant.

Table 2: Estimation of Factor Intensity of Land

	$\log(\chi_t^{nj})$
$\log(\pi_t^{nj})$	0.951*** (0.025)
Crop Fixed Effects (b^j)	
- Bananas	0.522*** (0.116)
- Cassava	-0.363* (0.143)
- Maize	-1.464*** (0.108)
- Oil palm fruit	-0.138 (0.243)
- Potato and sweet potato	0 (.)
- Rice	-0.994*** (0.094)
- Soybean	-1.767*** (0.085)
- Sugar cane	0.0440 (0.175)
- Tomatoes	1.381*** (0.145)
- Wheat	-1.840*** (0.103)
Observations	9,425
Adj R-squared	0.904
Country-Year FE	Yes

Notes: Standard errors in parenthesis. Significance levels are denoted as ***p<0.01, **p<0.05, and *p<0.1, respectively. Fixed effects are included at the country-by-year level, and standard errors are clustered at the country level. The regression employs country-level panel data for the period 2000-2020. The fixed effect for 'potato and sweet potato' is dropped as the baseline crop.

Table 3: Factor Intensity of Crop Production

Crop Name	Labor (α^{nj})	Intermediate (ρ^{nj})	Land (γ^{nj})
Bananas	0.255	0.705	0.040
Cassava	0.240	0.664	0.096
Maize	0.189	0.522	0.289
Oil palm fruit	0.245	0.678	0.077
Potato and sweet potato	0.248	0.685	0.067
Rice	0.218	0.602	0.181
Soybeans	0.162	0.447	0.391
Sugar cane	0.249	0.687	0.064
Tomatoes	0.261	0.722	0.017
Wheat	0.154	0.425	0.421

Notes: The table above shows the crop-level factor intensities used in the model simulation. Relative heterogeneity in land intensities across crops is estimated by targeting equation (41), with land intensity parameters (γ^{nj}) normalized such that the revenue-weighted input share of land matches with the input share of land for modern technology as reported in [Farrokhi and Pellegrina \(2023\)](#).

Table 4: Estimation Result: Migration Elasticity

	All Flows		Domestic Flows	
	OLS (1)	IV (2)	OLS (3)	IV (4)
1/ ν : migration elasticity	0.118*** (0.003)	0.127*** (0.003)	0.217*** (0.042)	0.281*** (0.043)
Kleibergen-Paap Wald rk F statistic		506,766.3		4,504.5
Observations	54,668	54,668	960	960
ν : inverse of migration elasticity	8.492	7.864	4.598	3.564
Origin-Destination-Year FE	Yes	Yes	Yes	Yes

Notes: Standard errors in parenthesis. Significance levels are denoted as ***p<0.01, **p<0.05, and *p<0.1, respectively. Fixed effects are included at the origin-destination-year level, and standard errors are clustered at the origin-by-destination level.

Appendix

A Proofs for the Model

A.1 Proof of Household Migration Problem

Proof. This section reintroduces the proof of the dynamic discrete choice problem of households in Caliendo et al. (2019) for the integrity of the model proofs. The only difference from Caliendo et al. (2019) is that I keep per-period utility u_t^{ns} in the value function expression when using dynamic hat algebra rather than using real wages.

Proof of Equation (7) — The Bellman equation of a household currently living in country n and working in sector s at time t is given by:

$$\mathbf{v}_t^{ns} = u_t^{ns} + \max_{m \in \mathcal{N}, z \in \mathcal{S}} \left\{ \beta \mathbb{E}_t(\mathbf{v}_{t+1}^{mz}) - \zeta^{ns, mz} + \nu \epsilon_t^{mz} \right\}, \quad (\text{A.1})$$

where ϵ_t^{mz} is i.i.d. over individuals, countries, sectors, and time and is assumed to follow Type-I Extreme Value distribution with mean zero. Specifically, the cumulative distribution function is given by:

$$F(\epsilon) = \exp(-\exp(-\epsilon - \bar{\delta})), \quad (\text{A.2})$$

where $\bar{\delta} = \int_{-\infty}^{\infty} x \exp(-x \exp(-x)) dx$. Its probability density function is $f(\epsilon) = \partial F(\epsilon)/\partial \epsilon$.

Let us define $\Xi_t^{ns} = \mathbb{E}_t \left[\max_{m \in \mathcal{N}, z \in \mathcal{S}} \left\{ \beta \mathbb{E}_t(\mathbf{v}_{t+1}^{mz}) - \zeta^{ns, mz} + \nu \epsilon_t^{mz} \right\} \right]$. The goal is to solve for $V_t^{ns} \equiv \mathbb{E}_t(\mathbf{v}_t^{ns})$ by obtaining Ξ_t^{ns} . For mz to be the utility maximizing country-sector pair in the period $t+1$, it must be:

$$\beta V_{t+1}^{\tilde{m}\tilde{z}} - \zeta^{ns, \tilde{m}\tilde{z}} + \nu \epsilon_t^{\tilde{m}\tilde{z}} \leq \beta V_{t+1}^{mz} - \zeta^{ns, mz} + \nu \epsilon_t^{mz}, \quad (\text{A.3})$$

for all other country-sector pair $\tilde{m}\tilde{z}$. The above expression is equivalent to the following:

$$\epsilon_t^{\tilde{m}\tilde{z}} \leq \left(\frac{\beta(V_{t+1}^{mz} - V_{t+1}^{\tilde{m}\tilde{z}}) - (\zeta^{ns, mz} - \zeta^{ns, \tilde{m}\tilde{z}})}{\nu} \right) + \epsilon_t^{mz}. \quad (\text{A.4})$$

Define $\bar{\epsilon}_t^{mz, \tilde{m}\tilde{z}} = \left(\frac{\beta(V_{t+1}^{mz} - V_{t+1}^{\tilde{m}\tilde{z}}) - (\zeta^{ns, mz} - \zeta^{ns, \tilde{m}\tilde{z}})}{\nu} \right)$ and obtain $\Pr(\epsilon_t^{\tilde{m}\tilde{z}} \leq \bar{\epsilon}_t^{mz, \tilde{m}\tilde{z}} + \epsilon_t^{mz}) = F(\bar{\epsilon}_t^{mz, \tilde{m}\tilde{z}} + \epsilon_t^{mz})$. Then Ξ_t^{ns} can be expressed as:

$$\Xi_t^{ns} = \sum_{m \in \mathcal{N}} \sum_{z \in \mathcal{S}} \int_{-\infty}^{\infty} (\beta V_{t+1}^{mz} - \zeta^{ns, mz} + \nu \epsilon_t^{mz}) f(\epsilon_t^{mz}) \prod_{\tilde{m}\tilde{z} \neq mz} F(\bar{\epsilon}_t^{mz, \tilde{m}\tilde{z}} + \epsilon_t^{mz}) d\epsilon_t^{mz}. \quad (\text{A.5})$$

Substituting for $F(\epsilon)$ and $f(\epsilon)$ leads to the following:

$$\begin{aligned}\Xi_t^{ns} &= \sum_{m \in \mathcal{N}} \sum_{z \in \mathcal{S}} \int_{-\infty}^{\infty} (\beta V_{t+1}^{mz} - \zeta^{ns,mz} + \nu \epsilon_t^{mz}) \\ &\quad \times e^{-\epsilon_t^{mz} - \bar{\delta}} e^{-\exp(-\epsilon_t^{mz} - \bar{\delta})} \prod_{\tilde{m}\tilde{z} \neq mz} e^{-\exp(-(\bar{\epsilon}_t^{mz, \tilde{m}\tilde{z}} + \epsilon_t^{mz}) - \bar{\delta})} d\epsilon_t^{mz} \\ &= \sum_{m \in \mathcal{N}} \sum_{z \in \mathcal{S}} \int_{-\infty}^{\infty} (\beta V_{t+1}^{mz} - \zeta^{ns,mz} + \nu \epsilon_t^{mz}) \\ &\quad \times e^{-\epsilon_t^{mz} - \bar{\delta}} e^{-\exp(-\epsilon_t^{mz} - \bar{\delta})} \sum_{\tilde{m} \in \mathcal{N}} \sum_{\tilde{z} \in \mathcal{S}} \exp(-\bar{\epsilon}_t^{mz, \tilde{m}\tilde{z}}) d\epsilon_t^{mz},\end{aligned}\tag{A.6}$$

where the rearrangement is based on $\bar{\epsilon}_t^{mz, mz} = 0$ and $\exp(-\bar{\epsilon}_t^{mz, mz}) = 1$.

Next, one can simplify the above expression by defining $\mathcal{Z}_t^{mz} \equiv \log \left(\sum_{\tilde{m} \in \mathcal{N}} \sum_{\tilde{z} \in \mathcal{S}} \exp(-\bar{\epsilon}_t^{mz, \tilde{m}\tilde{z}}) \right)$ and $\kappa_t^{mz} \equiv \epsilon_t^{mz} + \bar{\delta}$ as follows:

$$\Xi_t^{ns} = \sum_{m \in \mathcal{N}} \sum_{z \in \mathcal{S}} \int_{-\infty}^{\infty} (\beta V_{t+1}^{mz} - \zeta^{ns,mz} + \nu(\kappa_t^{mz} - \bar{\delta})) e^{-\kappa_t^{mz} - \exp(-(\kappa_t^{mz} - \mathcal{Z}_t^{mz}))} d\kappa_t^{mz}.\tag{A.7}$$

With an additional change of variable $\tilde{y}_t^{mz} = \kappa_t^{mz} - \mathcal{Z}_t^{mz}$, it follows:

$$\begin{aligned}\Xi_t^{ns} &= \sum_{m \in \mathcal{N}} \sum_{z \in \mathcal{S}} \int_{-\infty}^{\infty} (\beta V_{t+1}^{mz} - \zeta^{ns,mz} + \nu(\tilde{y}_t^{mz} + \mathcal{Z}_t^{mz} - \bar{\delta})) e^{-\tilde{y}_t^{mz} - \mathcal{Z}_t^{mz} - \exp(-\tilde{y}_t^{mz})} d\tilde{y}_t^{mz} \\ &= \sum_{m \in \mathcal{N}} \sum_{z \in \mathcal{S}} e^{-\mathcal{Z}_t^{mz}} \left[(\beta V_{t+1}^{mz} - \zeta^{ns,mz} + \nu(\mathcal{Z}_t^{mz} - \bar{\delta})) + \nu \underbrace{\int_{-\infty}^{\infty} \tilde{y}_t^{mz} e^{-\tilde{y}_t^{mz} \exp(-\tilde{y}_t^{mz})} d\tilde{y}_t^{mz}}_{=\bar{\delta}} \right] \\ &= \sum_{m \in \mathcal{N}} \sum_{z \in \mathcal{S}} e^{-\mathcal{Z}_t^{mz}} (\beta V_{t+1}^{mz} - \zeta^{ns,mz} + \nu \mathcal{Z}_t^{mz}).\end{aligned}\tag{A.8}$$

Substituting $\bar{\epsilon}_t^{mz, \tilde{m}\tilde{z}}$ into the definition of \mathcal{Z}_t^{mz} , one can express \mathcal{Z}_t^{mz} as:

$$\begin{aligned}\mathcal{Z}_t^{mz} &= \log \left(\sum_{\tilde{m} \in \mathcal{N}} \sum_{\tilde{z} \in \mathcal{S}} \exp \left(-\frac{\beta V_{t+1}^{mz} - \zeta^{ns,mz}}{\nu} + \frac{\beta V_{t+1}^{\tilde{m}\tilde{z}} - \zeta^{ns, \tilde{m}\tilde{z}}}{\nu} \right) \right) \\ &= \log \left(\exp \left(-\frac{\beta V_{t+1}^{mz} - \zeta^{ns,mz}}{\nu} \right) \sum_{\tilde{m} \in \mathcal{N}} \sum_{\tilde{z} \in \mathcal{S}} \exp \left(\frac{\beta V_{t+1}^{\tilde{m}\tilde{z}} - \zeta^{ns, \tilde{m}\tilde{z}}}{\nu} \right) \right) \\ &= - \left(\frac{\beta V_{t+1}^{mz} - \zeta^{ns,mz}}{\nu} \right) + \log \sum_{\tilde{m} \in \mathcal{N}} \sum_{\tilde{z} \in \mathcal{S}} \exp \left(\frac{\beta V_{t+1}^{\tilde{m}\tilde{z}} - \zeta^{ns, \tilde{m}\tilde{z}}}{\nu} \right).\end{aligned}\tag{A.9}$$

Again, substituting the above expression for \mathcal{Z}_t^{mz} into Ξ_t^n leads to the following:

$$\begin{aligned}
\Xi_t^{ns} &= \sum_{m \in \mathcal{N}} \sum_{z \in \mathcal{S}} \exp \left(\left(\frac{\beta V_{t+1}^{mz} - \zeta^{ns,mz}}{\nu} \right) - \log \sum_{\tilde{m} \in \mathcal{N}} \sum_{\tilde{z} \in \mathcal{S}} \exp \left(\frac{\beta V_{t+1}^{\tilde{m}\tilde{z}} - \zeta^{ns,\tilde{m}\tilde{z}}}{\nu} \right) \right) \\
&\quad \times \left(\beta V_{t+1}^{mz} - \zeta^{ns,mz} - \nu \left(\frac{\beta V_{t+1}^{mz} - \zeta^{ns,mz}}{\nu} \right) + \nu \log \sum_{\tilde{m} \in \mathcal{N}} \sum_{\tilde{z} \in \mathcal{S}} \exp \left(\frac{\beta V_{t+1}^{\tilde{m}\tilde{z}} - \zeta^{ns,\tilde{m}\tilde{z}}}{\nu} \right) \right) \\
&= \underbrace{\left[\sum_{m \in \mathcal{N}} \sum_{z \in \mathcal{S}} \exp \left(\frac{\beta V_{t+1}^{mz} - \zeta^{ns,mz}}{\nu} \right) \right]}_{=1} \underbrace{\left[\sum_{\tilde{m} \in \mathcal{N}} \sum_{\tilde{z} \in \mathcal{S}} \exp \left(\frac{\beta V_{t+1}^{\tilde{m}\tilde{z}} - \zeta^{ns,\tilde{m}\tilde{z}}}{\nu} \right) \right]^{-1}}_{\times \left[\nu \log \sum_{\tilde{m} \in \mathcal{N}} \sum_{\tilde{z} \in \mathcal{S}} \exp \left(\frac{\beta V_{t+1}^{\tilde{m}\tilde{z}} - \zeta^{ns,\tilde{m}\tilde{z}}}{\nu} \right) \right]} \\
&= \nu \log \sum_{\tilde{m} \in \mathcal{N}} \sum_{\tilde{z} \in \mathcal{S}} \exp \left(\frac{\beta V_{t+1}^{\tilde{m}\tilde{z}} - \zeta^{ns,\tilde{m}\tilde{z}}}{\nu} \right). \tag{A.10}
\end{aligned}$$

Therefore, the expected lifetime utility can be expressed as:

$$V_t^{ns} = u_t^{ns} + \underbrace{\nu \log \sum_{m \in \mathcal{N}} \sum_{z \in \mathcal{S}} \exp \left(\frac{\beta V_{t+1}^{mz} - \zeta^{ns,mz}}{\nu} \right)}_{=\Xi_t^{ns}}. \tag{A.11}$$

The above expression implies that the expected lifetime utility is the current period utility plus the option value that can be obtained when moving to a different labor market, net of migration costs.

Proof of Equation (8) — The fraction of migrating households from country-sector pair ns to mz is equal to the probability that moving to mz provides the maximum expected lifetime utility:

$$\begin{aligned}
\mu_t^{ns,mz} &= \Pr \left(\beta V_{t+1}^{mz} - \zeta^{ns,mz} + \nu \epsilon_t^{mz} \geq \max_{\tilde{m} \in \mathcal{N}, \tilde{z} \in \mathcal{S}} \left\{ \beta \mathbb{E}_t(\mathbf{v}_{t+1}^{\tilde{m}\tilde{z}}) - \zeta^{ns,\tilde{m}\tilde{z}} + \nu \epsilon_t^{\tilde{m}} \right\} \right) \\
&= \int_{-\infty}^{\infty} f(\epsilon_t^{mz}) \prod_{\tilde{m}\tilde{z} \neq mz} \Pr \left(\epsilon_t^{\tilde{m}\tilde{z}} \leq \frac{\beta(V_{t+1}^{mz} - V_{t+1}^{\tilde{m}\tilde{z}}) - (\zeta^{ns,mz} - \zeta^{ns,\tilde{m}\tilde{z}})}{\nu} + \epsilon_t^{mz} \right) d\epsilon_t^{mz} \\
&= \int_{-\infty}^{\infty} f(\epsilon_t^{mz}) \prod_{\tilde{m}\tilde{z} \neq mz} F \left(\epsilon_t^{\tilde{m}\tilde{z}} \leq \bar{\epsilon}_t^{mz,\tilde{m}\tilde{z}} + \epsilon_t^{mz} \right) d\epsilon_t^{mz}. \tag{A.12}
\end{aligned}$$

Similar to equation (A.6), it can be shown that:

$$\mu_t^{ns,mz} = \int_{-\infty}^{\infty} e^{-\epsilon_t^{mz} - \bar{\delta}} e^{-\exp(-\epsilon_t^{mz} - \bar{\delta}) \sum_{\tilde{m} \in \mathcal{N}} \sum_{\tilde{z} \in \mathcal{S}} \exp(-\bar{\epsilon}_t^{mz,\tilde{m}\tilde{z}})} d\epsilon_t^{mz}. \tag{A.13}$$

Again, taking similar steps in equation (A.7) and equation (A.8) leads to the following:

$$\begin{aligned}
\mu_t^{ns,mz} &= \int_{-\infty}^{\infty} e^{-\mathcal{Z}_t^{mz}} e^{-\tilde{y}_t^{mz} - \exp(-\tilde{y}_t^{mz})} d\tilde{y}_t^{mz} \\
&= \exp(-\mathcal{Z}_t^{mz}) \underbrace{\int_{-\infty}^{\infty} e^{-\tilde{y}_t^{mz} - \exp(-\tilde{y}_t^{mz})} d\tilde{y}_t^{mz}}_{=1}.
\end{aligned} \tag{A.14}$$

Substituting \mathcal{Z}_t^{mz} in equation (A.9) into the above expression, it follows that:

$$\begin{aligned}
\mu_t^{ns,mz} &= \exp\left(\left(\frac{\beta V_{t+1}^{mz} - \zeta^{ns,mz}}{\nu}\right) - \log \sum_{\tilde{m} \in \mathcal{N}} \sum_{\tilde{z} \in \mathcal{S}} \exp\left(\frac{\beta V_{t+1}^{\tilde{m}\tilde{z}} - \zeta^{ns,\tilde{m}\tilde{z}}}{\nu}\right)\right) \\
&= \exp\left(\frac{\beta V_{t+1}^{mz} - \zeta^{ns,mz}}{\nu}\right) \left[\sum_{\tilde{m} \in \mathcal{N}} \sum_{\tilde{z} \in \mathcal{S}} \exp\left(\frac{\beta V_{t+1}^{\tilde{m}\tilde{z}} - \zeta^{ns,\tilde{m}\tilde{z}}}{\nu}\right) \right]^{-1} \\
&= \frac{\exp\left((\beta V_{t+1}^{mz} - \zeta^{ns,mz})/\nu\right)}{\sum_{\tilde{m} \in \mathcal{N}} \sum_{\tilde{z} \in \mathcal{S}} \exp((\beta V_{t+1}^{\tilde{m}\tilde{z}} - \zeta^{ns,\tilde{m}\tilde{z}})/\nu)}.
\end{aligned} \tag{A.15}$$

■

A.2 Proof of Optimal Land Allocation

Proof. The proofs for the crop production component closely follow Sotelo (2020). In Sotelo (2020), a heterogeneous land model is employed to evaluate the impact of reduced domestic trade costs from road paving. One notable difference is that Sotelo (2020) assumes intermediate inputs used in agricultural production are all imported from abroad, with their prices taken as given. Consequently, the income of the representative consumer in Sotelo (2020) is characterized by the sum of agricultural wages, non-agricultural wages, and rental revenue from land, excluding rental revenues from intermediate inputs. In this paper, rental revenue from intermediate inputs in each country is absorbed as income for workers in the agricultural sector. Furthermore, income from the two sectors—agriculture and non-agriculture—is differentiated, providing motivation for labor mobility among households.

Proof of Equation (11) — The equilibrium rental rate of land can be derived by equating the marginal cost of crop production with the crop price under perfect competition. Let us start with the representative farmer's cost minimization problem:

$$\begin{aligned}
&\min_{\ell_t^{nj}(\omega), m_t^{nj}(\omega), h_t^{nj}(\omega)} \left\{ w_t^{nA}(\omega) \ell_t^{nj}(\omega) + z_t^n m_t^{nj}(\omega) + r_t^{nj}(\omega) h_t^{nj}(\omega) \right\} \\
&\text{s.t.} \quad B_t^n \left(\ell_t^{nj}(\omega) \right)^{\alpha^{nj}} \left(m_t^{nj}(\omega) \right)^{\rho^{nj}} \left(h_t^{nj}(\omega) A_t^{nj}(\omega) \right)^{\gamma^{nj}} \geq \bar{q}.
\end{aligned}$$

The Lagrangian function is obtained by:

$$\begin{aligned}
\mathcal{L} &= w_t^{nA}(\omega) \ell_t^{nj}(\omega) + z_t^n m_t^{nj}(\omega) + r_t^{nj}(\omega) h_t^{nj}(\omega) \\
&\quad - \Lambda \left(B_t^n \left(\ell_t^{nj}(\omega) \right)^{\alpha^{nj}} \left(m_t^{nj}(\omega) \right)^{\rho^{nj}} \left(h_t^{nj}(\omega) A_t^{nj}(\omega) \right)^{\gamma^{nj}} - \bar{q} \right).
\end{aligned}$$

The first-order conditions are given by:

$$[\ell_t^{nj}(\omega)] : \ell_t^{nj}(\omega) = \left(\frac{\Lambda \alpha^{nj} q_t^{nj}(\omega)}{w_t^{nA}} \right) \quad (\text{A.16})$$

$$[m_t^{nj}(\omega)] : m_t^{nj}(\omega) = \left(\frac{\Lambda \rho^{nj} q_t^{nj}(\omega)}{z_t^n} \right) \quad (\text{A.17})$$

$$[h_t^{nj}(\omega)] : h_t^{nj}(\omega) = \left(\frac{\Lambda \gamma^{nj} q_t^{nj}(\omega)}{r_t^{nj}(\omega)} \right). \quad (\text{A.18})$$

Rearranging the first-order conditions, the optimal demand for labor and intermediate inputs can be expressed in terms of the optimal demand for land input.

$$\begin{aligned} \ell_t^{nj}(\omega) &= \left(\frac{r_t^{nj}(\omega)}{w_t^{nA}} \right) \left(\frac{\alpha^{nj}}{\gamma^{nj}} \right) h_t^{nj}(\omega) \\ m_t^{nj}(\omega) &= \left(\frac{r_t^{nj}(\omega)}{z_t^n} \right) \left(\frac{\rho^{nj}}{\gamma^{nj}} \right) h_t^{nj}(\omega). \end{aligned} \quad (\text{A.19})$$

Substituting the above equation into the constraint leads to the conditional input demands of land for producing the output quantity of \bar{q} :

$$h_t^{nj}(\omega) = \left(\frac{\bar{q}}{B_t^n(A_t^{nj}(\omega))^{\gamma^{nj}}} \right) \left(\frac{r_t^{nj}(\omega)}{w_t^{nA}} \right)^{-\alpha^{nj}} \left(\frac{r_t^{nj}(\omega)}{z_t^n} \right)^{-\rho^{nj}} \left(\frac{\alpha^{nj}}{\gamma^{nj}} \right)^{-\alpha^{nj}} \left(\frac{\rho^{nj}}{\gamma^{nj}} \right)^{-\rho^{nj}}. \quad (\text{A.20})$$

Then the cost of production is obtained as:

$$c(\bar{q}) = \left(\frac{\bar{c}^{nj}(w_t^{nA})^{\alpha^{nj}}(z_t^n)^{\rho^{nj}}(r_t^{nj}(\omega))^{\gamma^{nj}}}{B_t^n(A_t^{nj}(\omega))^{\gamma^{nj}}} \right) \bar{q}, \quad (\text{A.21})$$

where $\bar{c}^{nj} = (\alpha^{nj})^{-\alpha^{nj}}(\rho^{nj})^{-\rho^{nj}}(\gamma^{nj})^{-\gamma^{nj}}$.

Under perfect competition, the marginal cost of production is equalized to the crop price in equilibrium:

$$p_t^{nj} = \left(\frac{\bar{c}^{nj}(w_t^{nA})^{\alpha^{nj}}(z_t^n)^{\rho^{nj}}(r_t^{nj}(\omega))^{\gamma^{nj}}}{B_t^n(A_t^{nj}(\omega))^{\gamma^{nj}}} \right). \quad (\text{A.22})$$

Therefore, the equilibrium rental rate of land can be expressed as:

$$r_t^{nj}(\omega) = R_t^{nj} A_t^{nj}(\omega), \quad (\text{A.23})$$

where

$$R_t^{nj} \equiv \left(\frac{p_t^{nj} B_t^n}{\bar{c}^{nj}(w_t^{nA})^{\alpha^{nj}}(z_t^n)^{\rho^{nj}}} \right)^{1/\gamma^{nj}}. \quad (\text{A.24})$$

Proof of Equation (13) — The distributional assumption on $A_t^{nj}(\omega)$ implies that $R_t^{nj} A_t^{nj}(\omega)$ is independently and identically Fréchet distributed with shape parameter $\theta > 1$ and scale parameter

$\Upsilon R_t^{nj} A_t^{nj}$:

$$\begin{aligned}\Pr(R_t^{nj} A_t^{nj}(\omega) \leq x) &= \Pr\left(A_t^{nj}(\omega) \leq \frac{x}{R_t^{nj}}\right) \\ &= \exp\left\{-\left(\frac{x}{\Upsilon R_t^{nj} A_t^{nj}}\right)^{-\theta}\right\}.\end{aligned}\tag{A.25}$$

The probability that crop j generates the highest land rent and is planted in a parcel ω of a field f in the country n is given by:

$$\pi_t^{nj} \equiv \Pr\left(R_t^{nj} A_t^{nj}(\omega) \geq \max_{k \neq j} \{R_t^{nk} A_t^{nk}(\omega)\}\right).\tag{A.26}$$

By denoting the cumulative probability of $R_t^{nj} A_t^{nj}(\omega)$ as $F_j(x) = \Pr(R_t^{nj} A_t^{nj}(\omega) \leq x)$, it follows:

$$\begin{aligned}\pi_t^{nj} &= \int_0^\infty \Pr\left(\max_{k \in \mathcal{J}^c \setminus j} R_t^{nk} A_t^{nk}(\omega) \leq x\right) F'_j(x) dx \\ &= \Pr\left(\bigcap_{k \in \mathcal{J}^c \setminus j} \{R_t^{nk} A_t^{nk}(\omega) \leq x\}\right) F'_j(x) dx \\ &= \int_0^\infty \prod_{k \in \mathcal{J}^c \setminus j} F_k(x) F'_j(x) dx.\end{aligned}\tag{A.27}$$

Substituting $F_j(x) = \Pr(R_t^{nj} A_t^{nj}(\omega) \leq x)$ into the above equation leads to the following:

$$\begin{aligned}\pi_t^{nj} &= \int_0^\infty \prod_{k \in \mathcal{J}^c \setminus j} \exp\left\{-\left(\frac{x}{\Upsilon R_t^{nk} A_t^{nk}}\right)^{-\theta}\right\} \\ &\quad \times \exp\left\{-\left(\frac{x}{\Upsilon R_t^{nj} A_t^{nj}}\right)^{-\theta}\right\} \left(\frac{x}{\Upsilon R_t^{nj} A_t^{nj}}\right)^{-\theta-1} \left(\frac{\theta}{\Upsilon R_t^{nj} A_t^{nj}}\right) dx.\end{aligned}\tag{A.28}$$

Rearranging terms leads to the following:

$$\begin{aligned}\pi_t^{nj} &= \int_0^\infty \prod_{k \in \mathcal{J}^c} \exp\left\{-\left(\frac{x}{\Upsilon R_t^{nk} A_t^{nk}}\right)^{-\theta}\right\} \left(\frac{x}{\Upsilon R_t^{nj} A_t^{nj}}\right)^{-\theta-1} \left(\frac{\theta}{\Upsilon R_t^{nj} A_t^{nj}}\right) dx \\ &= (\Upsilon R_t^{nj} A_t^{nj})^\theta \int_0^\infty \exp\left\{-\sum_{k=1}^J \left(\frac{x}{\Upsilon R_t^{nk} A_t^{nk}}\right)^{-\theta}\right\} \theta x^{-\theta-1} dx \\ &= \frac{(R_t^{nj} \Upsilon A_t^{nj})^\theta}{\sum_{k=1}^J (R_t^{nk} A_t^{nk})^\theta} \underbrace{\left[\exp\left\{-x^{-\theta} \sum_{k=1}^J (\Upsilon R_t^{nk} A_t^{nk})^\theta\right\}\right]_0^\infty}_=\end{aligned}\tag{A.29}$$

Therefore, it follows that:

$$\pi_t^{nj} = \frac{(R_t^{nj} A_t^{nj})^\theta}{\sum_{k=1}^J (R_t^{nk} A_t^{nk})^\theta}.\tag{A.30}$$

A.3 Proof of Optimal Revenue and Crop Supply

Proof. Proof of Equation (14) — From equation (11), recall that $r_t^{nj}(\omega) = R_t^{nj} A_t^{nj}(\omega)$ follows the Fréchet distribution with shape parameter $\theta > 1$ and scale parameter $\Upsilon R_t^{nj} A_t^{nj}$. Then the probability of $R_t^{nj} A_t^{nj}(\omega)$ conditional on crop j being the most profitable in parcel ω in country n , is given by:

$$\begin{aligned}
& \Pr \left(R_t^{nj} A_t^{nj}(\omega) = x \mid R_t^{nj} A_t^{nj}(\omega) \in \arg \max_{k \in \mathcal{J}^c} R_t^{nk} A_t^{nk}(\omega) \right) \\
&= \frac{\Pr \left(R_t^{nj} A_t^{nj}(\omega) = x \right) \prod_{k \in \mathcal{J}^c \setminus j} \Pr \left(R_t^{nk} A_t^{nk}(\omega) \leq x \right)}{\Pr \left(R_t^{nj} A_t^{nj}(\omega) \in \arg \max_{k \in \mathcal{J}^c} R_t^{nk} A_t^{nk}(\omega) \right)} \\
&= \frac{F'_j(x) \prod_{k \in \mathcal{J}^c \setminus j} F_k(x)}{\pi_t^{nj}} \\
&= \exp \left\{ - \left(\frac{x}{\Upsilon R_t^{nj} A_t^{nj}} \right)^{-\theta} \right\} \left(\frac{x}{\Upsilon R_t^{nj} A_t^{nj}} \right)^{-\theta-1} \left(\frac{\theta}{\Upsilon R_t^{nj} A_t^{nj}} \right) \\
&\quad \times \exp \left\{ - \sum_{k \in \mathcal{J}^c \setminus j} \left(\frac{x}{\Upsilon R_t^{nk} A_t^{nk}} \right)^{-\theta} \right\} (\pi_t^{nj})^{-1} \\
&= \exp \left\{ - \sum_{k=1}^J \left(\frac{x}{\Upsilon R_t^{nk} A_t^{nk}} \right)^{-\theta} \right\} \theta x^{-\theta-1} (\Upsilon R_t^{nj} A_t^{nj})^\theta (\pi_t^{nj})^{-1}.
\end{aligned} \tag{A.31}$$

The conditional expectation of $R_t^{nj} A_t^{nj}(\omega)$ can be obtained as follows:

$$\begin{aligned}
& E \left[R_t^{nj} A_t^{nj}(\omega) \mid R_t^{nj} A_t^{nj}(\omega) \in \arg \max_{k \in \mathcal{J}^c} R_t^{nk} A_t^{nk}(\omega) \right] \\
&= \int_0^\infty x \Pr \left(R_t^{nj} A_t^{nj}(\omega) = x \mid R_t^{nj} A_t^{nj}(\omega) \in \arg \max_{k \in \mathcal{J}^c} R_t^{nk} A_t^{nk}(\omega) \right) dx \\
&= \int_0^\infty \exp \left\{ - \sum_{k=1}^J \left(\frac{x}{\Upsilon R_t^{nk} A_t^{nk}} \right)^{-\theta} \right\} \theta x^{-\theta} (\Upsilon R_t^{nj} A_t^{nj})^\theta (\pi_t^{nj})^{-1} dx \\
&= \int_0^\infty \exp \left\{ -x^{-\theta} \sum_{k=1}^J (\Upsilon R_t^{nk} A_t^{nk})^\theta \right\} \theta x^{-\theta} \sum_{k=1}^J (\Upsilon R_t^{nk} A_t^{nk})^\theta dx.
\end{aligned} \tag{A.32}$$

Let $u = x^{-\theta} \sum_{k=1}^J (\Upsilon R_t^{nk} A_t^{nk})^\theta$. Integration by substitution yields:

$$\begin{aligned}
& E \left[R_t^{nj} A_t^{nj}(\omega) \mid R_t^{nj} A_t^{nj}(\omega) \in \arg \max_{k \in \mathcal{J}^c} R_t^{nk} A_t^{nk}(\omega) \right] \\
&= \int_\infty^0 \exp(-u) \theta u (-\theta x^{-\theta-1})^{-1} \left(\sum_{k=1}^J (\Upsilon R_t^{nk} A_t^{nk})^\theta \right)^{-1} du \\
&= \int_0^\infty \exp(-u) u^{1-(\theta+1)/\theta} \left(\sum_{k=1}^J (\Upsilon R_t^{nk} A_t^{nk})^\theta \right)^{(\theta+1)/\theta-1} du \\
&= \Upsilon \left(\sum_{k=1}^J (R_t^{nk} A_t^{nk})^\theta \right)^{1/\theta} \int_0^\infty u^{(\theta-1)/\theta-1} \exp(-u) du.
\end{aligned} \tag{A.33}$$

Note that $\Upsilon \equiv \Gamma(1 - \frac{1}{\theta})^{-1}$ and $\Gamma(z) = \int_0^\infty x^{z-1} e^{-x} dx$. Therefore, it follows:

$$\Phi_t^n = \mathbb{E}_t \left[R_t^{nj} A_t^{nj}(\omega) \mid R_t^{nj} A_t^{nj}(\omega) \in \arg \max_{k \in \mathcal{J}^c} R_t^{nk} A_t^{nk}(\omega) \right] = \left(\sum_{k=1}^J (R_t^{nk} A_t^{nk})^\theta \right)^{1/\theta}. \quad (\text{A.34})$$

Proof of Equation (15) — Recall the relationship between optimal demand for labor, intermediate, and land inputs from equation (A.19):

$$\begin{aligned} \ell_t^{nj}(\omega) &= \left(\frac{r_t^{nj}(\omega)}{w_t^{nA}} \right) \left(\frac{\alpha^{nj}}{\gamma^{nj}} \right) h_t^{nj}(\omega) \\ m_t^{nj}(\omega) &= \left(\frac{r_t^{nj}(\omega)}{z_t^n} \right) \left(\frac{\rho^{nj}}{\gamma^{nj}} \right) h_t^{nj}(\omega). \end{aligned} \quad (\text{A.35})$$

Using the above equations, the optimal revenue per unit of land when the farmer plants crop j on a given plot ω in the country n is obtained by:

$$\begin{aligned} \psi_t^{nj}(\omega) &= p_t^{nj} q_t^{nj}(\omega) \Big|_{h_t^{nj}(\omega)=1} \\ &= p_t^{nj} B_t^n \left(\ell_t^{nj}(\omega) \right)^{\alpha^{nj}} \left(m_t^{nj}(\omega) \right)^{\rho^{nj}} \left(h_t^{nj}(\omega) A_t^{nj}(\omega) \right)^{\gamma^{nj}} \Big|_{h_t^{nj}(\omega)=1} \\ &= p_t^{nj} B_t^n \left(\frac{\alpha^{nj} r_t^{nj}(\omega)}{\gamma^{nj} w_t^{nA}} \right)^{\alpha^{nj}} \left(\frac{\rho^{nj} r_t^{nj}(\omega)}{\gamma^{nj} z_t^n} \right)^{\rho^{nj}} \left(A_t^{nj}(\omega) \right)^{\gamma^{nj}}. \end{aligned} \quad (\text{A.36})$$

Substituting the optimal rental rate from equation (11), the optimal revenue per unit of land for a given plot ω is derived as:

$$\begin{aligned} \psi_t^{nj}(\omega) &= \left(\frac{p_t^{nj} B_t^n}{\bar{c}^{nj} (w_t^{nA})^{\alpha^{nj}} (z_t^n)^{\rho^{nj}}} \right) \left(\frac{1}{\gamma^{nj}} \right) \left(R_t^{nj} A_t^{nj}(\omega) \right)^{\alpha^{nj} + \rho^{nj}} \left(A_t^{nj}(\omega) \right)^{\gamma^{nj}} \\ &= \frac{R_t^{nj} A_t^{nj}(\omega)}{\gamma^{nj}}. \end{aligned} \quad (\text{A.37})$$

Finally, the optimal revenue from growing crop j in country n is the product of the total amount of land in country n , the share of land allocated to crop j , and the average revenue from the production of crop j , conditional on crop j being selected. Considering that $\psi_t^{nj}(\omega)$ is simply a scaled version of $r_t^{nj}(\omega)$ by $1/\gamma^{nj}$, it is straightforward to demonstrate that:

$$\begin{aligned} \Psi_t^{nj} &= \mathbb{E}_t \left[\psi_t^{nj}(\omega) \mid R_t^{nj} A_t^{nj}(\omega) \in \arg \max_{k \in \mathcal{J}^c} R_t^{nk} A_t^{nk}(\omega) \right] \pi_t^{nj} H_t^n \\ &= \mathbb{E}_t \left[R_t^{nj} A_t^{nj}(\omega) \mid R_t^{nj} A_t^{nj}(\omega) \in \arg \max_{k \in \mathcal{J}^c} R_t^{nk} A_t^{nk}(\omega) \right] \left(\frac{\pi_t^{nj} H_t^n}{\gamma^{nj}} \right) \\ &= \left(\sum_{k=1}^J (R_t^{nk} A_t^{nk})^\theta \right)^{1/\theta} \left(\frac{\pi_t^{nj} H_t^n}{\gamma^{nj}} \right) \\ &= (R_t^{nj} A_t^{nj})^\theta (\Phi_t^n)^{1-\theta} \left(\frac{H_t^n}{\gamma^{nj}} \right), \end{aligned} \quad (\text{A.38})$$

where $\Phi_t^n = \left(\sum_{k=1}^J (R_t^{nk} A_t^{nk})^\theta \right)^{1/\theta}$. ■

A.4 Proof of Optimal Input Demands

Proof. **Proof of Equation (17)** — From equation (A.37), recall that the optimal revenue per unit of land for a given plot (ω) is given by:

$$\psi_t^{nj}(\omega) = \frac{R_t^{nj} A_t^{nj}(\omega)}{\gamma^{nj}}. \quad (\text{A.39})$$

Then the optimal input demand per unit of land for plot (ω) for labor and intermediate inputs are respectively given by:

$$\begin{aligned} \ell_t^{nj}(\omega) &= \left(\frac{\alpha^{nj}}{\gamma^{nj}} \right) \left(\frac{R_t^{nj} A_t^{nj}(\omega)}{w_t^{nA}} \right) \\ m_t^{nj}(\omega) &= \left(\frac{\rho^{nj}}{\gamma^{nj}} \right) \left(\frac{R_t^{nj} A_t^{nj}(\omega)}{z_t^n} \right). \end{aligned} \quad (\text{A.40})$$

The labor input demand for the production of crop j is the product of the land size of each country, the fraction of land allocated to the crop j , and the average labor input demand conditional on crop j being chosen as the rent-maximizing crop among all crop varieties:

$$\begin{aligned} \ell_t^{nj} &= \mathbb{E}_t \left[\ell_t^{nj}(\omega) \mid R_t^{nj} A_t^{nj}(\omega) \in \arg \max_{k \in \mathcal{J}^c} R_t^{nk} A_t^{nk}(\omega) \right] \pi_t^{nj} H_t^n \\ &= \mathbb{E}_t \left[R_t^{nj} A_t^{nj}(\omega) \mid R_t^{nj} A_t^{nj}(\omega) \in \arg \max_{k \in \mathcal{J}^c} R_t^{nk} A_t^{nk}(\omega) \right] \left(\frac{\alpha^{nj}}{\gamma^{nj}} \right) \left(\frac{\pi_t^{nj} H_t^n}{w_t^{nA}} \right) \\ &= \left(\frac{\alpha^{nj}}{w_t^{nA}} \right) \Psi_t^{nj}. \end{aligned} \quad (\text{A.41})$$

Similarly, for the intermediate input, it follows:

$$m_t^{nj} = \mathbb{E}_t \left[m_t^{nj}(\omega) \mid R_t^{nj} A_t^{nj}(\omega) \in \arg \max_{k \in \mathcal{J}^c} R_t^{nk} A_t^{nk}(\omega) \right] \pi_t^{nj} H_t^n = \left(\frac{\rho^{nj}}{z_t^n} \right) \Psi_t^{nj}. \quad (\text{A.42})$$

Proof of Equation (18) — Given the above expression for the country- and crop-level input demands, the aggregate country-level labor demand for all crops in the country n is expressed as:

$$\begin{aligned} \ell_t^{nA} &= \sum_{j=1}^J \ell_t^{nj} = \sum_{j=1}^J \left(\frac{\alpha^{nj}}{w_t^{nA}} \right) \Psi_t^{nj} \\ &= \sum_{j=1}^J \left(\frac{\alpha^{nj}}{w_t^{nA}} \right) (R_t^{nj} A_t^{nj})^\theta (\Phi_t^n)^{1-\theta} \left(\frac{H_t^n}{\gamma^{nj}} \right) \\ &= \left(\frac{H_t^n \Phi_t^n}{w_t^{nA}} \right) \sum_{j=1}^J \alpha^{nj} (\gamma^{nj})^{-1} \pi_t^{nj}. \end{aligned} \quad (\text{A.43})$$

It is beneficial to note that the revenue share of the crop, χ_t^{nj} , can be expressed as a function of land

allocation share, π_t^{nk} , as follows.

$$\begin{aligned}\chi_t^{nj} &= \frac{\Psi_t^{nj}}{\sum_{k=1}^J \Psi_t^{nk}} \\ &= \frac{(R_t^{nj} A_t^{nj})^\theta (\Phi_t^n)^{1-\theta} H_t^n (\gamma^{nj})^{-1}}{\sum_{k=1}^J (R_t^{nk} A_t^{nk})^\theta (\Phi_t^n)^{1-\theta} H_t^n (\gamma^{nk})^{-1}} \\ &= \frac{(\gamma^{nj})^{-1} \pi_t^{nj}}{\sum_{k=1}^J (\gamma^{nk})^{-1} \pi_t^{nk}}.\end{aligned}\tag{A.44}$$

Rearranging the terms, land allocation share, π_t^{nj} , can be expressed as follows:

$$\pi_t^{nj} = \gamma^{nj} \chi_t^{nj} \sum_{k=1}^J (\gamma^{nk})^{-1} \pi_t^{nk}.\tag{A.45}$$

Replacing the aforementioned expression for π_t^{nj} into equation (A.43) and subsequently substituting Ψ_t^n from equation (15), the country-level aggregate labor demand is then simplified to the following form:

$$\begin{aligned}\ell_t^{nA} &= \left(\frac{H_t^n \Phi_t^n}{w_t^{nA}} \right) \sum_{j=1}^J \alpha^{nj} (\gamma^{nj})^{-1} \pi_t^{nj} \\ &= \left(\frac{H_t^n \Phi_t^n}{w_t^{nA}} \right) \sum_{j=1}^J \alpha^{nj} \chi_t^{nj} \sum_{k=1}^J (\gamma^{nk})^{-1} \pi_t^{nk} \\ &= \left(\frac{\Psi_t^n}{w_t^{nA}} \right) \sum_{j=1}^J \alpha^{nj} \chi_t^{nj} = \frac{\bar{\alpha}_t^n}{w_t^{nA}} \Psi_t^n,\end{aligned}\tag{A.46}$$

where $\bar{\alpha}_t^n = \sum_{j=1}^J \alpha^{nj} \chi_t^{nj}$. Taking a similar approach, the country-level aggregate intermediate input demand is expressed as:

$$m_t^n = \sum_{j=1}^J m_t^{nj} = \frac{\bar{\rho}_t^n}{z_t^n} \Psi_t^n,\tag{A.47}$$

where $\bar{\rho}_t^n = \sum_{j=1}^J \chi_t^{nj} \rho^{nj}$.

■

B Proofs for Dynamic Hat Algebra

B.1 Proof of Proposition 1

Proof. Consider the allocation of temporary equilibrium $\{\pi_t, s_t, L_t, X_t\}$ at time t and the changes $\{\dot{L}_{t+1}, \dot{\Theta}_{t+1}\}$ as given. The following set of proofs demonstrates how to express the equilibrium conditions for the temporary equilibrium using dot notation $\dot{x}_{t+1} = (x_{t+1}/x_t)$, without relying on the information on the level of fundamental variables.

1) Aggregate-level demand

Proof of Equation (24) — From equation (3), the expression for \dot{C}_t^{ns} is simply given by taking a ratio between C_{t+1}^{ns} and C_t^{ns} as follows:

$$\dot{C}_t^{ns} = \frac{C_{t+1}^{ns}}{C_t^{ns}} = \left(\dot{c}_{t+1}^{ns, \mathbf{A}} \right)^{\phi^n} \left(\dot{c}_{t+1}^{ns, \mathbf{M}} \right)^{1-\phi^n}. \quad (\text{A.48})$$

Proof of Equation (25) — Consider the utility maximization problem of a household working in the labor market ns , whose income is E_t^{ns} . The non-agricultural good is considered as a numeraire.

$$\begin{aligned} & \max_{c_t^{ns, \mathbf{A}}, c_t^{ns, \mathbf{M}}} \left(c_t^{ns, \mathbf{A}} \right)^{\phi^n} \left(c_t^{ns, \mathbf{M}} \right)^{1-\phi^n} \\ & \text{s.t.} \quad P_t^n c_t^{ns, \mathbf{A}} + c_t^{ns, \mathbf{M}} = E_t^{ns}. \end{aligned} \quad (\text{A.49})$$

The optimal consumption of the agricultural and non-agricultural goods are respectively given by:

$$c_t^{ns, \mathbf{A}} = \frac{\phi^n E_t^{ns}}{P_t^n} \quad \text{and} \quad c_t^{ns, \mathbf{M}} = (1 - \phi^n) E_t^{ns}. \quad (\text{A.50})$$

Then it follows:

$$\begin{aligned} \dot{c}_t^{ns, \mathbf{A}} &= \frac{c_{t+1}^{ns, \mathbf{A}}}{c_t^{ns, \mathbf{A}}} = \frac{\dot{E}_{t+1}^{ns}}{\dot{P}_{t+1}^n} \\ \dot{c}_{t+1}^{ns, \mathbf{M}} &= \frac{c_{t+1}^{ns, \mathbf{M}}}{c_t^{ns, \mathbf{M}}} = \dot{E}_{t+1}^{ns}. \end{aligned} \quad (\text{A.51})$$

2) Crop-level demand

Proof of Equation (26) — Given the assumption of CES aggregation of agricultural goods, the optimal crop consumption is given by:

$$c_t^{ns, j} = \phi^{n, j} \left(\frac{P_t^{nj}}{P_t^n} \right)^{-\varkappa} c_t^{ns, \mathbf{A}}, \quad \text{for } j \in \mathcal{J}^c. \quad (\text{A.52})$$

Then it follows:

$$\dot{c}_{t+1}^{ns, j} = \frac{c_{t+1}^{ns, j}}{c_t^{ns, j}} = \left(\frac{\dot{P}_{t+1}^{nj}}{\dot{P}_{t+1}^n} \right)^{-\varkappa} \dot{c}_{t+1}^{ns, \mathbf{A}}. \quad (\text{A.53})$$

Proof of Equation (27) — Recall that the CES price index for the aggregate agricultural good is

given by:

$$P_t^n = \left(\sum_{j \in \mathcal{J}} \phi^{n,j} (P_t^{nj})^{1-\varkappa} \right)^{1/(1-\varkappa)}. \quad (\text{A.54})$$

Note that under the CES assumption, the expenditure share on crop j is identical for all households across all sectors s .

$$s_t^{nj} = \left(\frac{P_t^{nj} c_t^{ns,j}}{P_t^n c_t^{ns,\mathbf{A}}} \right) = \phi^{n,j} \left(\frac{P_t^{nj}}{P_t^n} \right)^{1-\varkappa}, \quad \text{for } j \in \mathcal{J}^c, s \in \mathcal{S} \quad (\text{A.55})$$

Then it follows:

$$\begin{aligned} \dot{P}_{t+1}^n &= \frac{P_{t+1}^n}{P_t^n} = \left(\frac{\sum_{j \in \mathcal{J}} \phi^{n,j} (P_t^{nj})^{1-\varkappa} (\dot{P}_{t+1}^{nj})^{1-\varkappa}}{(P_t^n)^{1-\varkappa}} \right)^{1/(1-\varkappa)} \\ &= \left(\sum_{j \in \mathcal{J}} s_t^{nj} (\dot{P}_{t+1}^{nj})^{1-\varkappa} \right)^{1/(1-\varkappa)}. \end{aligned} \quad (\text{A.56})$$

Proof of Equation (28) — The transition of crop-level expenditure share is captured by:

$$s_{t+1}^{nj} = s_t^{nj} \left(\frac{\dot{P}_{t+1}^{nj} \dot{c}_{t+1}^{ns,j}}{\dot{P}_{t+1}^n \dot{c}_{t+1}^{ns,\mathbf{A}}} \right) = s_t^{nj} \left(\frac{\dot{P}_{t+1}^{nj}}{\dot{P}_{t+1}^n} \right)^{1-\varkappa}. \quad (\text{A.57})$$

3) Crop- and origin-level demand

Proof of Equation (29) — The Armington (CES) assumption implies the optimal demand for crops of each origin is given by:

$$c_t^{m,ns,j} = \phi^{m,n,j} \left(\frac{p_t^{m,n,j}}{P_t^{nj}} \right)^{-\delta} c_t^{ns,j}. \quad (\text{A.58})$$

Then it follows:

$$\begin{aligned} \dot{c}_{t+1}^{m,ns,j} &= \frac{c_{t+1}^{m,ns,j}}{c_t^{m,ns,j}} = \left(\frac{\dot{p}_t^{m,n,j}}{\dot{P}_t^{nj}} \right)^{-\delta} \dot{c}_{t+1}^{ns,j} \\ &= \left(\frac{\dot{p}_{t+1}^{m,n,j} \dot{p}_{t+1}^{mj}}{\dot{P}_{t+1}^{nj}} \right)^{-\delta} \dot{c}_{t+1}^{ns,j}. \end{aligned} \quad (\text{A.59})$$

Proof of Equation (30) — Due to the Armington assumption, the price index of each crop is given by:

$$P_t^{nj} = \left[\sum_{m \in \mathcal{N}} \phi^{m,n,j} (p_t^{m,n,j})^{1-\delta} \right]^{1/(1-\delta)}, \quad j \in \mathcal{J}^c. \quad (\text{A.60})$$

Again, the expenditure share on a crop from each import origin remains identical for consumers across all sectors:

$$s_t^{mnj} = \left(\frac{p_t^{m,n,j} c_t^{m,ns,j}}{P_t^{nj} c_t^{ns,j}} \right) = \phi^{m,n,j} \left(\frac{p_t^{m,n,j}}{P_t^{nj}} \right)^{1-\delta}. \quad (\text{A.61})$$

Then it follows:

$$\begin{aligned}
\dot{P}_{t+1}^{nj} &= \frac{P_{t+1}^{nj}}{P_t^{nj}} = \left(\frac{\sum_{m \in \mathcal{N}} \phi^{m,n,j} (p_t^{m,n,j})^{1-\delta} (\dot{p}_{t+1}^{m,n,j})^{1-\delta}}{(P_t^{nj})^{1-\delta}} \right)^{1/(1-\delta)} \\
&= \left(\sum_{m \in \mathcal{N}} s_t^{mnj} (\dot{p}_{t+1}^{m,n,j})^{1-\delta} \right)^{1/(1-\delta)} \\
&= \left(\sum_{m \in \mathcal{N}} s_t^{mnj} (\dot{\tau}_{t+1}^{m,n,j} \dot{p}_{t+1}^{mj})^{1-\delta} \right)^{1/(1-\delta)}.
\end{aligned} \tag{A.62}$$

Proof of Equation (31) — The transition of origin- and crop-level expenditure share is given by:

$$\begin{aligned}
s_{t+1}^{mnj} &= s_t^{mnj} \left(\frac{\dot{p}_{t+1}^{m,n,j} \dot{c}_{t+1}^{m,ns,j}}{\dot{P}_{t+1}^{nj} \dot{c}_{t+1}^{ns,j}} \right) \\
&= s_t^{mnj} \left(\frac{\dot{p}_t^{m,n,j}}{\dot{P}_t^{nj}} \right)^{1-\delta} = s_t^{mnj} \left(\frac{\dot{\tau}_{t+1}^{m,n,j} \dot{p}_t^{m,j}}{\dot{P}_t^{nj}} \right)^{1-\delta}.
\end{aligned} \tag{A.63}$$

4) Crop production

Proof of Equation (32) — Taking a ratio of R_t^{nj} from equation (12) between time $t + 1$ and t , it follows:

$$\begin{aligned}
\dot{R}_{t+1}^{nj} &= \frac{R_{t+1}^{nj}}{R_t^{nj}} = \frac{\left(p_{t+1}^{nj} B_{t+1}^n (\bar{c}^{nj})^{-1} (w_{t+1}^n \mathbf{A})^{-\alpha^{nj}} (z_{t+1}^n)^{-\rho^{nj}} \right)^{1/\gamma^{nj}}}{\left(p_t^{nj} B_t^n (\bar{c}^{nj})^{-1} (w_t^n \mathbf{A})^{-\alpha^{nj}} (z_t^n)^{-\rho^{nj}} \right)^{1/\gamma^{nj}}} \\
&= \left(\dot{p}_{t+1}^{nj} \dot{B}_{t+1}^n (\dot{w}_{t+1}^n \mathbf{A})^{-\alpha^{nj}} (\dot{z}_{t+1}^n)^{-\rho^{nj}} \right)^{1/\gamma^{nj}}.
\end{aligned} \tag{A.64}$$

Proof of Equation (33) — Consider the optimal share of land allocation from equation (13) at time $t + 1$. Multiplying and dividing by $(R_t^{nk} A_t^{nk})^\theta$ and $\sum_{f=1}^J (R_t^{nf} A_t^{nf})^\theta$, and then using the definition of π_t^{nj} , it follows:

$$\begin{aligned}
\pi_{t+1}^{nj} &= \frac{(R_{t+1}^{nj} A_{t+1}^{nj})^\theta}{\sum_{k=1}^J (R_{t+1}^{nk} A_{t+1}^{nk})^\theta} \\
&= \left(\dot{R}_{t+1}^{nj} \dot{A}_{t+1}^{nj} \right)^\theta \left(\frac{\left(R_t^{nj} A_t^{nj} \right)^\theta}{\sum_{k=1}^J (R_t^{nk} A_t^{nk})^\theta} \right) \left(\frac{\sum_{f=1}^J (R_t^{nf} A_t^{nf})^\theta}{\sum_{k=1}^J (\dot{R}_{t+1}^{nk} \dot{A}_{t+1}^{nk})^\theta \left(R_t^{nk} A_t^{nk} \right)^\theta} \right) \\
&= \left(\dot{R}_{t+1}^{nj} \dot{A}_{t+1}^{nj} \right)^\theta \pi_t^{nj} \left(\frac{1}{\sum_{k=1}^J (\dot{R}_{t+1}^{nk} \dot{A}_{t+1}^{nk})^\theta \left(\frac{\left(R_t^{nk} A_t^{nk} \right)^\theta}{\sum_{f=1}^J (R_t^{nf} A_t^{nf})^\theta} \right)} \right).
\end{aligned} \tag{A.65}$$

Substituting π_t^{nj} into the denominator, the expression for π_{t+1}^{nj} is given by:

$$\pi_{t+1}^{nj} = \frac{\pi_t^{nj} (\dot{R}_{t+1}^{nj} \dot{A}_{t+1}^{nj})^\theta}{\sum_{k=1}^J \pi_t^{nk} (\dot{R}_{t+1}^{nk} \dot{A}_{t+1}^{nk})^\theta}. \tag{A.66}$$

Proof of Equation (34) — Consider the average rental rate of land for each crop from equation (14). Multiplying and dividing by $(R_t^{nk} A_t^{nk})^\theta$, it follows:

$$\begin{aligned}\dot{\Phi}_{t+1}^n &= \frac{\Phi_{t+1}^n}{\Phi_t^n} = \left(\frac{\sum_{k=1}^J (\dot{R}_{t+1}^{nk} \dot{A}_{t+1}^{nk})^\theta (R_t^{nk} A_t^{nk})^\theta}{\sum_{j=1}^J (R_t^{nj} A_t^{nj})^\theta} \right)^{1/\theta} \\ &= \left(\sum_{k=1}^J \pi_t^{nk} (\dot{R}_{t+1}^{nk} \dot{A}_{t+1}^{nk})^\theta \right)^{1/\theta}.\end{aligned}\quad (\text{A.67})$$

Proof of Equation (35) — Given $L_t^{n\mathbf{A}}$ and equilibrium conditions (18) and (23), the market wage for the agricultural sector is given by:

$$w_t^{n\mathbf{A}} = \frac{\bar{\alpha}_t^n}{L_t^{n\mathbf{A}}} \Psi_t^n, \quad (\text{A.68})$$

where $\bar{\alpha}_t^n = \sum_{j=1}^J \alpha^{nj} \chi_t^{nj}$ and $\chi_t^{nj} = \frac{(\gamma^{nj})^{-1} \pi_t^{nj}}{\sum_{k=1}^J (\gamma^{nk})^{-1} \pi_t^{nk}}$. Substituting Ψ_t^n from equation (16) and $\bar{\alpha}_t^n$ into $w_t^{n\mathbf{A}}$, it follows:

$$\begin{aligned}w_t^{n\mathbf{A}} &= \left(\frac{\sum_{j=1}^J \alpha^{nj} (\gamma^{nj})^{-1} \pi_t^{nj}}{\sum_{k=1}^J (\gamma^{nk})^{-1} \pi_t^{nk}} \right) \frac{\Phi_t^n H_t^n}{L_t^n} \sum_{j=1}^J (\gamma^{nj})^{-1} \pi_t^{nj} \\ &= \left(\sum_{j=1}^J \alpha^{nj} (\gamma^{nj})^{-1} \pi_t^{nj} \right) \left(\frac{\Phi_t^n H_t^n}{L_t^{n\mathbf{A}}} \right).\end{aligned}\quad (\text{A.69})$$

Expressing $w_t^{n\mathbf{A}}$ in time differences, it follows:

$$\dot{w}_{t+1}^{n\mathbf{A}} = \frac{w_{t+1}^{n\mathbf{A}}}{w_t^{n\mathbf{A}}} = \left(\frac{\sum_{j=1}^J \alpha^{nj} (\gamma^{nj})^{-1} \pi_{t+1}^{nj}}{\sum_{k=1}^J \alpha^{nk} (\gamma^{nk})^{-1} \pi_t^{nk}} \right) \left(\frac{\dot{\Phi}_{t+1}^n \dot{H}_{t+1}^n}{\dot{L}_{t+1}^{n\mathbf{A}}} \right). \quad (\text{A.70})$$

For the intermediate input, similar steps can be followed to obtain:

$$\dot{z}_{t+1}^n = \left(\frac{\sum_{j=1}^J \rho^{nj} (\gamma^{nj})^{-1} \pi_{t+1}^{nj}}{\sum_{k=1}^J \rho^{nk} (\gamma^{nk})^{-1} \pi_t^{nk}} \right) \left(\frac{\dot{\Phi}_{t+1}^n \dot{H}_{t+1}^n}{\dot{M}_{t+1}^n} \right) \quad (\text{A.71})$$

5) Budget constraint

Proof of Equation (36) — Consider the income of households in the agricultural sector from equation (21). Substituting Ψ_t^n from equation (16) into $E_t^{n\mathbf{A}}$, it follows:

$$E_t^{n\mathbf{A}} = \left(\frac{\Psi_t^n}{L_t^{n\mathbf{A}}} \right) = \left(\frac{\Phi_t^n H_t^n}{L_t^{n\mathbf{A}}} \right) \sum_{j=1}^J (\gamma^{nj})^{-1} \pi_t^{nj}. \quad (\text{A.72})$$

Taking time differences of $E_t^{n\mathbf{A}}$, it follows:

$$\dot{E}_{t+1}^{n\mathbf{A}} = \frac{E_{t+1}^{n\mathbf{A}}}{E_t^{n\mathbf{A}}} = \left(\frac{\sum_{j=1}^J (\gamma^{nj})^{-1} \pi_{t+1}^{nj}}{\sum_{k=1}^J (\gamma^{nk})^{-1} \pi_t^{nk}} \right) \left(\frac{\dot{\Phi}_{t+1}^n \dot{H}_{t+1}^n}{\dot{L}_{t+1}^{n\mathbf{A}}} \right). \quad (\text{A.73})$$

Next, consider the income of households working in the non-agricultural sector from equation (21). Taking time differences of $E_t^n M$, it is straight to show:

$$\dot{E}_{t+1}^n M = \frac{E_{t+1}^n M}{E_t^n M} = \dot{A}_{t+1}^n (\dot{L}_{t+1}^n)^{\xi^n - 1} (\dot{S}_{t+1}^n)^{1 - \xi^n}. \quad (\text{A.74})$$

6) Crop market clearing

Proof of Equation (37) — Consider the market clearing condition for goods in equation (22). Multiplying p_t^{nj} on both sides, the market clearing condition now becomes equating the value of production and the total value of exports:

$$\begin{aligned} p_t^{nj} q_t^{nj} &= \sum_{m \in \mathcal{N}} \tau_t^{n,m,j} p_t^{nj} c_t^{n,m,j} \\ &= \sum_{m \in \mathcal{N}} X_t^{n,m,j}, \end{aligned} \quad (\text{A.75})$$

where $c_t^{n,m,j} = \sum_{s \in \mathcal{S}} c_t^{n,ms,j} L_t^{ms}$ is the total consumption of good j in country m , imported from country n . Note that $X_t^{n,m,j} = \tau_t^{n,m,j} p_t^{nj} c_t^{n,m,j}$ is the trade value of crop j from country n to country m . Expressing the above equation in time differences, it follows:

$$\dot{p}_{t+1}^{nj} \dot{q}_{t+1}^{nj} = \frac{\sum_{m \in \mathcal{N}} X_{t+1}^{n,m,j}}{\sum_{\tilde{m} \in \mathcal{N}} X_t^{n,\tilde{m},j}}, \quad (\text{A.76})$$

By definition, the country- and crop-level optimal revenue is $\Psi_t^{nj} = p_t^{nj} q_t^{nj}$, hence $\dot{\Psi}_t^{nj} = \dot{p}_{t+1}^{nj} \dot{q}_{t+1}^{nj}$. Taking time differences of Ψ_t^{nj} from equation (15), the LHS of the above equation is obtained by:

$$\dot{\Psi}_{t+1}^{nj} = \frac{\Psi_{t+1}^{nj}}{\Psi_t^{nj}} = (\dot{R}_{t+1}^{nj} \dot{A}_{t+1}^{nj})^\theta (\dot{\Phi}_{t+1}^n)^{1-\theta} \dot{H}_{t+1}^n. \quad (\text{A.77})$$

Then the market clearing condition becomes:

$$\begin{aligned} \sum_{m \in \mathcal{N}} X_{t+1}^{n,m,j} &= (\dot{R}_{t+1}^{nj} \dot{A}_{t+1}^{nj})^\theta (\dot{\Phi}_{t+1}^n)^{1-\theta} \dot{H}_{t+1}^n \left(\sum_{\tilde{m} \in \mathcal{N}} X_t^{n,\tilde{m},j} \right), \quad \text{for } j \in \mathcal{J}^c \\ \text{with } X_{t+1}^{n,m,j} &= \dot{i}_{t+1}^{n,m,j} \dot{p}_{t+1}^{nj} \dot{c}_{t+1}^{n,m,j} X_t^{n,m,j}. \end{aligned} \quad (\text{A.78})$$

Now, consider the definition of $c_t^{n,m,j}$, where the country-level consumption of each imported crop is the sum of all consumption of that crop consumed by households across all sectors. Substituting the expressions for optimal consumption $c_t^{n,ms,j}$, $c_t^{ns,j}$, and $c_t^{ns,A}$ from equation (A.58), (A.52), and (A.50), respectively, it follows:

$$\begin{aligned} c_t^{n,m,j} &= \sum_{s \in \mathcal{S}} c_t^{n,ms,j} L_t^{ms} \\ &= \phi^{n,m,j} \phi^{m,j} \phi^m \left(\frac{p_t^{n,m,j}}{P_t^{mj}} \right)^{-\delta} \left(\frac{P_t^{mj}}{P_t^m} \right)^{-\varkappa} \left(\frac{1}{P_t^m} \right) \sum_{s \in \mathcal{S}} E_t^{ms} L_t^{ms}. \end{aligned} \quad (\text{A.79})$$

Taking time differences, $\dot{c}_{t+1}^{n,m,j}$ is obtained by

$$\begin{aligned}\dot{c}_{t+1}^{n,m,j} &= \frac{\sum_{s \in \mathcal{S}} c_{t+1}^{n,ms,j} L_{t+1}^{ms}}{\sum_{z \in \mathcal{S}} c_t^{n,mz,j} L_t^{mz}} \\ &= \left(\frac{\dot{p}_{t+1}^{n,m,j}}{\dot{P}_{t+1}^{mj}} \right)^{-\delta} \left(\frac{\dot{P}_{t+1}^{mj}}{\dot{P}_{t+1}^m} \right)^{-\varkappa} \left(\frac{1}{\dot{P}_{t+1}^m} \right) \left(\frac{\sum_{s \in \mathcal{S}} \dot{E}_{t+1}^{ms} \dot{L}_{t+1}^{ms} E_t^{ms} L_t^{ms}}{\sum_{z \in \mathcal{S}} E_t^{mz} L_t^{mz}} \right).\end{aligned}\quad (\text{A.80})$$

Substituting $\dot{c}_{t+1}^{n,m,j}$ from the above into $X_{t+1}^{n,m,j}$, the transition of trade flows is captured by:

$$\begin{aligned}X_{t+1}^{n,m,j} &= \dot{\tau}_{t+1}^{n,m,j} \dot{p}_{t+1}^{nj} \dot{c}_{t+1}^{n,m,j} X_t^{n,m,j} \\ &= \left(\frac{\dot{\tau}_{t+1}^{n,m,j} \dot{p}_{t+1}^{nj}}{\dot{P}_{t+1}^{mj}} \right)^{1-\delta} \left(\frac{\dot{P}_{t+1}^{mj}}{\dot{P}_{t+1}^m} \right)^{1-\varkappa} \left(\frac{\sum_{s \in \mathcal{S}} \dot{E}_{t+1}^{ms} \dot{L}_{t+1}^{ms} E_t^{ms} L_t^{ms}}{\sum_{z \in \mathcal{S}} E_t^{mz} L_t^{mz}} \right) X_t^{n,m,j}.\end{aligned}\quad (\text{A.81})$$

■

B.2 Proof of Proposition 2

Proof. The proof of the dynamic hat algebra for the sequential equilibrium component is following Caliendo et al. (2019). Consider the initial allocation of the economy, $(L_0, \pi_0, s_0, \mu_{-1}, X_0)$, and the converging sequence of exogenous time-varying fundamentals, $\{\dot{\Theta}_t\}_{t=0}^\infty$, as given.

Proof of Equation (38) — Consider the migration share from equation (8). Taking a ratio between $\mu_{t+1}^{ns,mz}$ and $\mu_t^{ns,mz}$, and multiplying and dividing by $\exp((\beta V_{t+1}^{\tilde{m}\tilde{z}} - \zeta^{ns,\tilde{m}\tilde{z}})/\nu)$ in the denominator, it follows:

$$\begin{aligned}\frac{\mu_{t+1}^{ns,mz}}{\mu_t^{ns,mz}} &= \frac{\frac{\exp((\beta V_{t+2}^{mz} - \zeta^{ns,mz})/\nu)}{\exp((\beta V_{t+1}^{mz} - \zeta^{ns,mz})/\nu)}}{\frac{\sum_{\tilde{m} \in \mathcal{N}} \sum_{\tilde{z} \in \mathcal{S}} \exp((\beta V_{t+2}^{\tilde{m}\tilde{z}} - \zeta^{ns,\tilde{m}\tilde{z}})/\nu)}{\sum_{\tilde{m} \in \mathcal{N}} \sum_{\tilde{z} \in \mathcal{S}} \exp((\beta V_{t+1}^{\tilde{m}\tilde{z}} - \zeta^{ns,\tilde{m}\tilde{z}})/\nu)} \left(\frac{\exp((\beta V_{t+1}^{\tilde{m}\tilde{z}} - \zeta^{ns,\tilde{m}\tilde{z}})/\nu)}{\exp((\beta V_{t+1}^{\tilde{m}\tilde{z}} - \zeta^{ns,\tilde{m}\tilde{z}})/\nu)} \right)} \\ &= \frac{\exp(V_{t+2}^{mz} - V_{t+1}^{mz})^{\beta/\nu}}{\sum_{\tilde{m} \in \mathcal{N}} \sum_{\tilde{z} \in \mathcal{S}} \exp(V_{t+2}^{\tilde{m}\tilde{z}} - V_{t+1}^{\tilde{m}\tilde{z}})^{\beta/\nu} \mu_t^{ns,\tilde{m}\tilde{z}}}.\end{aligned}\quad (\text{A.82})$$

Denoting $v_t^{ns} = \exp(V_t^{ns})$ and substituting into the above expression, $\mu_{t+1}^{ns,mz}$ is given by:

$$\mu_{t+1}^{ns,mz} = \frac{\mu_t^{ns,mz} (\dot{v}_{t+2}^{mz})^{\beta/\nu}}{\sum_{\tilde{m} \in \mathcal{N}} \sum_{\tilde{z} \in \mathcal{S}} \mu_t^{ns,\tilde{m}\tilde{z}} (\dot{v}_{t+2}^{\tilde{m}\tilde{z}})^{\beta/\nu}}. \quad (\text{A.83})$$

Proof of Equation (40) — Consider the Bellman equation (7) and take differences between V_{t+1}^{ns}

and V_t^{ns} . Multiplying and dividing by $\exp((V_{t+2}^{mz} - V_{t+1}^{mz})^{\beta/\nu})$ within the log term, it follows:

$$\begin{aligned}
V_{t+1}^{ns} - V_t^{ns} &= u_{t+1}^{ns} - u_t^{ns} \\
&\quad + \nu \log \left(\frac{\sum_{m \in \mathcal{N}} \sum_{z \in \mathcal{S}} \exp((\beta V_{t+2}^{mz} - \zeta^{ns,mz})/\nu)}{\sum_{\tilde{m} \in \mathcal{N}} \sum_{\tilde{z} \in \mathcal{S}} \exp((\beta V_{t+1}^{\tilde{m}\tilde{z}} - \zeta^{ns,\tilde{m}\tilde{z}})/\nu)} \left(\frac{\exp((\beta V_{t+1}^{mz} - \zeta^{ns,mz})/\nu)}{\exp((\beta V_{t+2}^{mz} - \zeta^{ns,mz})/\nu)} \right) \right) \\
&= u_{t+1}^{ns} - u_t^{ns} + \nu \left(\sum_{m \in \mathcal{N}} \sum_{z \in \mathcal{S}} \exp((V_{t+2}^{mz} - V_{t+1}^{mz})^{\beta/\nu}) \mu_t^{ns,mz} \right).
\end{aligned} \tag{A.84}$$

Taking exponential function on both sides yields the equilibrium condition (40):

$$\dot{v}_{t+1}^{ns} = \dot{\psi}_{t+1}^{ns} \left(\sum_{m \in \mathcal{N}} \sum_{z \in \mathcal{S}} \mu_t^{ns,mz} (\dot{v}_{t+2}^{mz})^{\beta/\nu} \right)^{\nu}, \tag{A.85}$$

where $\psi_t^{ns} = \exp(u_t^{ns})$, and u_t^{ns} satisfies the temporary equilibrium. ■

B.3 Policy analysis: Migration Costs

This subsection explains how the counterfactual analysis on migration costs is conducted in section 6.2. Let $\bar{\zeta}^{ns,mz}$ represent a counterfactual migration cost. The first analysis considers the counterfactual economy facing a sudden shock to migration cost in the initial period, which remains permanently, such that all migration costs become infinitely high, i.e., $\bar{\zeta}^{ns,mz} \rightarrow \infty$ for all n, s, m, z . Then it is straightforward to show that for, all $t \geq 0$,

$$\mu_t^{ns,mz} = \begin{cases} 1, & \text{if } n = m \text{ and } s = z, \\ 0, & \text{otherwise.} \end{cases} \tag{A.86}$$

Then the consumption equivalent variation can be obtained using the equation (50).

The second analysis considers a counterfactual economy where the cross-country international migration costs become infinitely large starting in the initial period and remain so permanently. In other words, the bilateral migration cost is $\zeta^{ns,mz}$ before the initial period ($t \leq -1$), but there is a sudden shock to the migration costs in the initial period ($t = 0$) such that $\bar{\zeta}^{ns,mz} \rightarrow \infty$, for $\forall n \neq m$. The migration costs for the domestic sectoral reallocation are assumed to remain unchanged, i.e., $\bar{\zeta}^{ns,mz} = \zeta^{ns,mz}$ for $\forall n = m$.

Given $\mu_{-1}^{ns,mz}$, the transition in migration share for the initial period is captured by,

$$\begin{aligned}
\frac{\mu_0^{ns,mz}}{\mu_{-1}^{ns,mz}} &= \frac{\frac{\exp((\beta V_1^{mz} - \bar{\zeta}^{ns,mz})/\nu)}{\exp((\beta V_0^{mz} - \zeta^{ns,mz})/\nu)}}{\frac{\sum_{\tilde{m} \in \mathcal{N}} \sum_{\tilde{z} \in \mathcal{S}} \exp((\beta V_1^{\tilde{m}\tilde{z}} - \bar{\zeta}^{ns,\tilde{m}\tilde{z}})/\nu)}{\sum_{\hat{m} \in \mathcal{N}} \sum_{\hat{z} \in \mathcal{S}} \exp((\beta V_0^{\hat{m}\hat{z}} - \zeta^{ns,\hat{m}\hat{z}})/\nu)} \left(\frac{\exp((\beta V_0^{\tilde{m}\tilde{z}} - \zeta^{ns,\tilde{m}\tilde{z}})/\nu)}{\exp((\beta V_0^{\hat{m}\hat{z}} - \zeta^{ns,\hat{m}\hat{z}})/\nu)} \right)} \\
&= \frac{\exp((V_1^{mz} - V_0^{mz}) - \frac{1}{\beta}(\bar{\zeta}^{ns,mz} - \zeta^{ns,mz}))^{\beta/\nu}}{\sum_{\tilde{m} \in \mathcal{N}} \sum_{\tilde{z} \in \mathcal{S}} \exp((V_1^{\tilde{m}\tilde{z}} - V_0^{\tilde{m}\tilde{z}}) - \frac{1}{\beta}(\bar{\zeta}^{ns,\tilde{m}\tilde{z}} - \zeta^{ns,\tilde{m}\tilde{z}}))^{\beta/\nu} \mu_t^{ns,\tilde{m}\tilde{z}}}.
\end{aligned} \tag{A.87}$$

Applying $\bar{\zeta}^{ns,mz} \rightarrow \infty$, for $\forall n \neq m$, and $\bar{\zeta}^{ns,mz} = \zeta^{ns,mz}$ for $\forall n = m$, the transition in migration share, for all $t \geq -1$, is captured by:

$$\mu_{t+1}^{ns,mz} = \begin{cases} 0, & \text{if } n \neq m \\ \frac{\mu_t^{ns,nz}(\dot{v}_{t+2}^{nz})^{\beta/\nu}}{\sum_{\tilde{z} \in S} \mu_t^{ns,n\tilde{z}}(\dot{v}_{t+2}^{n\tilde{z}})^{\beta/\nu}}, & \text{if } n = m \end{cases} \quad (\text{A.88})$$

Then, as in the previous analysis, the consumption equivalent variation can be obtained using the equation (50).

C Details of Data

C.1 GAEZ: Potential Yield

This section outlines the calculation of potential yield at the country level, adjusted for irrigation availability. Let $f \in \mathcal{F}^n$ denote a field in the GAEZ data (at 5 arc-minute spatial resolution), where \mathcal{F}^n is the set of fields in the country n . The GAEZ data provides potential yields for both irrigated conditions, $\mathcal{A}_t^{nj,\text{irr}}(f)$, and rain-fed conditions, $\mathcal{A}_t^{nj,\text{rain}}(f)$, for each field f . It also includes information on the spatial distribution of irrigation availability, given as the share of total croplands, $s^{n,\text{total}}(f)$, and the share of irrigated croplands, $s^{n,\text{irr}}(f)$, for each field f . It is straightforward to calculate the share of rain-fed croplands in field f as $s^{n,\text{rain}}(f) = s^{n,\text{total}}(f) - s^{n,\text{irr}}(f)$. For each field f where the share of croplands is nonzero, the average potential yield—adjusted for irrigation availability—is calculated as follows:

$$\tilde{\mathcal{A}}_t^{nj}(f) = \frac{\mathcal{A}_t^{nj,\text{irr}}(f)s^{n,\text{irr}}(f) + \mathcal{A}_t^{nj,\text{rain}}(f)s^{n,\text{rain}}(f)}{s^{n,\text{total}}(f)}, \quad \text{for } s^{n,\text{total}}(f) \neq 0 \quad (\text{A.89})$$

The country-level potential yield, adjusted for irrigation availability, is constructed as follows:

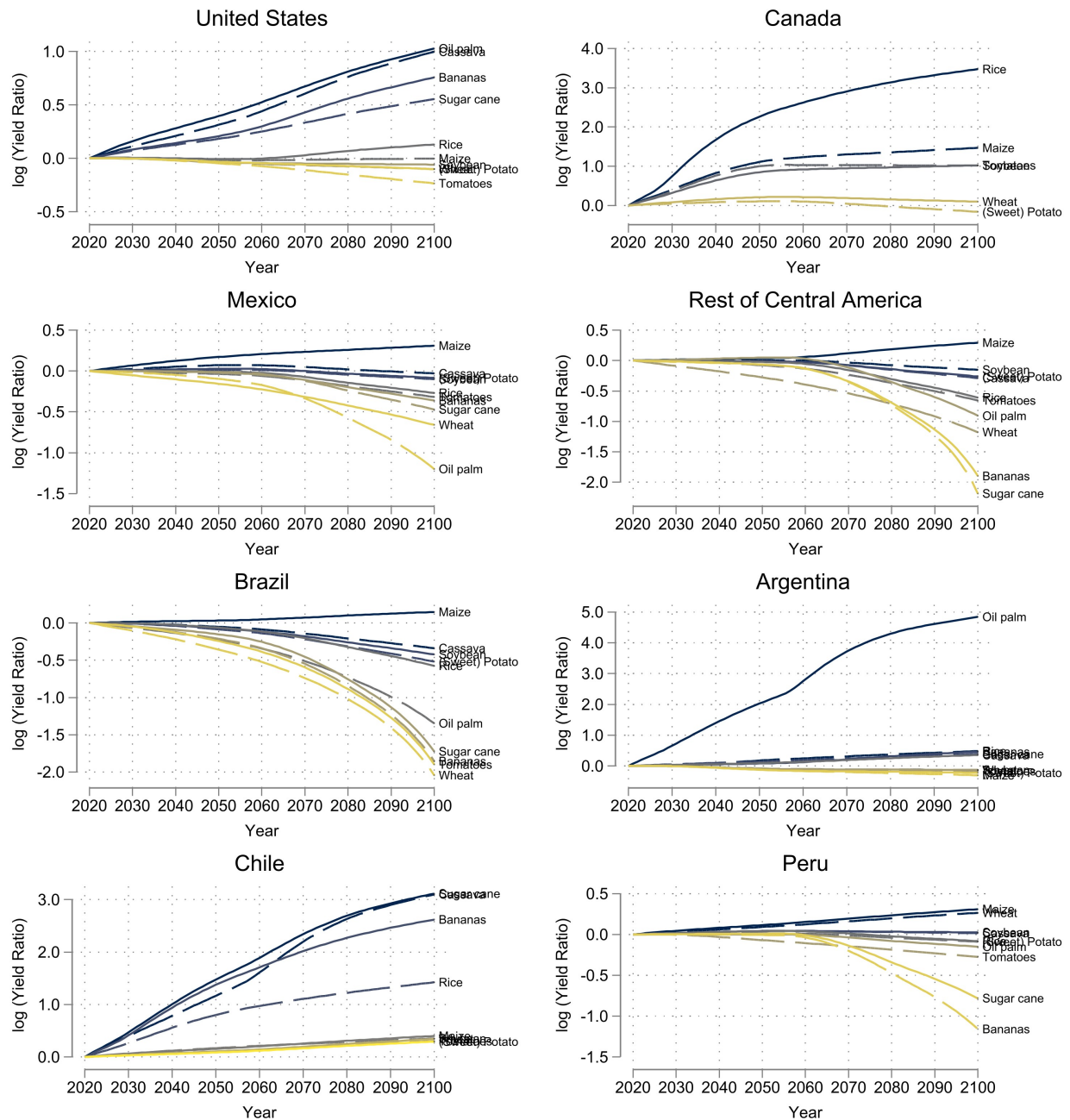
$$\mathcal{A}_t^{nj} = \frac{\sum_{f \in \mathcal{F}^n} \tilde{\mathcal{A}}_t^{nj}(f) \mathbb{1}\{s^{n,\text{total}}(f) > 0\}}{F^n}, \quad (\text{A.90})$$

where F^n is the total number of fields in country n . Note that if a field is currently not used as cropland, then there is no weight assigned to that field to compute the country-level potential yield. In other words, this study evaluates the changes in potential yield for land within a country that is currently utilized as cropland. The conversion between croplands and non-croplands is out of the scope of this study.

The agro-climatic potential yield estimates are provided as 30-year averages for both historical and future periods under each climate change scenario: 1981-2010 (1990s) for the current period, and 2011-2040 (2020s), 2041-2070 (2050s), and 2071-2100 (2080s) for the future. After constructing the irrigation-adjusted potential yields for these 30-year averages, I assign the average values as the annual yield for the years 1995, 2025, 2055, and 2085, respectively. Using the potential yield values for 2055 and 2085, I perform linear extrapolation to generate a prediction for 2100. Then, based on the values for 2025, 2055, and 2085, and the predicted values for 2100, I apply cubic interpolation to create a smooth annual time path from 2020 to 2100. Given the annual time path, the time differences over 5-year step sizes, $\dot{\mathcal{A}}_{t+1}^{nj}$, are constructed. It is assumed $\dot{\mathcal{A}}_{t+1}^{nj} = 1$, after 2100.

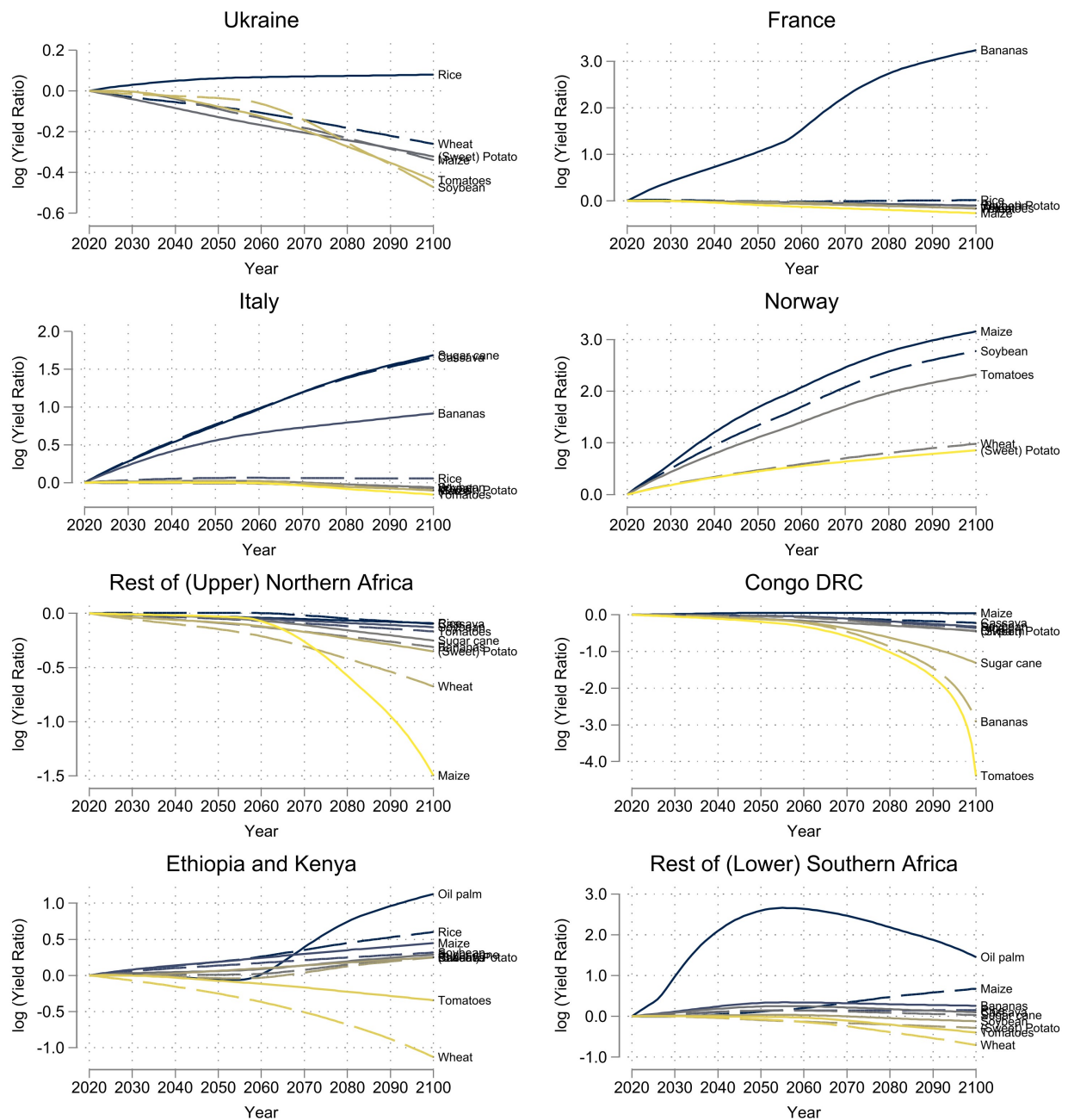
Figures C.1 to C.3 show the resulting dynamic transition in potential yield for major countries. The y-axis represents the logarithm of the yield ratio relative to the year 2020.

Figure C.1: Transition in Potential Yield - North and South America



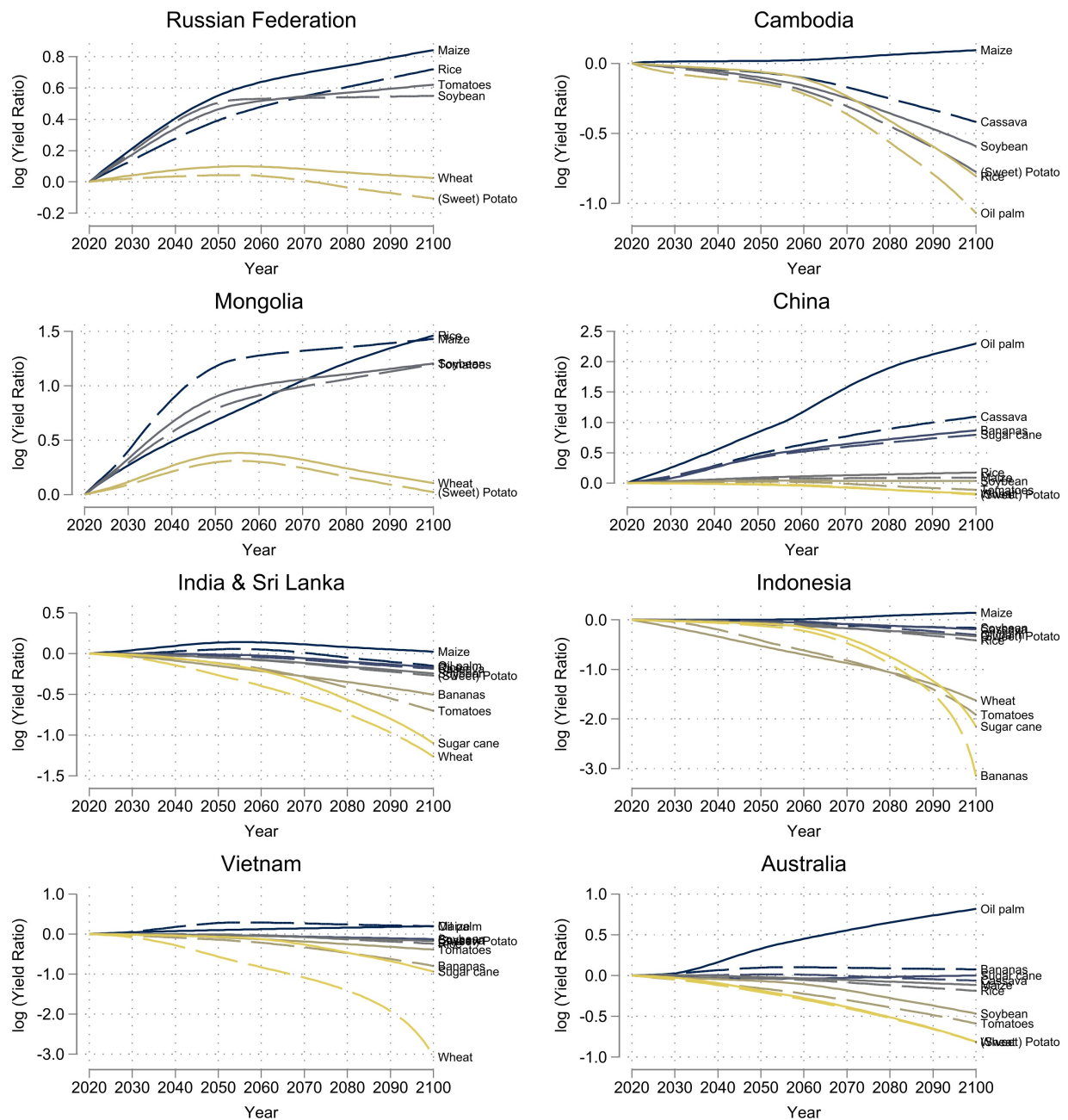
Notes: The figure above shows the changes in potential yield for major countries under the baseline climate change scenario RCP 8.5 (HadGEM2-ES). The x-axis shows the year for the period 2020-2100, and the y-axis represents the logarithm of the yield ratio relative to the year 2020. For each country, crops are plotted when their potential yield is nonzero in the base year 2020.

Figure C.2: Transition in Potential Yield - Europe and Africa



Notes: The figure above shows the changes in potential yield for major countries under the baseline climate change scenario RCP 8.5 (HadGEM2-ES). The x-axis shows the year for the period 2020-2100, and the y-axis represents the logarithm of the yield ratio relative to the year 2020. For each country, crops are plotted when their potential yield is nonzero in the base year 2020.

Figure C.3: Transition in Potential Yield - Asia and Oceania



Notes: The figure above shows the changes in potential yield for major countries under the baseline climate change scenario RCP 8.5 (HadGEM2-ES). The x-axis shows the year for the period 2020-2100, and the y-axis represents the logarithm of the yield ratio relative to the year 2020. For each country, crops are plotted when their potential yield is nonzero in the base year 2020.

C.2 GAEZ: Multicropping classification

Table 5 presents the multicropping zone classifications from the GAEZ Module 2, version 4. The GAEZ project categorizes global land into 9 zones based on their multicropping potential, ranging from no cropping to triple rice cropping (Fischer et al., 2021). Multicropping can involve either planting different crops (e.g., maize and beans) or growing the same crop (e.g., rice) sequentially in the same field after harvest. While multicropping in practice often entails specific crop combinations to optimize production, the current GAEZ data only indicates the number of potential multicropping practices for all crops, excluding rice. To address this data limitation and simplify model quantification, I have consolidated the 9 zones into 4 classifications, ranging from zero to triple cropping, regardless of crop type. I take a conservative approach in regrouping the classifications, reassigning multicropping zones only when all crops, including rice, can be grown multiple times. These classifications are summarized in the third column of Table 5.

Table 5: Multicropping zone classification (GAEZ v4)

Zone	Name	Value
A	Zone of no cropping	0
B	Zone of single cropping	1
C	Zone of limited double cropping (relay cropping; single wetland rice may be possible)	1
D	Zone of double cropping (sequential double cropping including wetland rice is not possible)	1
E	Zone of double cropping with rice (sequential cropping with one wetland rice crop is possible)	2
F	Zone of double rice cropping or limited triple cropping (may partly involve relay cropping; a third crop is not possible in case of two wetland rice crops)	2
G	Zone of triple cropping (sequential cropping of three short-cycle crops; two wetland rice crops are possible)	2
H	Zone of triple rice cropping (sequential cropping of three wetland rice crops is possible)	3

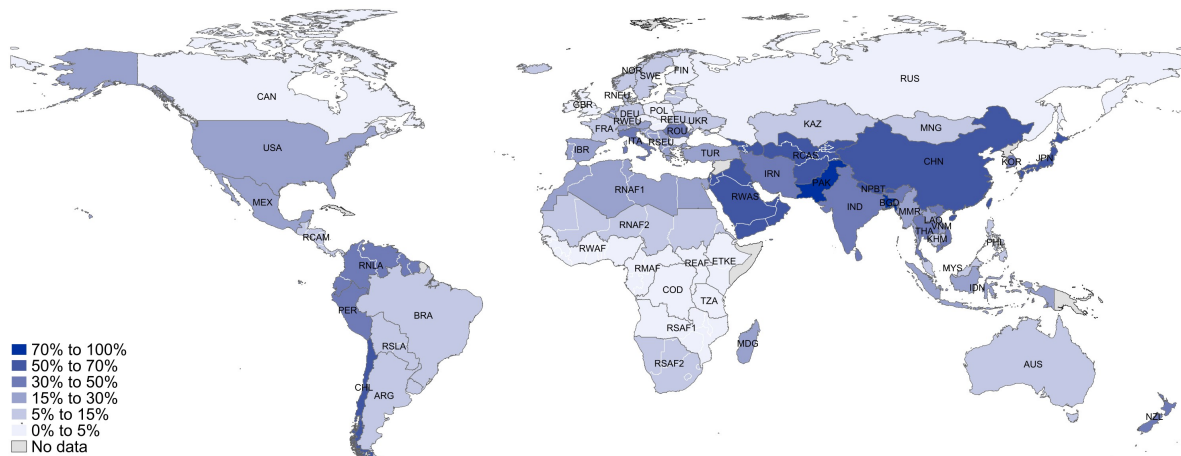
After reassigning the potential number of multicropping practices at the spatial unit level in the original GAEZ data, I aggregate the results at the country level, which is the unit of analysis for this study. Given the field-level multicropping potentials at irrigated conditions, $N_t^{n,\text{irr}}(f)$, and rain-fed conditions, $N_t^{n,\text{rain}}(f)$, the country-level multicropping potential adjusted for irrigation, N_t^n , is constructed using an approach similar to that used for potential yield, as detailed in Appendix C.1.²⁵

²⁵The only difference here is the use of the annual projection for the year 2099 from the GAEZ data, rather than using a linear extrapolation to generate a prediction for the year 2100. Cubic interpolation is then applied to fill in the annual values, similar to the potential yield data. While the GAEZ data offers both annual and 30-year average projections for multicropping zone information, the annual projections are not smooth over time. Therefore, the 30-year averages are used to construct a smoother trajectory to reflect the long-term trend.

C.3 GAEZ: Irrigation Distribution

Figure C.4 presents the share of croplands equipped for full control irrigation across countries in the current period, based on GAEZ data. Asian countries with a strong tradition of rice production tend to have a high share of irrigated lands. The figure also highlights that some of the most climate-vulnerable regions—particularly African countries—are less equipped with irrigation facilities, making them more severely impacted by climate change shocks in terms of both potential yield and multicropping capacity.

Figure C.4: Share of Croplands with Irrigation by Country



Note: The graph above illustrates the share of croplands equipped for irrigation among croplands in each country in the current period.

C.4 Details for Other Dataset

FAO: Price, Production, and Harvest areas — As noted in previous studies ([Costinot et al., 2016](#); [Gouel and Laborde, 2021](#)), the crop-level variables from the FAO data contain missing values in the database. Motivated by the approach in [Costinot et al. \(2016\)](#), missing values for price, production, and harvest areas in the FAO dataset are imputed by regressing the logarithm of each variable on a set of fixed effects: country-by-crop fixed effects, time-by-crop fixed effects, country fixed effects, and time fixed effects. Standard errors are clustered at the country-by-crop level. The imputation is performed using panel data covering the period from 1990 to 2021. For production and harvest area variables, zeros are assigned when the entire set of observations for a given country-crop pair is either zero or missing in the original panel data.

For crop price data, a slightly modified approach is used. First, missing values are imputed using the same set of fixed effects applied to the production and harvest area variables, provided that at least one observation exists for the country-crop pair (with the country identified by ISO3 code) over the entire data period. If no data are available at the country-crop level, the country fixed effects and country-by-crop fixed effects are replaced with “iso-major” fixed effects and “iso-major”-by-crop fixed effects, respectively, where “iso-major” refers to an aggregated country classification. Then the regression is repeated to impute missing values. This process is further continued by sequentially replacing “iso-major” fixed effects (and the corresponding “iso-major”-by-crop fixed effects) with “sub-region” fixed effects and, subsequently, with “region” fixed effects until all missing values are filled. The idea is to utilize the most closely related available data for imputation. The classifications of “iso-major”, “sub-region”, and “region” are provided in Table 10 in Appendix 10.

WIOD — The labor intensity parameter for non-agricultural production (ξ^n) is obtained as the share of labor compensation in total value added from the World Input-Output Database (WIOD) in the year 2014. The WIOD data primarily covers OECD countries, with limited representation of developing economies. For missing developing countries, the average labor share of the “sub-region” group to which the country belongs is used (see Table 10) if such data is available. When sub-regional averages are unavailable—primarily for African and ‘Central Asia’ countries—the average labor share of four observable low-income countries (India, Mexico, Turkey, and Indonesia) is applied.

D Details of Model Quantification

D.1 Solution Algorithm

The computational algorithm used to solve the sequential equilibrium similarly follows the approach in [Caliendo et al. \(2019\)](#). The model solution in this paper is obtained using GAMS (General algebraic modeling system) version 45.07 with CONOPT solver.

Step1) Initialization

Take the initial allocation of the observed economy $(L_0^{ns}, \pi_0^{nj}, s_0, \mu_{-1}^{ns,mz}, X_0^{n,m,j})$ and the converging sequence of exogenous time-varying fundamentals $\{\dot{\Theta}_t\}_{t=1}^T$ as given. Generate an initial guess ($i = 1$) of the path $\{\dot{v}_{t+1}^{ns(i)}\}_{t=0}^T$.

Step2) Updating path of labor supply

Given $\mu_{-1}^{ns,mz}$ and i -th guess $\{\dot{v}_{t+1}^{ns(i)}\}_{t=0}^T$, generate a path of $\{\mu_t^{ns,mz(i)}\}_{t=0}^T$ using equation (38). Next, given $L_0^{ns(i)}$ and path of $\{g_t^n\}_{t=0}^T$ and $\{\mu_t^{ns,mz(i)}\}_{t=0}^T$, compute a path of $\{\dot{L}_{t+1}^{ns(i)}\}_{t=0}^T$ using equation (39).

Step3) Solving the temporary equilibrium

Given the path of labor supply $\{\dot{L}_{t+1}^{ns(i)}\}_{t=0}^T$, solve the set of nonlinear equations (24)-(37) for each period $t \geq 0$. Constrained optimization solver CONOPT is used with the objective of minimizing the goods market residual $\epsilon_t^{X(i)}$ defined from equation (37) as follows:

$$\epsilon_t^{X(i)} = \max_{n \in \mathcal{N}, j \in \mathcal{J}} \left| \sum_{m \in \mathcal{N}} X_{t+1}^{n,m,j} - (\dot{R}_{t+1}^{nj} \dot{A}_{t+1}^{nj})^\theta (\dot{\Phi}_{t+1}^n)^{1-\theta} \dot{H}_{t+1}^n \left(\sum_{\tilde{m} \in \mathcal{N}} X_t^{n,\tilde{m},j} \right) \right|. \quad (\text{A.91})$$

Check if $\epsilon_t^{X(i)} < \epsilon^X$, where ϵ^X denotes the tolerance for market clearing condition.

Step4) Updating path of utility

Given the path of temporary equilibrium $\{\dot{C}_{t+1}^{ns(i)}\}_{t=0}^T$, update the path of $\{\dot{u}_{t+1}^{ns(i)}\}_{t=0}^T$. Note that $\dot{v}_T^{ns} = 1$ for a large enough $T > 0$. Given $\{\dot{u}_{t+1}^{ns(i)}\}_{t=0}^T$, update $(i + 1)$ -th guess $\{\dot{v}_{t+1}^{ns(i+1)}\}_{t=0}^T$ backward using equation (40) from the terminal period $T > 0$.

Step5) Check convergence

Check if $\{\dot{v}_{t+1}^{ns(i+1)}\}_{t=0}^T \simeq \{\dot{v}_{t+1}^{ns(i)}\}_{t=0}^T$ using the criteria as follows. Iterate through Steps 2 to 4 for $i = 1, 2, \dots$ until convergence.

$$\left| \frac{\dot{v}_{t+1}^{ns(i+1)} - \dot{v}_{t+1}^{ns(i)}}{\dot{v}_{t+1}^{ns(i+1)}} \right| < \epsilon^v. \quad (\text{A.92})$$

D.2 Construction of Migration Flows

This section details the construction of expanded migration flow estimates at both the cross-country and cross-sector levels. The analysis utilizes international migration flow estimates from [Abel and Cohen \(2019\)](#), which provide data at the cross-country level for the period 1990-2015 in 5-year intervals.²⁶ The primary objective is to extend these cross-country migration flow estimates to incorporate cross-sector dimensions, as illustrated in Table 6. Expanding this migration flow matrix to the sectoral level is crucial, particularly because it captures structural transformation between sectors—within-country labor reallocation from agriculture to non-agriculture.

Table 6: Expanding Migration Flow Estimates

		t+1		t+1	
		n	m	n, A	n, M
t		n		m, A	m, M

expand \Rightarrow

		t+1		t+1	
		n, A	n, M	m, A	m, M
t		n, A		m, A	m, M

Notes: The rows represent the origin of migration flows at time t , while the columns represent the destination of migration flows at time $t + 1$. For instance, the element $(n \mathbf{A}, m \mathbf{M})$ refers to migration flows from the labor market of country n in sector \mathbf{A} at time t to the labor market of country m in sector \mathbf{M} at time $t + 1$.

Step 1) International Gross Migration Flows

The first step is to match international gross migration flows from [Abel and Cohen \(2019\)](#) with the model. Recall the transition of labor supply from equation (39),

$$L_{t+1}^{ns} = \sum_{m \in \mathcal{N}} \sum_{z \in \mathcal{S}} \mu_t^{mz, ns} (1 + g_t^m) L_t^{mz}. \quad (\text{A.93})$$

Note that we are provided with country-level migration flow estimates. Let $\mathbb{L}_{t+1}^{m,n}$ denote the cross-country migration flows from country m to country n . Matching $\mathbb{L}_{t+1}^{m,n}$ with data from [Abel and Cohen \(2019\)](#), by definition, it follows:

$$\mathbb{L}_{t+1}^{m,n} = \sum_{s \in \mathcal{S}} \sum_{z \in \mathcal{S}} \mu_t^{mz, ns} (1 + g_t^m) L_t^{mz}, \quad \text{for } m \neq n. \quad (\text{A.94})$$

Assuming population growth is realized at the end of the period, the cross-country migration flows before population growth is given by:

$$\frac{\mathbb{L}_{t+1}^{m,n}}{(1 + g_t^m)} = \sum_{s \in \mathcal{S}} \sum_{z \in \mathcal{S}} \mu_t^{mz, ns} L_t^{mz}, \quad \text{for } m \neq n, \quad (\text{A.95})$$

where the population growth rate is calculated as the difference between the birth rate and the death rate, sourced from World Bank data. While agricultural populations often have a higher birth rate

²⁶Among the several international migration flow estimates provided by [Abel and Cohen \(2019\)](#), estimates using closed demographic accounting methods with pseudo-Bayesian method were employed.

than populations in non-agriculture, due to data limitations, the same population growth rate is applied to both sectors.

Step 2) International Cross-Sectoral Migration Flows

To construct international cross-sectoral migration flows, an additional assumption is introduced: international cross-sector migration flows are assumed to be proportional to the sectoral population compositions of the origin and destination countries, respectively. Denoting e_t^{ns} as the employment share in country n and sector s at time t , cross-country migration flows from labor market mz to labor market ns before population growth is given by:

$$\mu_t^{mz,ns} L_t^{mz} = e_t^{mz} e_t^{ns} \mathbb{L}_{t+1}^{m,n} / (1 + g_t^m), \quad \text{for } m \neq n, \quad (\text{A.96})$$

where $\sum_{s \in S} e_t^{ns} = 1$ by definition. This assumption is applied exclusively to international migration flows, i.e., $m \neq n$. While international cross-sector migration flows constructed under this approach may inherently contain some errors, their impact on the results is likely to be negligible, given that gross international migration flows remain relatively small—below 1% at the global level, as depicted in Table 6. Instead, the focus is on capturing domestic cross-sector migration flows, which play a more critical role in driving structural changes in labor markets.

Step 3) Domestic Sectoral Net Migration Flows

Given international cross-sector migration flows and population growth rates, domestic cross-sector net migration flows can be recovered. Let us first focus on the population inflows based on population at time $t + 1$. The equation (A.93) can be decomposed into international inflows and domestic inflows for the non-agricultural and agricultural sectors, respectively, as follows:

$$L_{t+1}^{nM} = \underbrace{\sum_{m \neq n} \sum_{z \in S} \mu_t^{mz,nM} (1 + g_t^m) L_t^{mz}}_{\text{Cross-border inflows}} + \underbrace{\mu_t^n A, nM (1 + g_t^n) L_t^{nA} + \mu_t^n M, nM (1 + g_t^n) L_t^{nM}}_{\text{Domestic inflows}} \quad (\text{A.97})$$

$$L_{t+1}^{nA} = \underbrace{\sum_{m \neq n} \sum_{z \in S} \mu_t^{mz,nA} (1 + g_t^m) L_t^{mz}}_{\text{Cross-border inflows}} + \underbrace{\mu_t^n M, nA (1 + g_t^n) L_t^{nA} + \mu_t^n A, nA (1 + g_t^n) L_t^{nA}}_{\text{Domestic inflows}}, \quad (\text{A.98})$$

where the first component on the RHS is the international migration inflows into the labor market nM (or nA), while the second and third components together are domestic migration inflows. A similar decomposition can be done for the population outflows based on the population at time t . For each sector, the population at time t prior to population growth is, by definition, given by:

$$L_t^{nM} = \underbrace{\sum_{m \neq n} \sum_{z \in S} \mu_t^{nM,mz} L_t^{nM}}_{\text{Cross-border outflows}} + \underbrace{\mu_t^n M, nA L_t^{nM} + \mu_t^n M, nM L_t^{nM}}_{\text{Domestic outflows}} \quad (\text{A.99})$$

$$L_t^{nA} = \underbrace{\sum_{m \neq n} \sum_{z \in S} \mu_t^{nA,mz} L_t^{nA}}_{\text{Cross-border outflows}} + \underbrace{\mu_t^n A, nM L_t^{nA} + \mu_t^n A, nA L_t^{nA}}_{\text{Domestic outflows}}, \quad (\text{A.100})$$

where the first term on the RHS is the international migration outflows departing from the labor market nM , and the second and third terms are domestic migration outflows.

Given the identity equations in inflows and outflows, domestic cross-sector net flows can be recovered. Dividing equation (A.97) by $(1 + g_t^n)$ on both sides and subtracting with equation (A.99), it follows:

$$\frac{L_{t+1}^n M}{(1 + g_t^n)} - L_t^n M = \underbrace{\left(\mu_t^{n A, n M} L_t^n A - \mu_t^{n M, n A} L_t^n M \right)}_{= \mathcal{P}_t^n} + \left(\underbrace{\frac{1}{(1 + g_t^n)} \sum_{m \neq n} \sum_{z \in S} \mu_t^{mz, n M} (1 + g_t^m) L_t^{mz}}_{\text{Cross-border inflows}} - \underbrace{\sum_{m \neq n} \sum_{z \in S} \mu_t^{n M, mz} L_t^n M}_{\text{Cross-border outflows}} \right) \quad (\text{A.101})$$

Note that the first term on the RHS, defined as $\mathcal{P}_t^n = \left(\mu_t^{n A, n M} L_t^n A - \mu_t^{n M, n A} L_t^n M \right)$, is domestic cross-sector net flows. If $\mathcal{P}_t^n > 0$, there is a positive net flow from agriculture to non-agricultural sector within the country, and if $\mathcal{P}_t^n < 0$, vice versa. Given the cross-country migration flows from equation (A.96), the domestic sectoral net flows \mathcal{P}_t^n is obtained by:

$$\mathcal{P}_t^n = \left(\frac{L_{t+1}^n M}{(1 + g_t^n)} - L_t^n M \right) - \left(\underbrace{\frac{1}{(1 + g_t^n)} \sum_{m \neq n} \sum_{z \in S} e_t^{mz} e_t^n M \mathbb{L}_{t+1}^{m,n}}_{\text{Cross-border inflows}} - \underbrace{\frac{1}{(1 + g_t^n)} \sum_{m \neq n} \sum_{z \in S} e_t^n M e_t^{mz} \mathbb{L}_{t+1}^{n,m}}_{\text{Cross-border outflows}} \right) \quad (\text{A.102})$$

The above equation suggests that domestic cross-sector net flows can be constructed such that they exactly capture observed changes in sectoral population over time. Note, however, that only the net flows can be captured, not the level of cross-sector migration flows. In other words, in order to identify the level of domestic migration flows from agriculture to non-agriculture, this approach requires additional information on the level of domestic migration flows from non-agriculture to agriculture (or vice versa). While it is reasonable to expect that the share of migration flows from non-agriculture to agriculture is relatively smaller than the opposite flows in most countries, one cannot simply assume this flow to be zero. Such an assumption not only misrepresents actual migration flows but may also prevent the model from obtaining the sequential equilibrium solution. Note that, under steady-state conditions, the inflow and outflow of population should be balanced in every labor market, such that there are no changes in any labor markets over time. If a labor market experiences only population outflows, with no inflows from either within or across countries, its population will continuously decline over time and will never reach a steady state.

Step4) Domestic Sectoral Migration Flows

To recover the level of domestic sectoral migration flows, I obtain additional information on domestic migration flows from non-agriculture to agriculture. Given the limited data availability for most countries, I consider domestic sectoral flows in the U.S. as a reference. The Census Bureau's March Current Population Survey (CPS) provides individual-level data, including information on the previous year's employment, industry, wages, and current employment status and industry at the time of the survey. Following a similar approach to [Artuç et al. \(2010\)](#), I clean the data to construct migration flows. I focus on male respondents aged 25 to 65 who are currently employed

and worked at least 26 weeks in the previous year. Individuals with zero wage and salary income are excluded, as well as those in the top 99th percentile of wage and salary income. A worker's industry is classified as agriculture if it falls under 'Crop production,' 'Animal production,' 'Forestry except logging,' 'Logging,' 'Fishing, hunting, and trapping,' or 'Support activities for agriculture and forestry.' This definition of agriculture is broader than crop production itself but is used to be consistent with the definition of the agricultural sector in country-level macro data.

Using the CPS survey, I construct the annual domestic migration flow matrix for each period and then multiply the five consecutive annual matrices to construct a quinquennial domestic migration flow matrix. Using data covering the period 1990-2019, I construct the quinquennial domestic migration flow matrix for 1990-1994, 1995-1999, 2000-2004, 2005-2009, 2010-2014, and 2015-2019. The table 7 presents the mean of quinquennial domestic migration flows for the period 1990-2019, showing that, for non-agricultural workers, only 0.54% goes to the agricultural sector in the next period, while 99.46% stays in the non-agricultural sector.

Table 7: Quinquennial Domestic Migration Flows in the US (1990-2019)

	Ag	Non-ag
Ag	0.5730 (0.0898)	0.4270 (0.0898)
Non-ag	0.0054 (0.0009)	0.9946 (0.0009)

Notes: Rows represent the origin sector and columns represent the destination sector. Each cell shows the mean migration flow rates over 5-year intervals over the period 1990-2019, with standard deviation in parenthesis.

Using US data as a reference, I assume that the level of the domestic sectoral migration flow to be $\varpi = 0.54\%$ on the lower side for all countries.²⁷ Specifically, if there is a positive domestic net flow from agriculture to non-agriculture, i.e., $\mathcal{P}_t^n > 0$, then the domestic migration flows from non-agriculture to agriculture is set at $\varpi = 0.54\%$. Then the level of domestic cross-sector migration flows can be characterized as:

$$\begin{aligned}\mu_t^{nM,nA} L_t^{nM} &= \varpi L_t^{nM} \\ \mu_t^{nA,nM} L_t^{nA} &= \mathcal{P}_t^n + \mu_t^{nM,nA} L_t^{nM}\end{aligned}\tag{A.103}$$

The recovered share of domestic flows from agriculture to non-agriculture in the US from this approach is 39.07% for the period 2015-2019, which is comparable to the value 42.7% directly constructed from CPS individual data. Similarly, if there is a positive net flow from non-agriculture to agriculture, i.e., $\mathcal{P}_t^n < 0$, the level of domestic cross-sector migration flows is constructed as follows:

$$\begin{aligned}\mu_t^{nA,nM} L_t^{nA} &= \varpi L_t^{nA} \\ \mu_t^{nM,nA} L_t^{nM} &= \mu_t^{nA,nM} L_t^{nA} - \mathcal{P}_t^n\end{aligned}\tag{A.104}$$

²⁷This assumption may not fully represent actual migration flows, as it imposes constant minimum flows for domestic sectoral migration. However, despite its strictness, the assumption facilitates achieving sequential equilibrium by preventing zero inflows in certain labor markets. Furthermore, this limitation is less concerning in the model, as these flows are likely to be small for most countries, and, importantly, changes in wages are driven by total population changes in each labor market. Therefore, what matters is the net migration flow, which is adequately captured by the approach used here.

After recovering $\mu_t^{n\mathbf{M},n\mathbf{A}} L_t^{n\mathbf{M}}$ and $\mu_t^{n\mathbf{A},n\mathbf{M}} L_t^{nA}$, the flow of stayers can be also recovered based on equation (A.97) and equation (A.98) as follows:

$$\mu_t^{n\mathbf{M},n\mathbf{M}} L_t^{n\mathbf{M}} = \frac{L_{t+1}^{n\mathbf{M}}}{(1 + g_t^n)} - \left\{ \frac{1}{(1 + g_t^n)} \sum_{m \neq n} \sum_{z \in \mathcal{S}} \mu_t^{mz,n\mathbf{M}} (1 + g_t^m) L_t^{mz} + \mu_t^{n\mathbf{A},n\mathbf{M}} L_t^{nA} \right\} \quad (\text{A.105})$$

$$\mu_t^{n\mathbf{A},n\mathbf{A}} L_t^{n\mathbf{A}} = \frac{L_{t+1}^{n\mathbf{A}}}{(1 + g_t^n)} - \left\{ \frac{1}{(1 + g_t^n)} \sum_{m \neq n} \sum_{z \in \mathcal{S}} \mu_t^{mz,n\mathbf{A}} (1 + g_t^m) L_t^{mz} + \mu_t^{n\mathbf{M},n\mathbf{A}} L_t^{nA} \right\} \quad (\text{A.106})$$

The expanded migration flow matrix is then fully constructed.

D.3 Estimation of Migration Elasticity

This section presents the derivation of equation (48), which is used to estimate the migration elasticity. The estimation strategy closely follows the approach in [Artuç et al. \(2010\)](#) and [Caliendo et al. \(2019\)](#), and relies on the expanded migration matrix constructed in the Appendix D.2.

Recall the equation (A.10),

$$\Xi_t^{ns} = \nu \log \sum_{\tilde{m} \in \mathcal{N}} \sum_{\tilde{z} \in \mathcal{S}} \exp \left(\frac{\beta V_{t+1}^{\tilde{m}\tilde{z}} - \zeta^{ns,\tilde{m}\tilde{z}}}{\nu} \right). \quad (\text{A.107})$$

Substituting the above expression in to equation (8), it follows

$$\begin{aligned} \mu_t^{ns,mz} &= \frac{\exp((\beta V_{t+1}^{mz} - \zeta^{ns,mz})/\nu)}{\sum_{\tilde{m} \in \mathcal{N}} \sum_{\tilde{z} \in \mathcal{S}} \exp((\beta V_{t+1}^{\tilde{m}\tilde{z}} - \zeta^{ns,\tilde{m}\tilde{z}})/\nu)} \\ &= \exp((\beta V_{t+1}^{mz} - \zeta^{ns,mz} - \Xi_t^{ns})/\nu). \end{aligned} \quad (\text{A.108})$$

Taking a ratio between $\mu_t^{ns,mz}$ and $\mu_t^{ns,ns}$ and taking a log on both sides, it follows:

$$\log(\mu_t^{ns,mz}/\mu_t^{ns,ns}) = \frac{\beta}{\nu}(V_{t+1}^{mz} - V_{t+1}^{ns}) - \frac{1}{\nu}(\zeta^{ns,mz} - \zeta^{ns,ns}). \quad (\text{A.109})$$

Similarly, taking a ratio between $\mu_t^{ns,mz}$ and $\mu_t^{mz,mz}$ and taking a log on both sides, it follows:

$$\log(\mu_t^{ns,mz}/\mu_t^{mz,mz}) = -\frac{1}{\nu}(\zeta^{ns,mz} - \zeta^{mz,mz}) - \frac{1}{\nu}(\Xi_t^{ns} - \Xi_t^{mz}). \quad (\text{A.110})$$

Recall that our Bellman equation (7) is simply written using Ξ_t^{ns} as follows:

$$V_t^{ns} = u_t^{ns} + \Xi_t^{ns}. \quad (\text{A.111})$$

Substituting $(V_{t+1}^{mz} - V_{t+1}^{ns})$ using equation (A.111), and $(\Xi_{t+1}^{mz} - \Xi_{t+1}^{ns})$ using equation (A.110) into the equation (A.109), it follows:

$$\begin{aligned} \log(\mu_t^{ns,mz}/\mu_t^{ns,ns}) &= \frac{\beta}{\nu}(V_{t+1}^{mz} - V_{t+1}^{ns}) - \frac{1}{\nu}(\zeta^{ns,mz} - \zeta^{ns,ns}) \\ &= \frac{\beta}{\nu}(u_{t+1}^{mz} - u_{t+1}^{ns}) + \frac{\beta}{\nu}(\Xi_{t+1}^{mz} - \Xi_{t+1}^{ns}) - \frac{1}{\nu}(\zeta^{ns,mz} - \zeta^{ns,ns}) \\ &= \frac{\beta}{\nu}(u_{t+1}^{mz} - u_{t+1}^{ns}) + \beta \log(\mu_{t+1}^{ns,mz}/\mu_{t+1}^{mz,mz}) \\ &\quad + \frac{\beta}{\nu}(\zeta^{ns,mz} - \zeta^{mz,mz}) - \frac{1}{\nu}(\zeta^{ns,mz} - \zeta^{ns,ns}). \end{aligned} \quad (\text{A.112})$$

Assuming that there's no migration cost to stay in the same labor market, i.e., $\zeta^{ns,ns} = 0$, the above equation leads to the following.

$$\log(\mu_t^{ns,mz}/\mu_t^{ns,ns}) = \frac{\beta}{\nu}(u_{t+1}^{mz} - u_{t+1}^{ns}) + \beta \log(\mu_{t+1}^{ns,mz}/\mu_{t+1}^{mz,mz}) - \frac{(1-\beta)}{\nu} \zeta^{ns,mz}. \quad (\text{A.113})$$

This is the moment condition equivalent to the one used in [Artuç et al. \(2010\)](#) and [Caliendo et al.](#)

(2019), but generalized for any utility u_{t+1}^{ns} . Substituting the logarithm utility $u_t^{ns} = \log(C_t^{ns})$ into the above equation, the regression equation of interest becomes

$$\frac{1}{\beta} \log(\mu_t^{ns,mz} / \mu_t^{ns,ns}) = \frac{1}{\nu} \log(C_{t+1}^{mz} / C_{t+1}^{ns}) + \log(\mu_{t+1}^{ns,mz} / \mu_{t+1}^{mz,mz}) - \frac{(1-\beta)}{\nu\beta} \zeta^{ns,mz} + v_{t+1}, \quad (\text{A.114})$$

where v_{t+1} is the random error term realized at $t+1$. The coefficient $1/\nu$ then captures the elasticity of migration flows, i.e., how much the migration flow (relative to staying in the same labor market) responds to the changes in real consumption in the next period.

Although an ideal model would account for the bilateral migration costs $\zeta^{ns,mz}$, I impose the simplifying assumption that $\zeta^{ns,mz} = \zeta^{n,m}$ for $\forall s, z$. Substituting the optimal consumption in equation (A.50) into the aggregate real consumption C_{t+1}^{ns} , then above equation leads to the following:

$$\frac{1}{\beta} \log(\mu_t^{ns,mz} / \mu_t^{ns,ns}) - \log(\mu_{t+1}^{ns,mz} / \mu_{t+1}^{mz,mz}) = \frac{1}{\nu} \log(E_{t+1}^{mz} / E_{t+1}^{ns}) + D_t^{n,m} + v_{t+1}, \quad (\text{A.115})$$

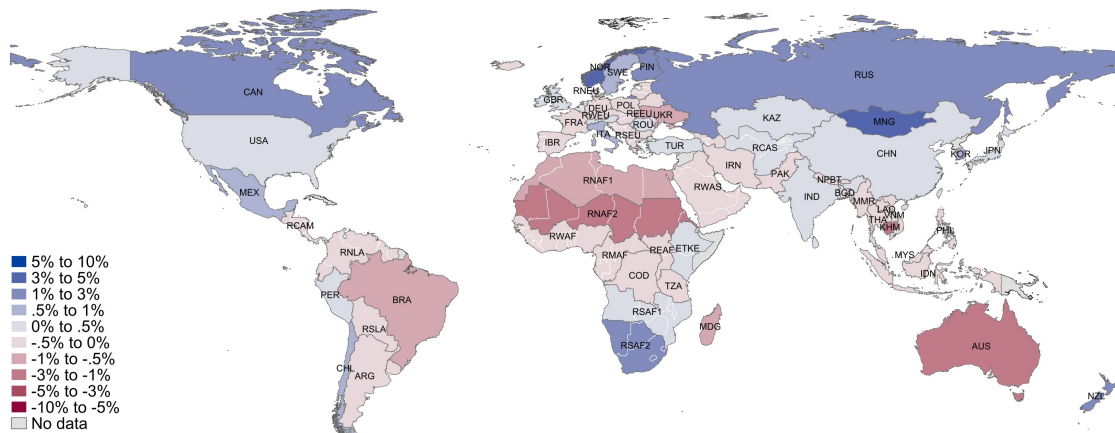
where the aggregate term $D_t^{n,m}$ is captured by origin-destination-time fixed effects, absorbing the preference parameters, price index, and bilateral migration cost terms as follows:

$$D_t^{n,m} = \frac{1}{\beta} \log \left(\frac{\phi^{m\phi^m} (1-\phi^m)^{1-\phi^m}}{\phi^{n\phi^n} (1-\phi^n)^{1-\phi^n}} \right) - \frac{1}{\beta} \log \left(\frac{P_{t+1}^m \phi^m}{P_{t+1}^n \phi^n} \right) - \frac{(1-\beta)}{\beta\nu} \zeta^{n,m}. \quad (\text{A.116})$$

E Additional Results

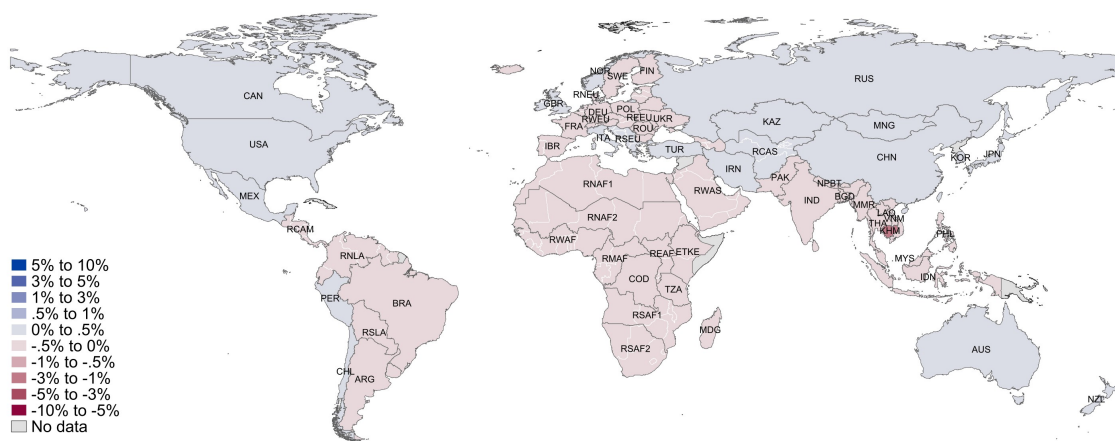
E.1 Baseline Scenario: Welfare Effects

Figure E.1: The Welfare Effects of Climate Change Shock RCP8.5



The Aggregate Global Welfare Effect of Workers in Agriculture: 0.01 %

(a) Welfare Effects of Workers in Agriculture

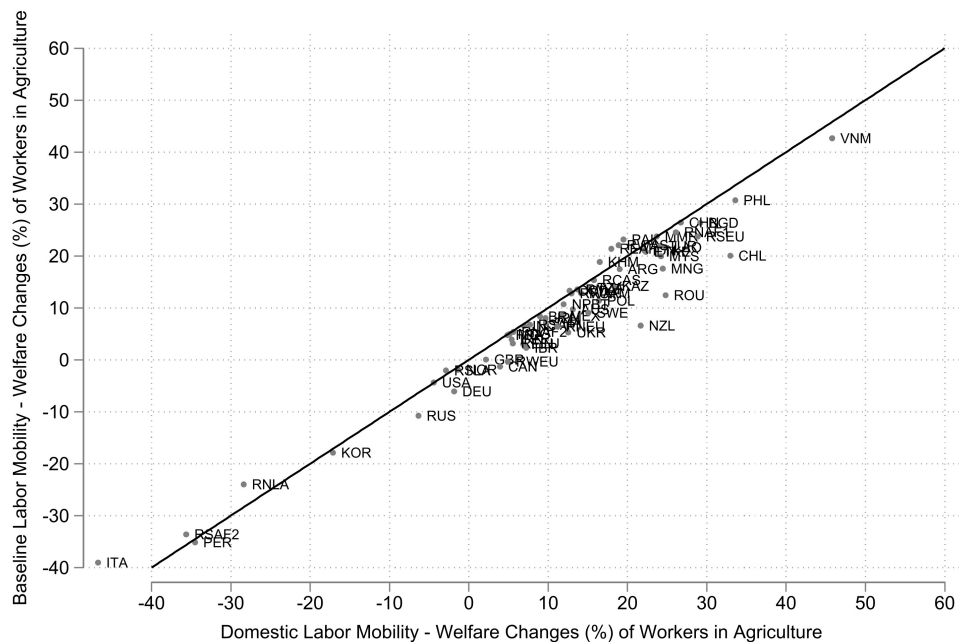


The Aggregate Global Welfare Effect of Workers in Non-Agriculture: -0.02 %

(b) Welfare Effects of Workers in Non-agriculture

Notes: The figures above show the welfare effects of labor mobility under the climate change RCP 8.5 scenario (HadGEM2-ES), measured by the consumption equivalent variation as percentage changes. Figure E.1a shows the welfare effects of climate change on an economy under the RCP 8.5, relative to an economy without climate change, for workers in the agricultural sector, while Figure E.1b depicts the corresponding effects for workers in the non-agricultural sector.

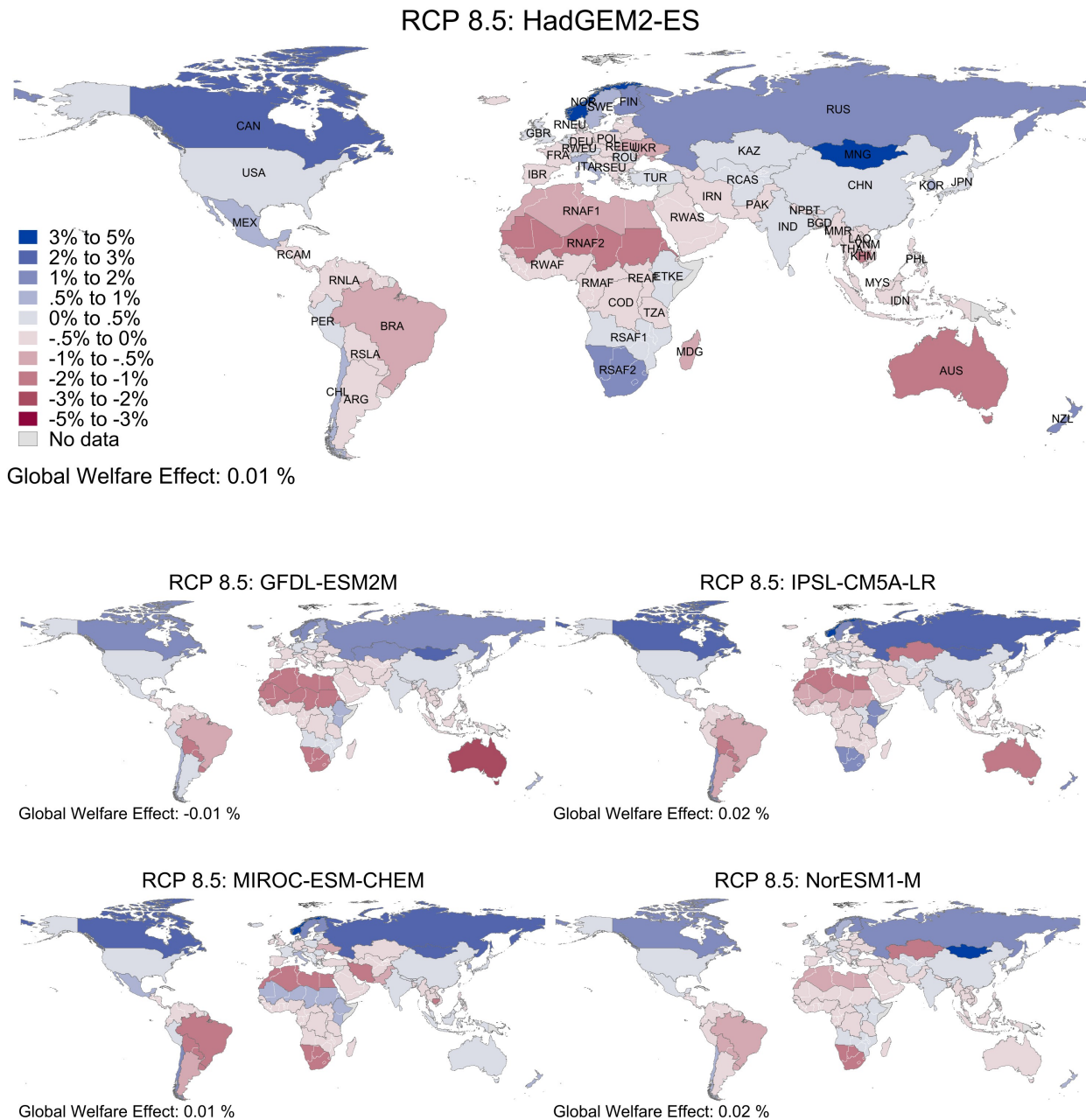
Figure E.2: The Welfare Effects: Counterfactual Migration Costs



Notes: This figure shows the correlation of welfare outcomes for agricultural workers under two different counterfactual migration cost analyses. The y-axis represents the welfare effects of allowing baseline labor mobility, while the x-axis represents the welfare effects of allowing only domestic sectoral labor mobility.

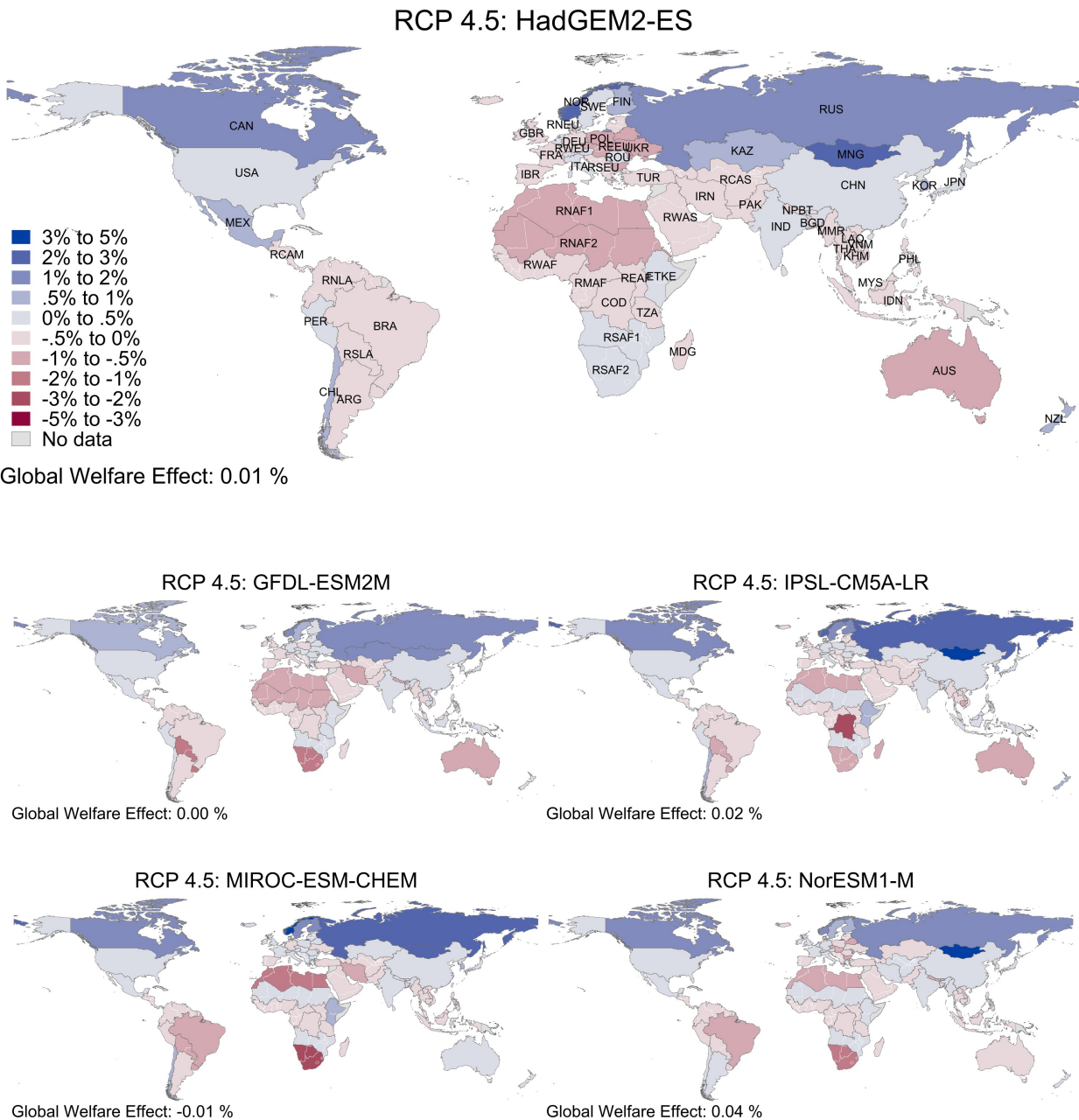
E.2 Sensitivity Test: Other Climate Scenarios

Figure E.3: The Welfare Effects: Climate Scenarios RCP8.5



Notes: The figures above illustrate the welfare effects of climate change shocks under RCP 8.5, relative to an economy without such shocks, for agricultural workers. The welfare effects are measured by the consumption equivalent variation as percentage changes.

Figure E.4: The Welfare Effects: Climate Scenarios RCP4.5



Notes: The figures above illustrate the welfare effects of climate change shocks under RCP 4.5, relative to an economy without such shocks, for agricultural workers. The welfare effects are measured by the consumption equivalent variation as percentage changes.

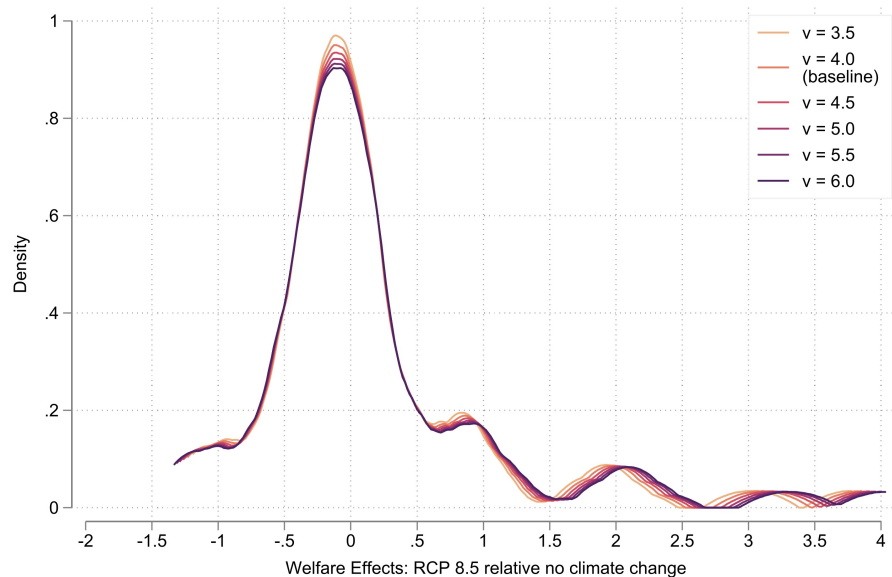
Table 8: Decomposition of Welfare Effects of Climate Change Shock RCP 8.5

	(1) Both Shocks		(2) Yield Only		(3) Multicropping Only	
	Ag workers	NA workers	Ag workers	NA workers	Ag workers	NA workers
Africa						
COD	-0.316	-0.276	-0.147	-0.195	-0.169	-0.082
ETH-KEN	0.361	0.047	0.549	0.057	-0.190	-0.011
MDG	-0.533	-0.171	-0.171	-0.061	-0.358	-0.111
Rest of (Lower) Northern Africa	-1.014	-0.458	-0.734	-0.351	-0.285	-0.111
Rest of (Lower) Southern Africa	1.151	0.531	0.990	0.480	0.157	0.048
Rest of (Upper) Northern Africa	-0.963	-0.076	-0.765	-0.069	-0.204	-0.008
Rest of (Upper) Southern Africa	0.060	-0.101	0.112	-0.102	-0.050	0.001
Rest of Eastern Africa	-0.092	-0.087	0.063	-0.011	-0.155	-0.076
Rest of Middle Africa	-0.110	-0.074	-0.025	-0.049	-0.086	-0.025
Rest of Western Africa	-0.277	-0.104	-0.200	-0.083	-0.076	-0.021
TZA	-0.115	-0.073	-0.046	-0.060	-0.068	-0.013
Asia						
BGD	-0.258	-0.030	-0.215	-0.038	-0.042	0.008
CHN	0.278	0.057	0.098	0.025	0.181	0.033
IDN	-0.074	-0.035	0.020	-0.023	-0.093	-0.012
IND	0.207	-0.062	0.226	-0.061	-0.016	-0.001
IRN	-0.319	0.035	-0.580	-0.005	0.263	0.041
JPN	0.192	0.020	0.050	0.007	0.142	0.013
KAZ	0.181	0.045	-0.011	0.024	0.193	0.021
KHM	-1.144	-1.328	-1.094	-1.335	-0.049	0.008
KOR	0.742	0.032	0.180	0.007	0.571	0.025
LAO	-0.119	-0.065	-0.087	-0.062	-0.033	-0.002
MMR	-0.115	-0.085	-0.004	-0.060	-0.111	-0.024
MNG	3.855	0.198	2.444	0.122	1.443	0.076
MYS	-0.013	-0.008	0.040	-0.005	-0.053	-0.003
NPL-BTN	-0.061	-0.115	-0.078	-0.126	0.020	0.011
PAK	-0.245	-0.041	-0.291	-0.063	0.049	0.022
PHL	-0.206	-0.022	-0.047	-0.016	-0.158	-0.007
Rest of Central Asia	0.251	0.082	0.024	0.022	0.228	0.059
Rest of Western Asia	-0.341	-0.021	-0.307	-0.019	-0.033	-0.001
THA	-0.340	-0.089	-0.278	-0.086	-0.060	-0.003
TUR	0.041	0.016	-0.102	0.001	0.143	0.016
VNM	-0.165	-0.023	-0.051	-0.015	-0.113	-0.009
Australia and New Zealand						
AUS	-1.233	-0.031	-1.026	-0.025	-0.210	-0.006
NZL	1.004	0.028	0.576	0.017	0.427	0.011
Europe						
DÉU	-0.003	0.006	0.059	-0.000	-0.061	0.006
FIN	1.808	0.033	1.813	0.033	-0.004	-0.000
FRA	-0.055	-0.019	-0.176	-0.021	0.121	0.001
GBR	0.047	0.004	0.091	0.003	-0.043	0.001
IBR	-0.115	-0.014	-0.235	-0.019	0.121	0.006
ITA	0.667	0.022	-0.007	-0.004	0.675	0.027
NOR	3.102	0.044	1.816	0.027	1.263	0.016
POL	-0.473	-0.012	-0.388	-0.012	-0.085	0.001
ROU	0.368	0.012	-0.230	-0.018	0.600	0.030
RUS	1.957	0.054	1.803	0.041	0.154	0.013
Rest of Eastern Europe	-0.450	-0.009	-0.428	-0.020	-0.021	0.012
Rest of Northern Europe	-0.057	0.009	0.026	0.007	-0.083	0.003
Rest of Southern Europe	-0.003	0.005	-0.187	-0.016	0.186	0.022
Rest of Western Europe	0.107	0.000	0.078	-0.004	0.029	0.004
SWE	0.843	0.010	0.748	0.009	0.095	0.001
UKR	-0.651	0.002	-0.574	-0.020	-0.077	0.023
Northern America						
CAN	2.157	0.044	2.079	0.042	0.078	0.002
MEX	0.685	0.037	0.663	0.034	0.021	0.003
Rest of Central America	-0.440	-0.034	0.016	-0.001	-0.449	-0.031
USA	0.004	0.005	-0.122	-0.000	0.127	0.006
South America						
ARG	-0.381	-0.051	-0.369	-0.041	-0.013	-0.010
BRA	-0.712	-0.037	-0.402	-0.025	-0.314	-0.012
CHL	0.938	0.028	0.461	0.015	0.470	0.013
PER	0.112	0.070	0.106	0.052	0.006	0.017
Rest of Northern Latin America	-0.100	-0.023	-0.021	-0.021	-0.078	-0.002
Rest of Southern Latin America	-0.237	-0.038	-0.027	-0.020	-0.212	-0.019
World						
Global	0.012	-0.012	0.032	-0.018	-0.019	0.006

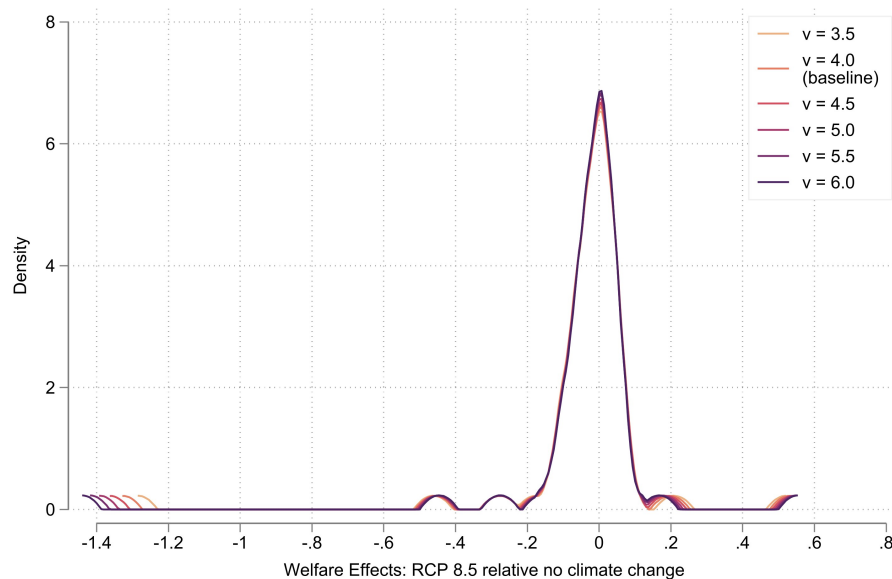
Notes: The table above presents the decomposition of welfare effects, with values expressed as percentage changes (%), measured by consumption equivalent variation. The first two columns report the welfare effects of the RCP 8.5 climate change scenario (HadGEM2-ES), with both yield and multicropping capacity shocks, for agricultural (Ag) and non-agricultural (NA) workers, respectively. The next two columns show the corresponding welfare effects of yield shocks only, while the last two columns show the welfare effects of multicropping capacity shocks only.

E.3 Sensitivity Test: Other Migration Elasticities

Figure E.5: Sensitivity to Migration Elasticity (ν)



(a) Welfare Effects of Workers in Agriculture



(b) Welfare Effects of Workers in Non-agriculture

Notes: The figures above show the density distribution of welfare effects of climate change RCP 8.5 scenario (HadGEM2-ES), measured by the consumption equivalent variation, across different migration elasticity parameters. Figure E.5a and E.1b describe the welfare distribution of workers in the agricultural and non-agricultural sectors, respectively.

F Other Supplementary Data

F.1 List of Crops and Countries

Table 9 shows the list of 10 major crops considered in this study. The first column (GAEZ Major Crops) provides the crop acronyms and names, which serve as the unit of analysis in this paper. The second column (FAO Trade Data) lists the corresponding trade items based on FAO classifications. The third column (GAEZ Module 3) details the subcategories of corresponding crop items from GAEZ Module 3, which provides potential yield information.

Table 9: List of Crops and Classifications

No.	GAEZ Major Crops		FAO Trade Data		GAEZ Module 3	
	Code	Name	Code	Name	Code	Name
1	RCW	Rice	27	Rice	ricd	Dryland rice
					ricw	Wetland rice
2	MZE	Maize	56	Maize (corn)	hmze	Highland maize (tropics)
					lmze	Lowland maize
					tmze	Temperate/sub-tropical maize
3	WHE	Wheat	15	Wheat	swhe	Spring wheat
					wwhe	Winter, sub-tropical and tropical highland wheat
4	RT1	Potato and sweet potato	116	Potatoes	wpot	White potato
				Sweet potatoes	spot	Sweet potato
5	SUC	Sugar cane	156	Sugar cane	sugc	Sugar cane
6	SOY	Soybean	236	Soya beans	soyb	Soybean
7	TMT	Tomatoes	388	Tomatoes	toma	Tomato
8	OLP	Oil palm fruit or its byproducts	254 256 257	Oil palm fruit	oilp	Oil palm
				Palm kernels		
				Palm oil		
9	RT2	Cassava	125	Cassava, fresh	casv	Cassava
10	BAN	Bananas	486	Bananas	bana	Banana

Notes: When the potential yield information is available for multiple crops under GAEZ Module 3 for each GAEZ major crop, I used the maximum value of crop yields.

Table 10: List of Countries and Classifications

No.	ISO-3 Code	Country Full Name	ISO-Major Code	Sub-region	Region	
1	ETH	Ethiopia	ETKE REAF - Rest of Eastern Africa	Eastern Africa	Africa	
2	KEN	Kenya				
3	MDG	Madagascar				
4	BDI	Burundi				
5	RWA	Rwanda				
6	SSD	South Sudan				
7	UGA	Uganda				
8	DJI	Djibouti				
9	TZA	Tanzania				
10	COD	Congo DRC				
11	GAB	Gabon				
12	CMR	Cameroon				
13	GNQ	Equatorial Guinea				
14	COG	Congo				
15	CAF	Central African Republic				
16	TUN	Tunisia	RNAF1 - Rest of (Upper) Northern Africa	Northern Africa		
17	EGY	Egypt				
18	LBY	Libya				
19	DZA	Algeria				
20	MAR	Morocco				
21	TCD	Chad				
22	NER	Niger				
23	MLI	Mali				
24	SDN	Sudan				
25	ERI	Eritrea				
26	MRT	Mauritania	RNAF2 - Rest of (Lower) Northern Africa	Northern Africa		
27	MWI	Malawi				
28	ZMB	Zambia				
29	AGO	Angola				
30	ZWE	Zimbabwe				
31	MOZ	Mozambique				
32	ZAF	South Africa				
33	LSO	Lesotho				
34	BWA	Botswana				
35	NAM	Namibia				
36	SWZ	Eswatini	RSAF1 - Rest of (Upper) Southern Africa	Southern Africa	Africa	
37	TGO	Togo				
38	BFA	Burkina Faso				
39	BEN	Benin				
40	SLE	Sierra Leone				
41	GNB	Guinea-Bissau				
42	GHA	Ghana				
43	SEN	Senegal				
44	CIV	Côte d'Ivoire				
45	LBR	Liberia				
46	GIN	Guinea	RSAF2 - Rest of (Lower) Southern Africa	Southern Africa		
47	NGA	Nigeria				
48	KAZ	Kazakhstan				
49	AFG	Afghanistan				
50	UZB	Uzbekistan				
51	TKM	Turkmenistan				
52	KGZ	Kyrgyzstan				
53	TJK	Tajikistan				
54	CHN	China	KAZ RCAS - Rest of Central Asia	Western Africa	Africa	
55	JPN	Japan				
56	KOR	South Korea				
57	MNG	Mongolia				
58	IDN	Indonesia				
59	KHM	Cambodia				
60	LAO	Laos				
61	MMR	Myanmar				
62	MYS	Malaysia				
63	PHL	Philippines				
64	THA	Thailand	KAZ NPBT	Central Asia	Asia	
65	VNM	Vietnam				
66	BGD	Bangladesh				
67	IND	India				
68	LKA	Sri Lanka				
69	IRN	Iran				
70	BTN	Bhutan				
71	NPL	Nepal				
72	PAK	Pakistan				

Continued on the next page

No.	ISO-3 Code	Country Full Name	ISO-Major Code	Sub-region	Region			
73	ARE	United Arab Emirates	RWAS - Rest of Western Asia	Western Asia				
74	AZE	Azerbaijan						
75	ISR	Israel						
76	IRQ	Iraq						
77	SAU	Saudi Arabia						
78	ARM	Armenia						
79	OMN	Oman						
80	KWT	Kuwait						
81	JOR	Jordan						
82	YEM	Yemen						
83	GEO	Georgia	TUR					
84	TUR	Turkiye						
85	AUS	Australia	AUS	Oceania	Oceania			
86	NZL	New Zealand	NZL					
87	POL	Poland	POL	Eastern Europe	Europe			
88	CZE	Czech Republic	REEU - Rest of Eastern Europe					
89	SVK	Slovakia						
90	HUN	Hungary						
91	BGR	Bulgaria						
92	BLR	Belarus						
93	MDA	Moldova						
94	ROU	Romania	ROU					
95	RUS	Russian Federation	RUS					
96	UKR	Ukraine	UKR					
97	FIN	Finland	FIN	Northern Europe				
98	GBR	United Kingdom	GBR					
99	IRL	Ireland	GBR					
100	NOR	Norway	NOR					
101	ISL	Iceland	RNEU - Rest of Northern Europe					
102	EST	Estonia						
103	LVA	Latvia						
104	DNK	Denmark						
105	LTU	Lithuania						
106	SWE	Sweden	SWE					
107	ESP	Spain	IBR					
108	PRT	Portugal	IBR					
109	ITA	Italy	ITA					
110	SVN	Slovenia	RSEU - Rest of Southern Europe	Southern Europe	Europe			
111	GRC	Greece						
112	HRV	Croatia						
113	MNE	Montenegro						
114	BIH	Bosnia and Herzegovina						
115	SRB	Serbia						
116	ALB	Albania						
117	MKD	North Macedonia						
118	DEU	Germany	DEU	Western Europe				
119	FRA	France	FRA					
120	AUT	Austria	RWEU - Rest of Western Europe					
121	BEL	Belgium						
122	CHE	Switzerland						
123	NLD	Netherlands						
124	MEX	Mexico	MEX		Central America			
125	BLZ	Belize	RCAM - Rest of Central America					
126	CRI	Costa Rica						
127	PAN	Panama						
128	GTM	Guatemala						
129	NIC	Nicaragua						
130	SLV	El Salvador						
131	HND	Honduras						
132	CAN	Canada	CAN	North America	Northern America			
133	USA	United States	USA					
134	ARG	Argentina	ARG	South America	South America			
135	BRA	Brazil	BRA					
136	CHL	Chile	CHL					
137	PER	Peru	PER					
138	ECU	Ecuador	RNLA - Rest of Northern Latin America	South America				
139	COL	Colombia						
140	SUR	Suriname						
141	GUY	Guyana						
142	VEN	Venezuela						
143	BOL	Bolivia	RSLA - Rest of Southern Latin America					
144	PRY	Paraguay						
145	URY	Uruguay	Latin America					